23

PETROLOGY, GEOCHEMISTRY AND MINERAL OCCURRENCES OF THE BIG DUBICHA METAULTRAMAFIC ROCKS, NORTHEAST OF KIBREMENGIST, SOUTHERN ETHIOPIA

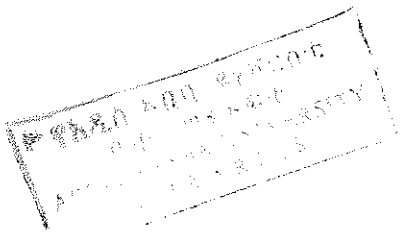

A Thesis Presented to

the School of Graduate Studies

Addis Ababa University

In Partial Fulfilment

of the Requirements for the Degree

of Master of Science in Geology

By

TESFAYE DEMISSIE

November, 1999

ABSTRACT

The Big Dubicha metaultramafic mass is part of the eastern belt (Kenticha belt) of Adola area. Lithologic units in the area include; biotite - muscovite - quartz schist, chlorite schist, talc schist and tremolite - actinolite - talc - serpentine schist.

Mineral assemblages of the Big Dubicha altered ultramafic rocks are characteristic of lower greenschist facies, representing serpentinization, chloritization and carbonation reactions among others. These reactions are the result of low temperature water-rock interactions. The metamorphic mineral assemblages of the enveloping metamorphosed sedimentary rock fall within lower to middle amphibolite facies, suggesting the presence of allofacial relationship between the Big Dubicha altered ultramafic rocks versus the enveloping rock. In addition shallow angle westward dipping foliation is related to the thrusting event .

Whole rock geochemical data examined in the system CaO - MgO - SiO_2 - H_2O - CO_2 for a tremolite - actinolite - talc - serpentine schist and chlorite schist suggest harzburgitic and dunitic anhydrous mineralogy, together with the limited metamorphic and structural observations, the Big Dubicha altered ultramafic rocks represent a slice or fragment of subcontinental mantle lithosphere.

From the geochemical maps of soil samples, anomalous zones of Ni, Cr, Co, Mn, and Zn are observed along the strongly deformed and serpentinized tremolite - actinolite - talc -serpentine schist, indicating insitu weathering (lateritization) of the bedrock was responsible for the observed mineral occurrences.

TABLE OF CONTENTS

ACKNOWLEDGMENT

I would like to express my deepest appreciation for the constant supervision and encouragement I received from my advisor, Dr. Teklewold Ayalew. Special thanks are due to Dr. Solomon Tadesse, Head, Geology and Geophysics Department (GGD) of Addis Ababa University for his help in arranging and providing vehicle for field work.

This study was mainly funded by the Ethio-Italian University Technical Cooperation through the research grant to Dr Teklewold Ayalew, entitled *Petrology and chemistry of the altered ultramafic masses of western and southern Ethiopia.*.I am also indebted to Professor Angelo Peccerillo for the analytical support at the Dipartimento di Scienze della Terra, University of Perujia, Italy.

Many thanks are also to Ethiopian Institute of Geological surveys (EIGS) central laboratory for preparation and analysis of thin - sections and soil samples. My acknowledgment also goes to Regional Geology and Geochemistry Department (RGGD) of EIGS for providing me vehicle during the second phase of field work and allowing me to use all facilities during preparation of the thesis.

I gratefully acknowledge the staff members of Geology and Geophysics Department, Regional Geology and Geochemistry Department (RGGD) and Mineral Operation Department (MOD) of Ministry of Mines and Energy for their endless great help to bring the thesis to its final form.

CHAPTER 1 - INTRODUCTION

1.1. Location, physiography, climate and access

The Big Dubicha metaultramafic mass has a total of about 5 sq. km areal extent. It is situated between $5^0$54'24" - $5^0$55'45" N and $39^0$01'36" - $39^0$02'41" E in Oromia Region (Fig. 1), about 478 km south of Addis Ababa and 8 km northeast of Kibremengist.

Ethiopia is divided into three distinct phsiographic units, which are the product of major geological evolution of the region (Fig. 2). These are:

1. The Ethiopian Rift System transects the territory into two and is bounded by spectacular fault scarps and accompanying rift floor that characterized by a series of horest – graben systems. The lowest elevation is 125 m below sea level (Afar depression).

2. The North – Western (Ethiopia) plateau and associated lowlands, covers more than half of the country, and where the lowlands slope westward into the Sudanese plain.

3. The South – Eastern (Somali) plateau and associated lowlands, most of which are extensively covered by flat plains starting from the Ogaden basin to the east and the Wabi – Shebelle and the Genale plains to the southeast. The Big Dubicha area is the part this phsiographic unit.

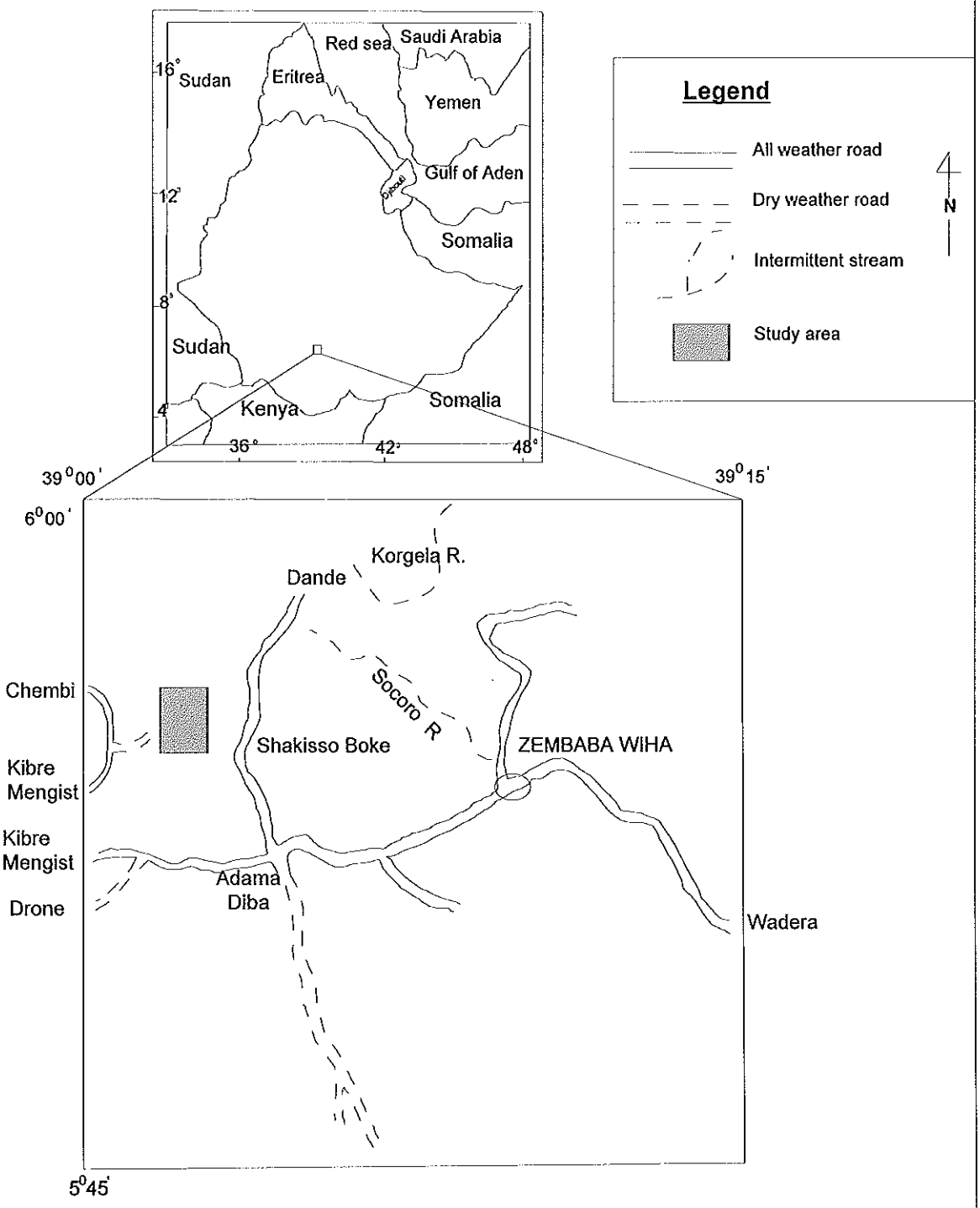

Figure 1. Location map of Big Dubicha area

Plate 1. Western view of the Big Dubicha area.

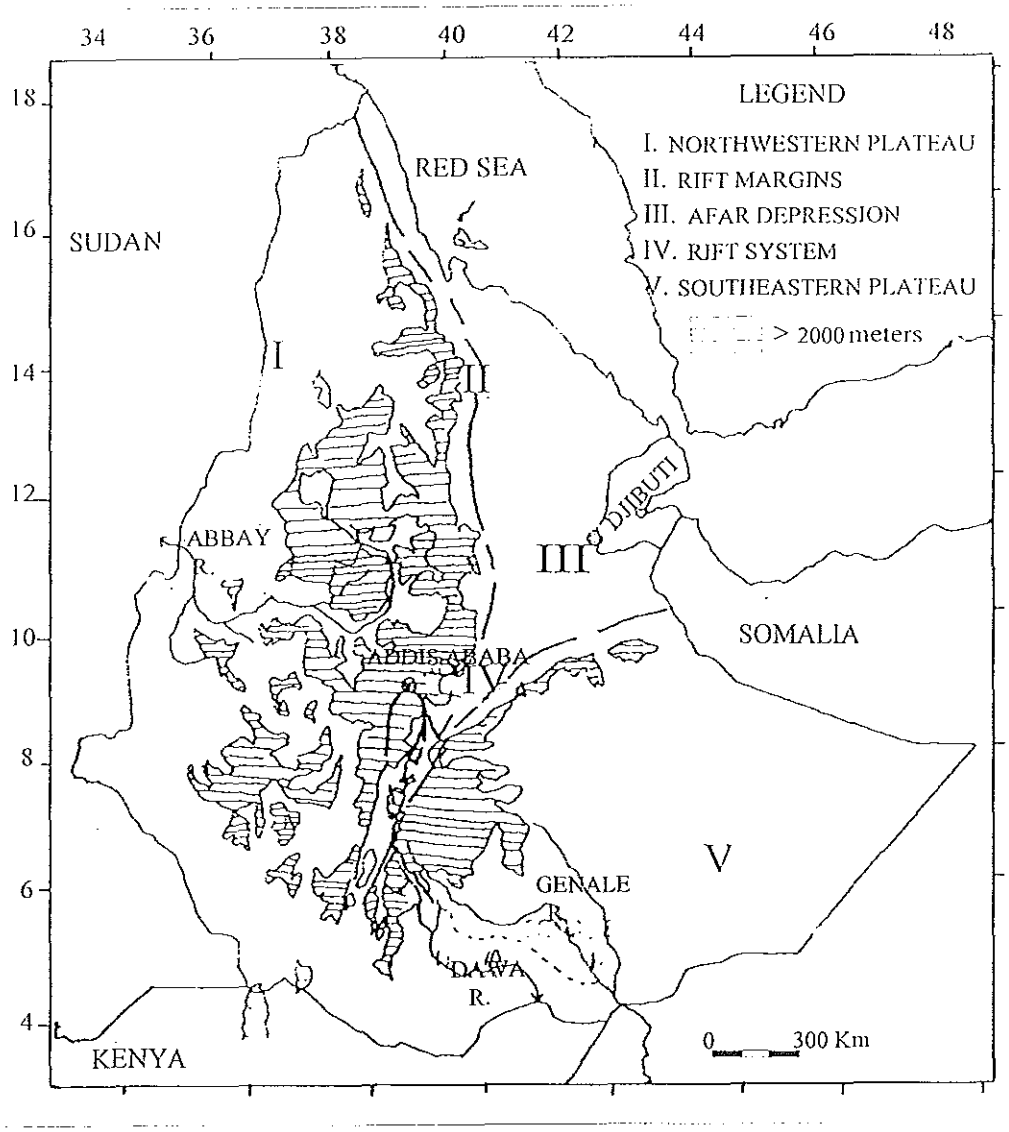

Figure 2. Physiographic units of Ethiopia (After Woldemariam, 1970).

The Big Dubicha metaultramafic mass is characterized by N – S striking subcircular to elongate ridge. It has flat top and gentle to steep slopes (Plate 1). The highest elevation is 1910m above sea level (a. s. l.), and the lowest elevation is 1740m a.s.l. Intermittent drainages with dendritic to subparallel pattern characterize the ridge and flow into the Kucho (to the west) and Benko (to the east) perennial streams.

The Big Dubicha area is characterized by scarce vegetation (Plate 1) except along the drainages, which have sparse vegetation including *zegba, bisana, kitkita, grar, wanza, shola, banana etc.* The area is marked by tropical climate with two rainy seasons: from September to November and from March to May. The mean annual rainfall ranges from 400mm to 800mm and the mean annual temperature is 18 ^{0}C (Ethiopian mapping agency, 1981).

The population density of the surrounding flat-lying area is relatively low and the inhabitants are Oromo. Their livelihood is subsistence farming of crops such as *barley, teff, maize, sorghum, wheat and the newly started coffee, and livestock.*

The Big Dubicha route is all-weather road that stretches from Addis Ababa through Awassa - Aposto - Aleta Wondo - Kibremengist, of which the road from Addis Ababa to Aleta Wondo junction (~ 320 kms) is asphalted. The road that bifurcates to the study area (~2kms) from Kibremengist – Chembi gravel road is accessible by four wheel drive vehicles during rainy season.

1.2. Review of previous work

The earliest geological investigation dates back to late 1930s following the discovery of placer gold in the Bedakessa valley of the Adola area. Extensive placer gold mining activities in later years enhanced the overall geological investigation of the region.

Jelenc (1966), in his compilation of the mineral occurrences and deposits of Ethiopia, divided the rocks of the Adola region into two: i) the high-grade metamorphic rock association, older series of the Gariboro which includes gneisses, amphibolites, migmatites and schists and: ii) the low-grade rocks, the younger rocks of the Adola, represented by dominant metasediments of the greenschist facies. He further noted the presence of nickeliferous laterites, which developed on the serpentinite masses and slivers that form two parallel array of the same. In addition he documented chromite occurrences along the eastern chain which are absent from those in the west.

Gilboy (1970) and Chater (1971) proposed a three – fold subdivision of the rocks into Lower, Middle and Upper lithostratigraphic groups. Kazmin (1971, 1972, 1975, 1976 and Kazmin et al., 1978), redefined the groups into complexes. Their stratigraphy and possible manner evolution was discussed by Kazmin (1972), Table 1 and 2 represent the stratigraphic correlation within the country as well as those of east Africa. Although not supported by isotopic works, the Lower Complex is referred as Archean and the Upper Complex as late Proterozoic (Kazmin, 1971, 1972, 1975, 1976 and Kazmin et al., 1978).

Age		Southern Ethiopia	Western Ethiopia	Northern Ethiopia		Harar and Aisha	
Eocambrian				Matheos Fm			Upper
Upper Proterozoic				Shiraro Fm			
				Dadikama Fm			
				Tambien Gr	Amota Fm		
					Mai Kental Fm		
					Arequa Fm		
		Mormora Group and Kajimiti beds	Birbir Group	Tsaliet Group		Boka and Boje Series	
		Adola Group	Greenstones and amphibolite				
Low. – Mid. Proterozoic		Wadera Group					Middle
Archean		Burgi gneiss	Gneisses Undifferentiated	Gneisses Undifferentiated		Mica Schist	Lower
	Arero Group	Yavello gneiss				Gneisses	
		Awata gneiss					
		Alghe gneiss					
		?					
		Konso gneiss	Granulites of the Beles basin				

Table 1. Precambrian Units in Ethiopia (After Kazmin, 1972)

Age		Saudi - Arabia	Egypt	Sudan	Ethiopia	Somalia	Kenya	Tanzania
Infracambrian or Eocambrian		Fatima, Abla Fm.	Hammat series	Awat Series	Shiraro Fm. Matheos Fm.			
Upper Proterozoic	Upper Part	Murrdama Fm. Halaban Fm.	Schist – mud stone – grey – wake series Dokhan series	Upper part Nafirdeib Series Lower Part	Tambien Group Tsaliet Group Birbir Group	Inda – Ad Series		
	Lower part	Beish; Lit Complexes	Shadli Series Barramia Rocks	Primitive system	Adola Group	Green – rock Series in The Basement System	Some green rock complexes in western Kenya (?) Embu and Ablun Sereies in central and eastern Kenya	Ukinga, Konse, Ndembera Series
Middle - Lower Proterozoic		?	?		Wadera Group	?	Turoka Series	Limestone Graphite Series
Archean		Ancient Gneiss	Orthogneisses of " Basement " Mitiq Series		Burji) Awata) Alghe) = Gneiss Konso)	Gneisses of the Basement System	Basement System	Usagarian System

Table 2. Correlation of Some Precambrian Units in East Africa and Arabia (After Kazmin, 1972)

The Lower Complex comprises thick successions of gneisses grading to migmatites and metamorphic granites (Kazmin, 1972) representing the older cratonic basement (Kazmin et al., 1978). The prominent rock associations include biotite and hornblende gneisses, with subordinate quartzofeldspathic gneisses, calc - silcate rocks and amphibolites (Kazmin et al., 1978). They are extensively exposed in southern and western Ethiopia.

The Middle Complex, known so far only in southern Ethiopia, is represented by the Wadera Group of moderately altered psammitic to pelitic metasediments including biotite and quartz – muscovite schists, metaarkoses, quartzite often with primary sedimentary features including cross – bedding (Kazmin, 1971, 1972, 1976). The relationship between the Lower and the Middle Complex is most probably that of basement and cover (Kazmin, 1976). Generally the Middle Complex rocks are considered as the Lower to Middle Proterozoic platform sediments (Kazmin et al., 1978).

The Upper Complex comprises a thick succession of low-grade metamorphic (greenschist facies, at places amphibolite facies) rocks in the following succession: ophioilitic rocks, andesitic metavolcanics and associated metasediments, clastic and to less extent carbonate sediments (Kazmin, et al., 1978). The contacts between these rocks and the Lower and Middle Complex rocks is tectonic (Kazmin, 1972, 1976, de Wit and Chewaka 1981). Kazmin (1976) accepted the ophiolitic origin for the rocks of the Adola group, and interpreted the Kenticha zone as a nappe or series of nappes overthrust on the margin of continental blocks. This opinion is supported by (de Wit and Chewaka, 1981 and Woldehaimanot, 1995). The altered ultramafics of the study area which belong to the Kenticha belt is interpreted also as thrust slice by current work supporting this thrust tectonic concept.

Kozyrev et al., (1985) recognized only the Middle and Upper Complex; with further classification of the Adola area into three N – S trending lithostructural blocks. Thus named as the Western, Central and Eastern blocks, the latter were subdivided into the Mormora and Awata subblocks separated by the Kenticha zone. In addition two N – S trending belts of ultramafic rocks, the Kenticha and the Megado, which are traced through the entire length of the Adola area are reported. Finally a geosynclinal basin formation is proposed in which volcanosedimentary assemblages of the Adola belt is evolved.

de Wit and Chewaka (1981) have attempted to classify the Ethiopian basement into five tectonostratigraphic zones, by grouping the Megado and Kenticha ophiolitic rocks under eastern metamophic belt (Fig. 3). They have also tried to reconstruct the tectonic evolution for Precambrian rocks of Ethiopia.

Worku and Yifa (1989), classified the Adola area into two main tectono-stratigraphic units, based on distinct deformational phases and intensity of metamorphism. In addition they interpreted the ensialic basin development on sialic basement is unrelated to Wilson cycle plate tectonics. Worku (1996) recognized five major lithotectonic terrains in the Adola belt and interpreted interms of Wilson cycle tectonics, which started by formation of passive continental margin sediments and development of an oceanic basin in the Kenticha terrain.

In continental and subcontinental scale Berhe (1990) identified five major ophiolitic sutures in NE Africa including the Adola and Moyale belt. He classified them as remnants of either suprasubduction zones or back-arc basins settings as they show island arc and MORB geochemistry. Hence there are wide variation in interpretation of the geologic evolution of the Adola area and origin of ultramafic rocks.

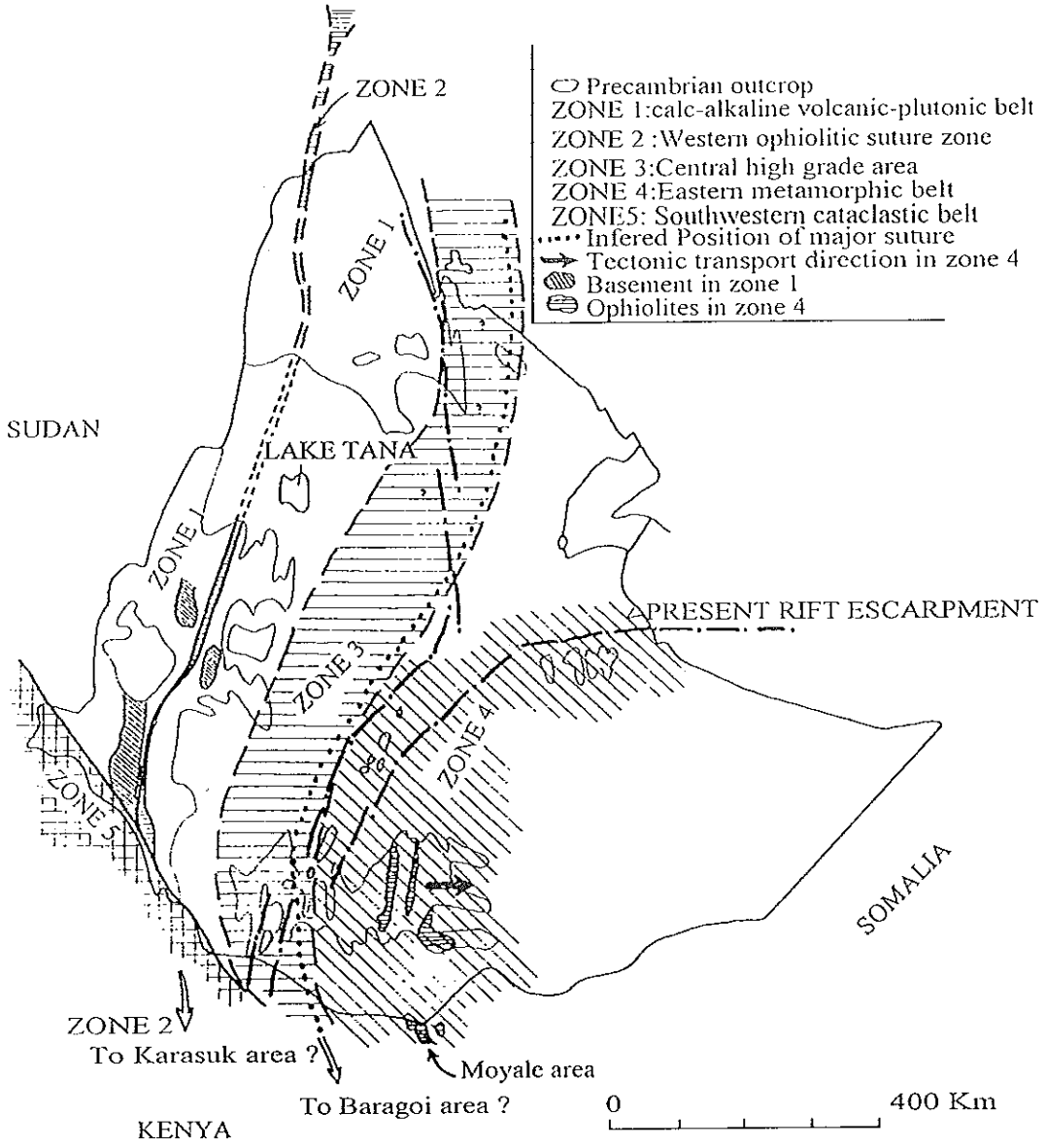

Figure 3. Major tectono-stratigraphic units of the Ethiopian Precambrian (After de Wit and Chewaka, 1981).

Levite and Kent (1968) reported a vertically sunk 200 m deep exploratory drill hole in the western slope of Big Dubicha. The documented lithologic sequences reveal that serpentinites grade into an altered peridotites suggesting insitu serpentinization. It is also reported occurrence of garnierite mineral as fracture filling and dissiminations, and chromite lenses, about 2 to 3 meters long, recorded within the weathered serpentinites. In the report the lateritic Ni reserve was estimated at 1,573,452 tons with a grade of 1.2 % Ni averaged from ninety eight exploratory pits sunk at Big Dubicha. The present work proved the presence of this lateritic Ni and identified the source rock.

1.3. Objective of the present work

This study embraces the petrology, geochemistry and mineral occurrences of the Big Dubicha metaultramafic mass. The major aspect of the study can be summerized as follows:

i. detailed geological and geochemical mapping.

ii. petrographic and chemical characterization of the rocks to approximate their anhydrous mineralogy in an attempt to discern the tectonic evolution of the area.

iii. evaluation of the mineral potential of the area, with particular emphasis to Ni and Cr occurrences.

1.4. Methodology

A detailed geological mapping of the Big Dubicha metaultramafic mass covering an area of about 5 sq. km was carried out at scale of 1:10,000. Base maps at the scale of 1:10,000 and 1:25,000 were prepared from 1:50,000 topographic maps; air-photographs were also used for geological interpretation prior to the field exercise. Thin-sections from a total of 88 rock samples collected from the various mappable units were carefully studied. Sample spacing is based on alteration intensity, lithologic variation and clues for mineral occurrences. Mineralogical compositions, textural patterns, fabric and replacement or alteration features are documented from outcrops, hand specimen and microscopic observations. Sample preparations for petrographic and chemical analysis were made at the EIGS central laboratory. Whole rock chemical analysis of 86 samples was performed in the Dipartimento di Scienze della Terra, Universty of Perujia, Italy using X–ray fluorescence (XRF).

Rock grinding (to reduce to fine chips) has been carried out by stainless steel jaw crusher and fine powders have been obtained by grinding in a tungsten carbide disk crusher. These crushing tools do not give significant elemental contamination, except for W and Co. Major and trace elements have been determined by combined wet chemistry and X-ray fluorescence (XRF) analysis. SiO_2, TiO_2, Al_2O_3, MnO, CaO, K_2O, P_2O_5, V, Cr, Co, Ni, Cu, Zn, Ga, Rb, Sr, Y, Zr, Nb, Ba, La, Pb, Ce and Th have been analyzed by XRF on pressed pellets made of pure rock powder. A full matrix correction method has been used to correct matrix effects for major elements. Trace elements have been determined using several international rock standards for curve calibration and correcting for matrix effects. Loss on ignition (LOI) has been determined by heating 500 mg dried samples to 1000^0 C, cooling in a disccator and

measuring the loss of weight during heating. LOI contains all the volatile components (H_2O, CO_2, F etc.) occurring in the rocks. Na_2O and MgO have been determined by wet methods. 200 mg samples have been attacked with HF + perchloric acid for several hours, reduced to dryness, dissolved in HCl and brougth to volume. Na_2O has been determined by flame photometry. MgO has been determined by Atomic Absorption Spectrophotometry. Trace elements precision expressed as relative standard deviation is between 5 - 10 %. The analytical data was statistically and graphically evaluated using a software known as *Newpet* with close review of the associated field and petrographic data.

Geochemical soil sampling was conducted using a compass grid of 250m line spacing and 100m sampling interval. 31 soil samples (25 along the grid and 6 from random locations outside the grid), 8 pit channel soil samples, 10 trench channel soil samples and 6 stream sediment samples were collected. They were analyzed for Au (except for pit and trench samples), Cu, Zn, Ni, Co, Pb, Mn and Cr using Atomic Absorption Spectroscopy (AAS). Fe was analyzed only for pit and trench samples using the same method. The geochemical samples were analyzed at EIGS central laboratory. During laboratory analysis of the soil and stream sediment samples, the samples were sieved into - 80 mesh size. For gold analysis a 20 gram sample was digested and with aquaregia ($1HNO_3$: 3HCl), and leached with 5 ml Di Isobutyl Ketone. The concentrate was read by Atomic Absorption Spectroscopy (AAS) for Gold. In this case the detection limit of the instrument is 0.1 ppm. For the trace elements, a 0.25 g samples was digested with 1 ml perchloric acid and leached with 9 ml (1 + 9) HCl. The detection limit of the instrument for trace elements is 1 ppm. Results of the twenty five soil samples from the established grid are contoured and grided using a *Surfer – 32* geochemical software. Inorder to identify the anomalous zones the thresholds of the population were selected from cumulative probability frequency curve using *pplot* software.

CHAPTER 2 - GEOLOGY

2.1. Regional geologic setting

Continent - wide geological understanding was that of Holmes (1951) who suggested that the region is the northern continuation of the Mozambique belt (MB), a North - South trending policyclic structural entity extending along the eastern margin of Africa including the Adola area of southern Ethiopia. The Adola volcanosedimentary - ultramafic association is regarded as the southern continuation of the Arabian - Nubian Sheild (ANS) (Gass, 1981), the gneissic rocks might represent the northward continuation of the high-grade rocks of the MB (Kazmin et al., 1978; Vail, 1976, 1983). Hence the Adola area occupies a unique position within the ANS and MB (Kazmin, 1972, 1975; Kazmin et al., 1978; Vail, 1983), which together known as East African Orogen (EAO) (Stern, 1993, 1994).

The Precambrian rocks of Ethiopia are classified into three groups (Lower, Middle and Upper complexes) (Gilboy, 1970, Chater, 1971, Kazmin, 1971, 1972, 1975; Kazmin et al., 1978). The Lower Complex is characterized by multiply deformed and metamorphosed high-grade gneisses, migmatites and associated granulites. These rocks are considered as the northern continuation of the basement system of Kenya, northeast Uganda and southeast Sudan. The Middle Complex consists of psammitic and pelitic metasediments. The Upper Complex is comprised of low-grade island-arc ophiolitic association of late Proterozoic age. Hence the MB corresponds to Lower and Middle Complex and the ANS correlated to the Upper Complex in Ethiopia. This approach is no longer applicable by recent geochronological works (Ayalew et al., 1990; Ayalew and Gichile, 1990; Teklay et al., 1993) argue against basement - cover relationship. The high-grade rocks such as the Konso granulites, which were previously

considered to be Archean are found to be the root zone of the Neoproterozoic - Pan - African collision event. Hence the traditional classification of the Precambrian rocks of Ethiopia into an Archean cratonic basement and Proterozoic mobile belt, is therefore modified and a two fold classification is adopted (Worku, 1996): i. the reworked early - or pre - Pan African crust and ii. the Pan - African juvenile crust. The recent geochronological studies in the ANS of Saudi - Arabia, Egypt, Sudan, Ethiopia and the MB of Kenya gave late Proterozoic ages and Kroner (1993) concluded that the ANS and the MB are mostly juvenile crust developed during the Pan - African Orogenesis.

The rocks of southern Ethiopia (Fig. 4) can be subdivided into two major lithologic domains separated by major tectonic boundaries (Worku, 1996): i. the gneiss and schist domain, a complex and heterogeneous association of high grade, poly deformed and metamorphosed granitoid gneisses, pelitic and psammitic gneisses/schists migmatites and associated mafic - ultramafic schilern and enclaves, all of which are intruded by syn- to post-collision granitoids, ii. low-grade metavolcano-sedimentary successions and associated mafic - ultramafic complexes forming distinctive N-S trending belts (Fig. 4).

In the Adola area the rocks of the Adola Group (altered ultramafic and mafic rocks) crop out in the two N-S striking areas known as the Adola and Kenticha zones (Fig. 4; Kazmin, 1976). According to Kazmin (1976) the Kenticha zone consists of two parallel belts of talc and talc-serpentine rocks extending for atleast 60 kms along strike. East of the Kenticha ultramafic mass these rocks are incontact with metasediments of Wadera Group (Kazmin, 1976). It seems also altered ultramafic is mainly concentrated in the eastern part of the belt, where bodies of serpentinized peridotites such as those at Lolotu and Big and Small Dubicha occur.

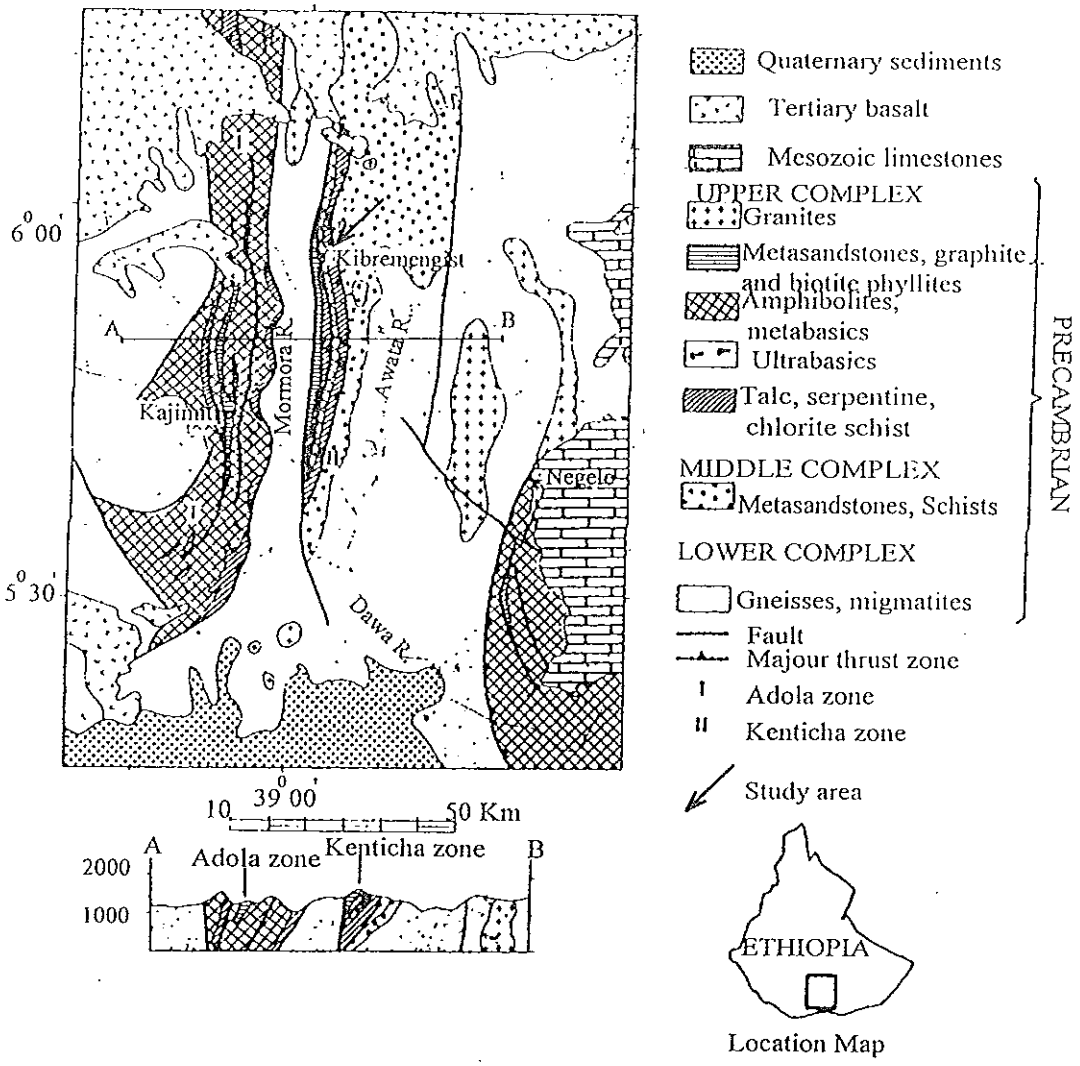

Figure 4. Geological sketch - map of the Adola area (After Kazmin, 1976).

2.2. Geology of the project area

Mappable lithologic units within the Big Dubicha metaultramafic mass and its surrounding consists of:

- quartz vein (Qv)
- tremolite - actinolite - talc - serpentine schist (Ttss)
- talc schist (Ts)
- chlorite schist (Cs)
- biotite - muscovite - quatrz schist (Bmqs)

2.2.1. Lithology

2.2.1.1. Biotite - muscovite - quartz schist (Bmqs)

This unit is mainly exposed in the northeastern part of the mapped area (Fig. 5). It occupies the top of the ridges. The unit is gray to greenish gray in colour (CI = 0 - 20), but the gray varieties are dominant. It is often medium grained, lepidoblastic and composed of quartz (40 - 50 %), muscovite (25 - 30 %), biotite (0 - 20 %), opaque minerals (0 – 20 %), plagioclase (0 – 5 %) and microcline (0 – 5 %). But at one locality (sample Nº TDB - 100); (Fig. 7), it is biotite free quartz - muscovite schist. The distribution and abundance of quartz and muscovite is so heterogeneous which is evident at the scale of a thin - section. The unit is weakly to strongly foliated, with N 30^0 E strike and 35^0 dip to NW (Fig. 5). The foliation is marked by alternating thin layers of biotite and muscovite on one hand and on the other hand quartz (Plate 2). Quartz veinlets and stringers criss - cross this unit at macro - and micro scale. Opaque minerals are also seen forming a network of veinlets.

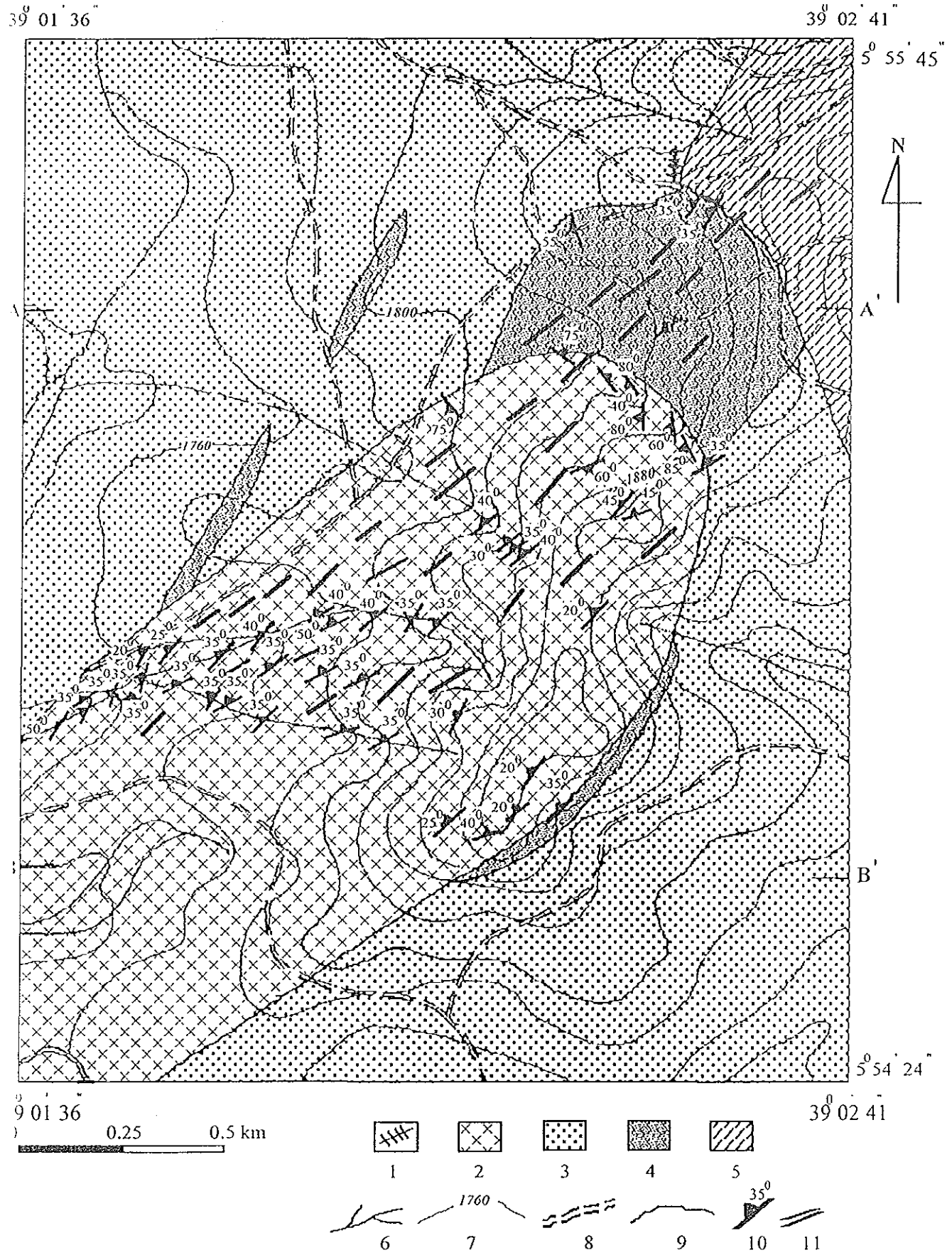

Figure 5. Geological map of Big Dubicha area. 1) Quartz vein 2) Tremolite - actinolite - talc - serpentine schist 3) Talc schist 4) Chlorite schist 5) Biotite - muscovite - quartz schist 6) Stream 7) Contour 8) Foot trail 9) Lithologic contact 10) Strike and dip of foliation 11) Strongly deformed zone

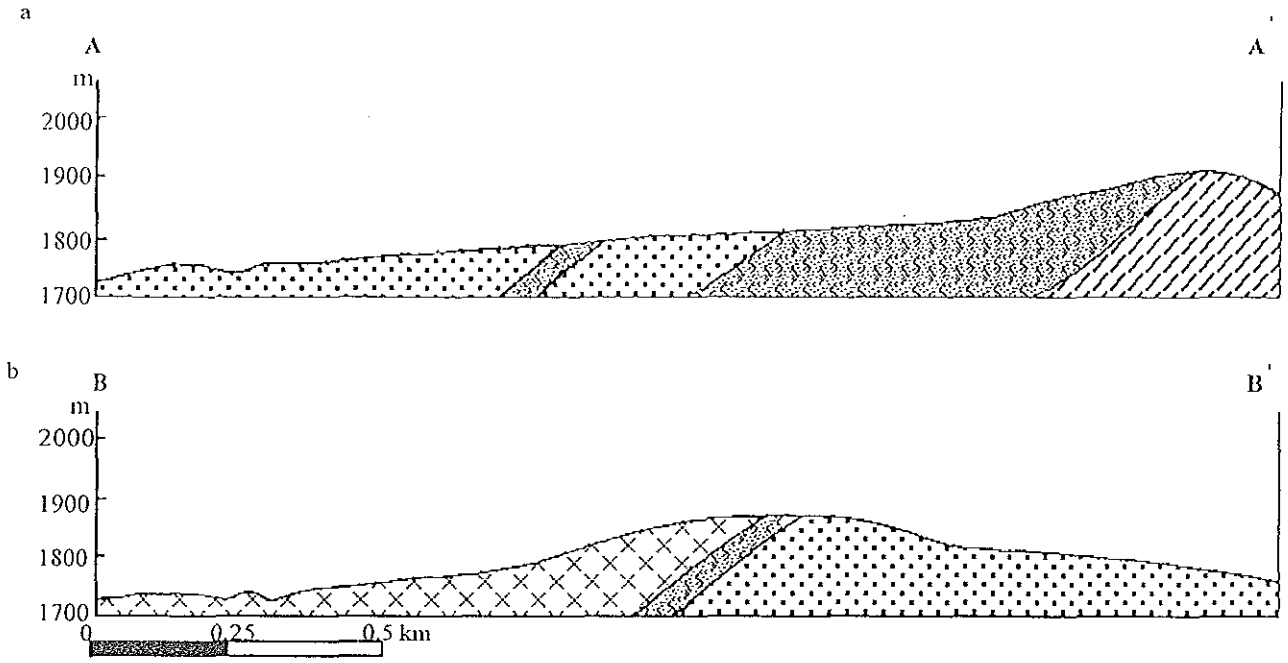

Figure 6. Geological cross section of Big Dubicha area. a) from A to A'
b) from B to B'

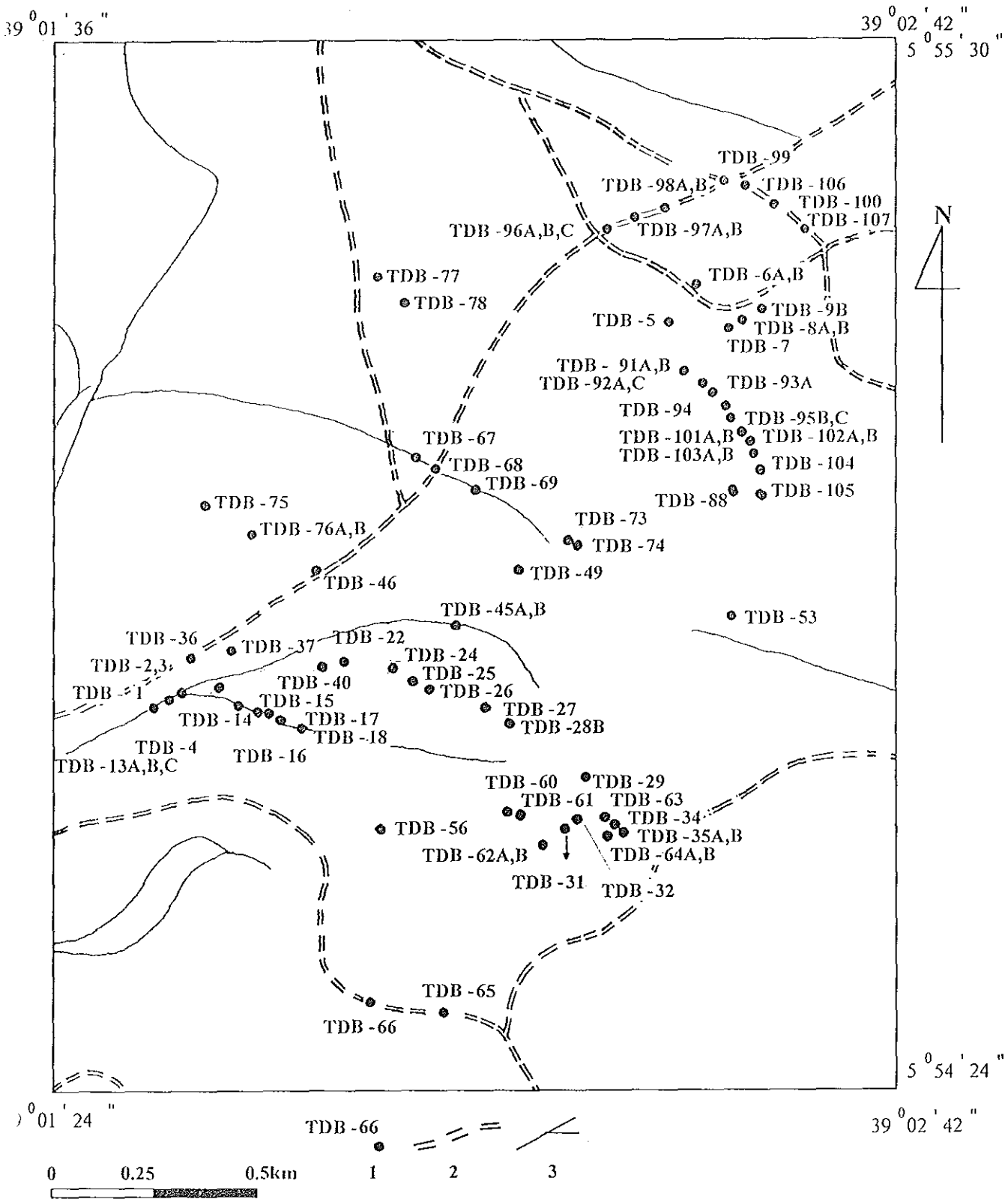

Figure 7. Rock sample location map of Big Dubicha area. 1) Rock sample location 2) Foot trail 3) Stream.

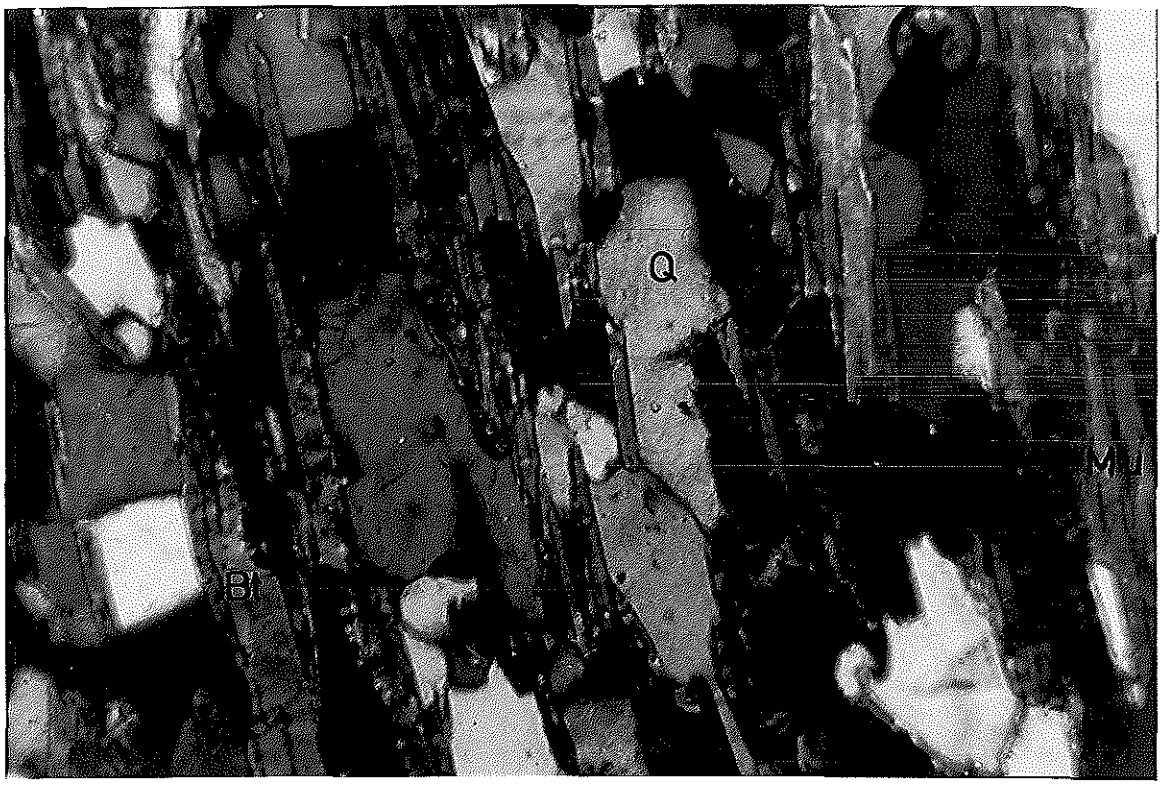

Plate 2. Schistosity in biotite - muscovite - quartz schist defined by, quartz (Q), muscovite (Mu) and biotite (Bt). Crossed nicols, magnification (20X).

2.2.1.2. Chlorite schist (Cs)

It is exposed mainly in the northeastern part of the Big Dubicha area (Fig. 5), as pockets and lenses within the talc schist unit. Outcrops are found frequently on the ridge tops; the flat topography is characterized by thick soil cover with some floats and fragments of the same.

The unit varies in color from greenish gray, light green to a dark green dominant variety (CI = 80 - 98 %). It is fine to medium grained and contain large crystals of euhedral magnetite (from mm to 2 cm). The distribution and abundance of magnetite crystals is significant in the lenses and pockets of western chlorite schist. The unit is composed of chlorite (45 - 98 %), tremolite – actinolite (0 – 43 %), magnetite (0 - 30 %), quartz (0 - 10 %) and epidote (0 - 3 %). The disseminated magnetite crystals sometimes have characteristic octahedral shape (Plate 3). In places the magnetite crystals also form microveinlets (Plate 4). Along its contact with tremolite - actinolite - talc - serpentine schist, chlorite schist has variable composition: chlorite (45 - 70 %), tremolite - actinolite (20 - 43 %), and talc (0 - 10 %) forming tremolite - actinolite - chlorite schist (sample Nº TDB - 92 A, TDB - 93 A, TDB - 101B; Fig. 7). Petrographic studies of sample Nº TDB - 103B showed hornblende (65 %), chlorite (25 %), actinolite (10 %), trace quartz and opaque minerals forming actinolite - chlorite - hornblende schist. Chloritization is prominent alteration feature observed in both hand specimens and thin - section. The unit is massive to weakly foliated; though it is very difficult to measure, the strike of the foliation varies from N - S to N 30^0 E with 35^0 dip angle to west (Fig. 5).

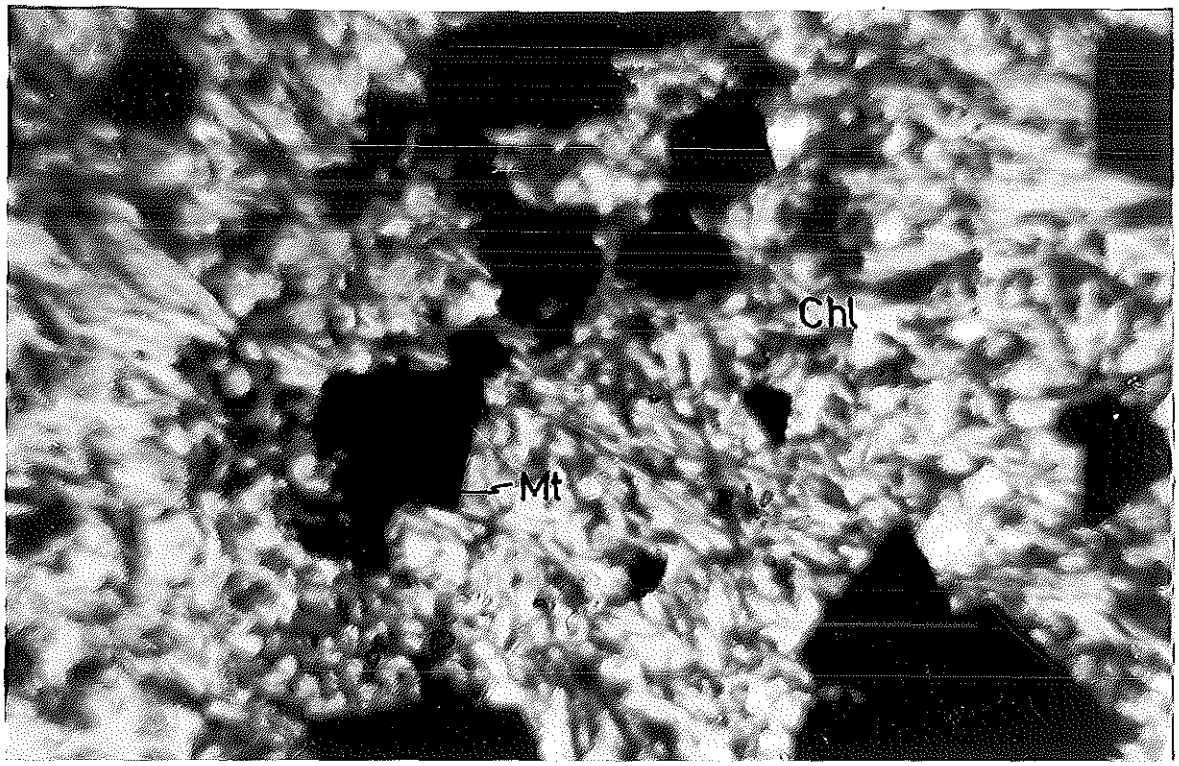

Plate 3. Disseminated magnetite crystals in chlorite schist ground mass, magnetite (Mt) and chlorite (Chl). Crossed nicols, magnification (4X).

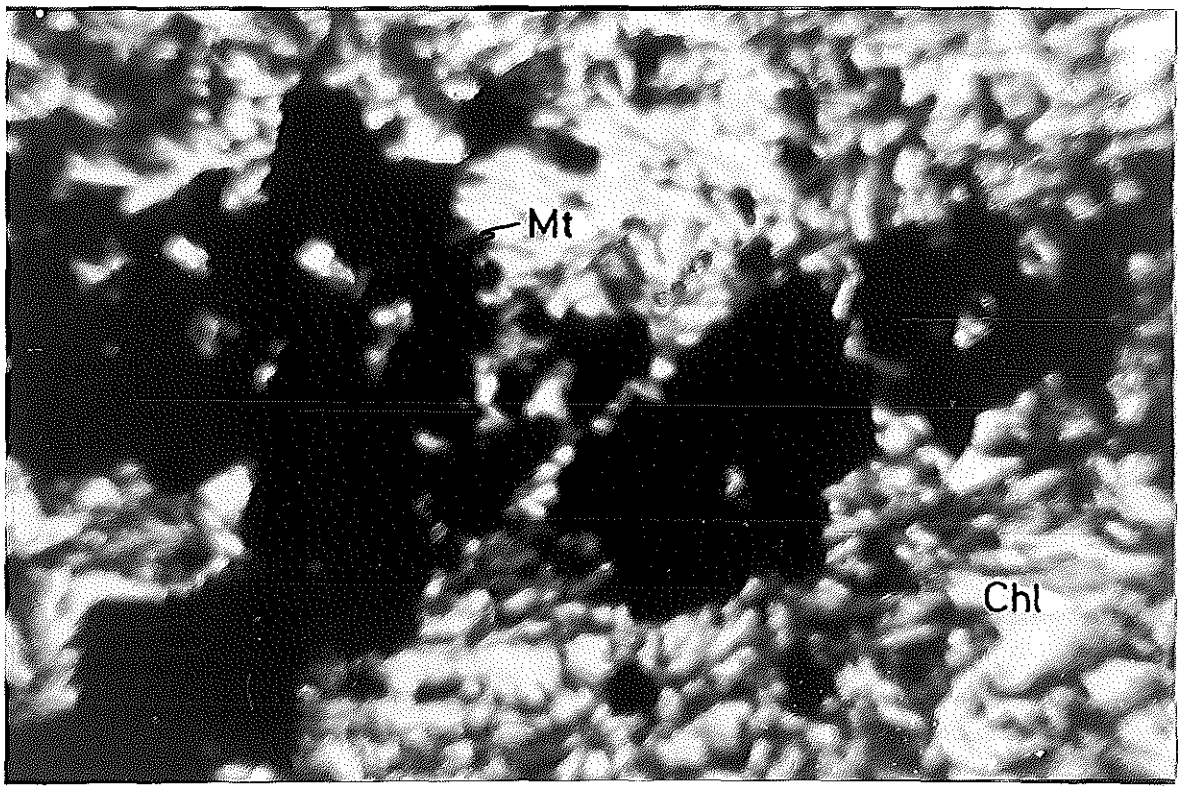

Plate 4. Magnetite microveinlet in chlorite schist ground mass, magnetite (Mt) and chlorite (Chl). Crossed nicols, magnification (4X).

2.2.1.3. Talc schist (Ts)

This unit is exposed in the northern, western and eastern part of the ridge (Fig. 5). It is exposed along ridge tops, slopes and the surrounding flat lying areas. Only small outcrops are preserved due to strong weathering. The talc schist unit contain pockets and lenses of chlorite schist which bear well developed magnetite crystals. The contact with tremolite - actinolite - talc - serpentine schist is marked by a relatively well developed soil covered by sparse vegetation (Plate 5).

The colour of this unit varies as: greenish gray, yellowish green and yellowish gray, but the last one is the most predominant. The greenish colour prevails along its contact with the chlorite schist and tremolite - actinolite - talc - serpentine schist. The unit is fine to medium in grain size, with characteristic silky luster. It is composed of talc (80 - 95 %), tremolite - actinolite (1 - 40 %) and opaque minerals (0 - 20 %). The opaque minerals are euhedral with some octahedral crystal forms (Plate 6) and some with aligned patterns. The unit is weakly to strongly schistosed, and the strike of the lithology varies from N 20 ^{0} W, N 10^0 W, N - S, N 30^0 E to N 50^0 E, dipping 35^0 towards northwest (Fig. 5). The modal composition of this unit is: talc (68 %), chlorite (30 %), magnetite (2 %) forming chlorite - talc schist (sample Nº TDB - 65). Samples taken from the northern contact with serpentine schist (sample Nº TDB - 101A, TDB - 102A) has a variable composition as talc (48 - 75 %) and tremolite - actinolite (25 - 40 %) forming tremolite - actinolite - talc schist. In all cases, tremolite - actinolites are elongated defining folaition (Plate 7) or form fibrous radiating aggregates.

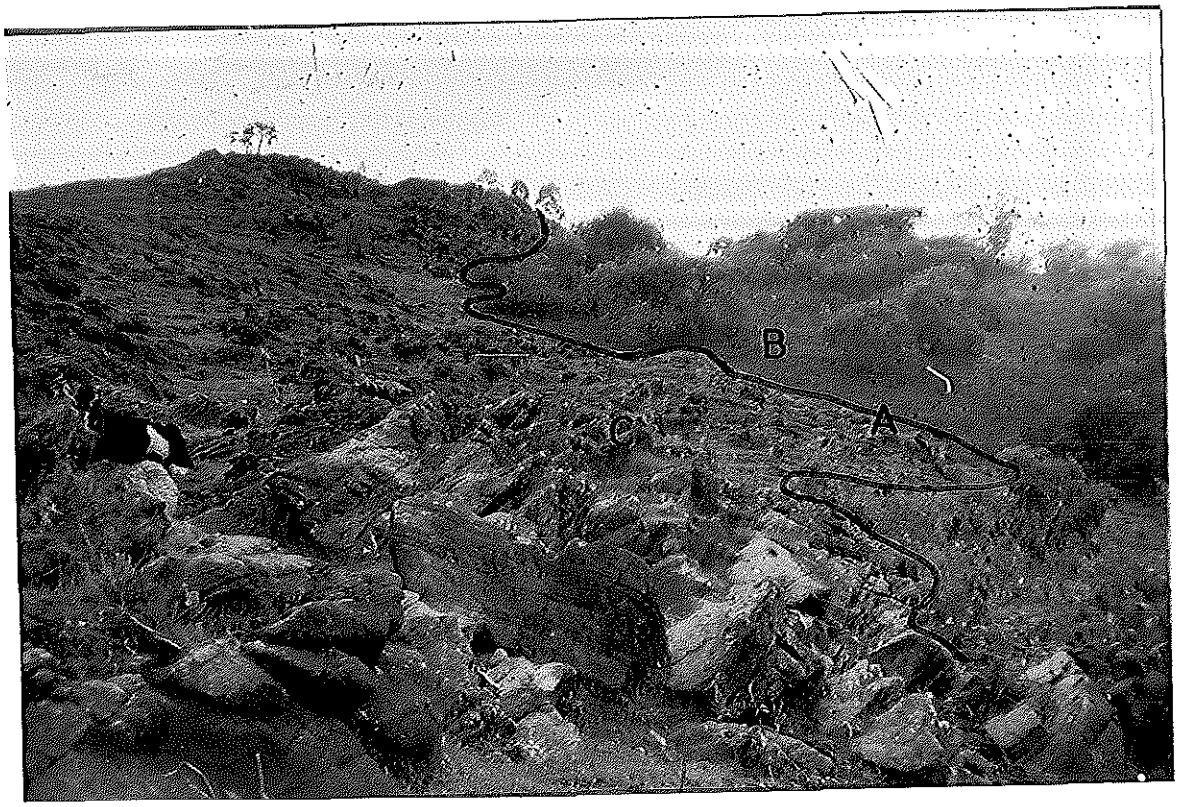

Plate 5. Lithologic contact (A) between, the eastern cholrite schist lense containing talc schist covered by sparse vegetation (B) and bare tremolite - actinolite - talc - serpentine schist (C).

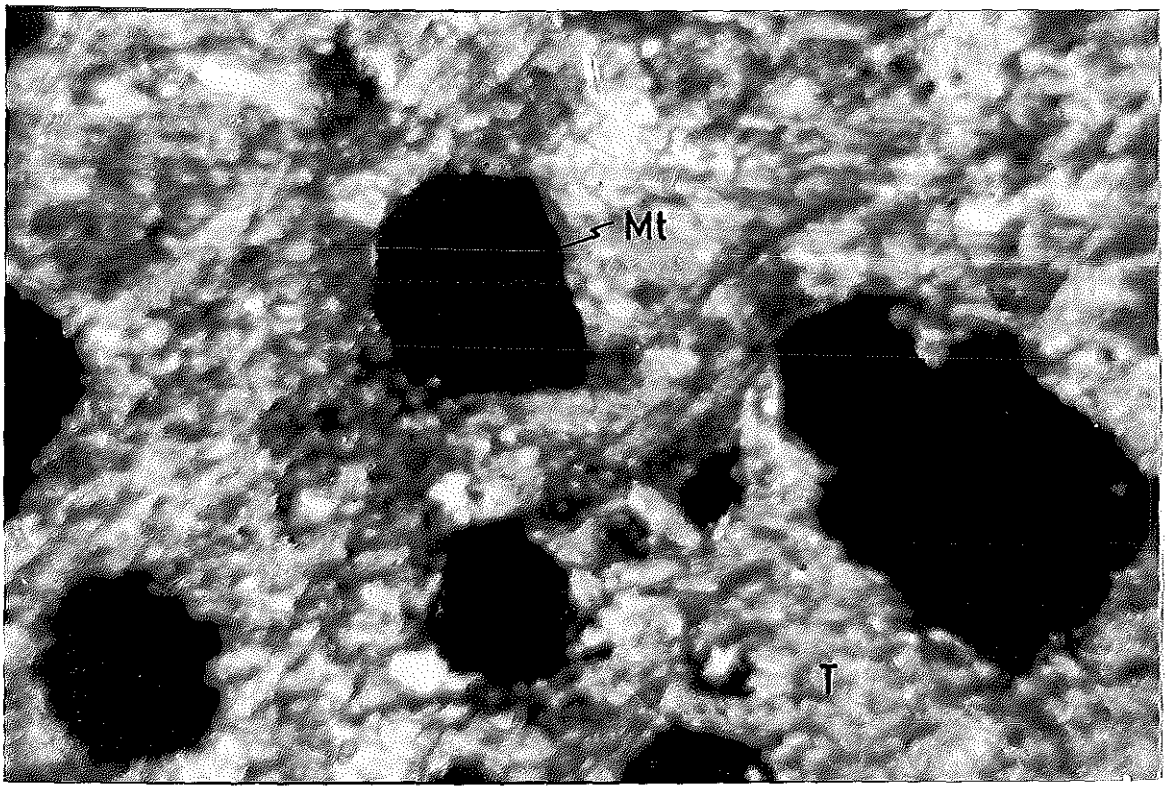

Plate 6. Disseminated magnetite in talc schist ground mass, magnetite (Mt) and talc (T).

Crossed nicols, magnification (4X).

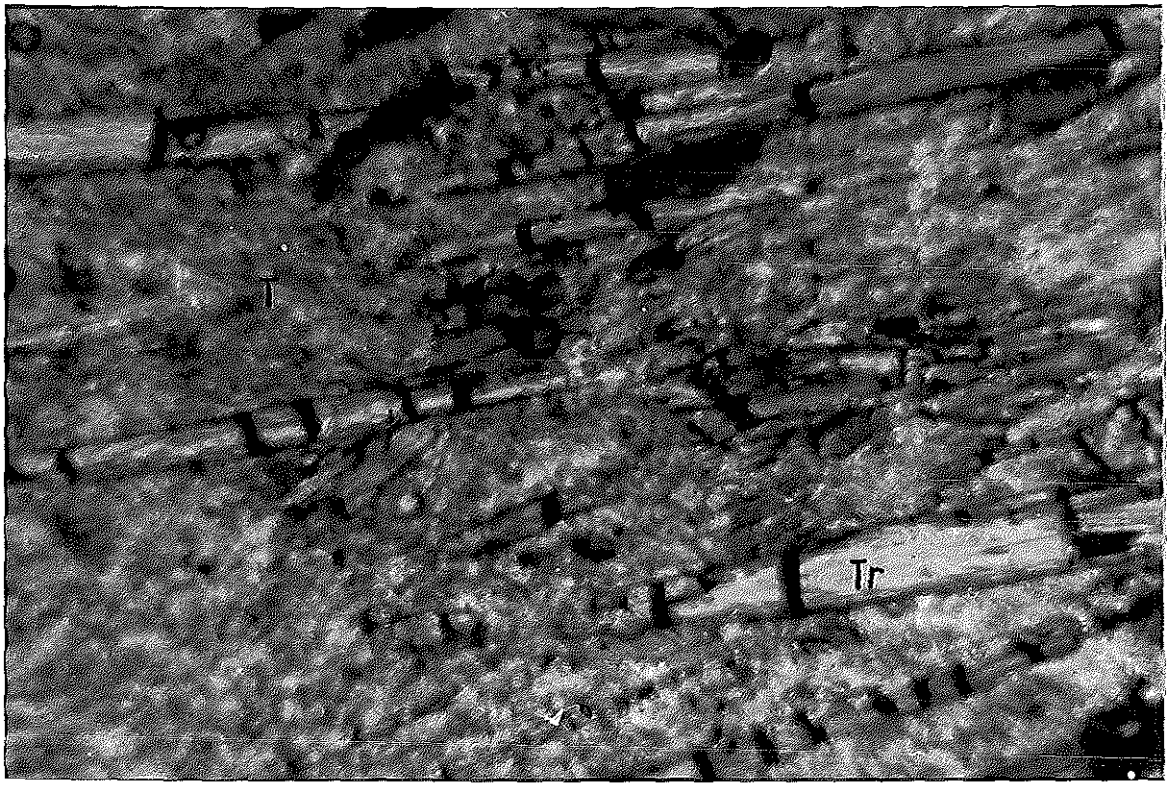

Plate 7. Elongated tremolites defining foliation in talc schist, tremolite (Tr) and talc(T).

Crossed nicols, magnification (4X)

2.2.1.4. Tremolite - actinolite - talc - serpentine schist (Ttss)

This unit covers the southwestern slopes and the crest of the ridge (Fig. 5). It is light green, dark green, greenish gray and yellowish green in colour, with dominant greenish gray varieties; the strongly weathered outcrops have yellowish colour. The unit is fine- to medium-grained, composed of serpentine (50 - 95 %), talc (0 - 30 %), tremolite - actinolite (0 - 20 %), opaque minerals (1 - 20 %) and trace quartz. The southern part of this unit is dominantly serpentine schist with composition, serpentine (85 - 95 %), talc (0 - 10 %), tremolite - actinolite (0 - 5 %) and opaque minerals (0 – 10 %) (sample Nº TDB - 15, TDB - 22, TDB - 32, TDB - 49, TDB - 60, TDB - 63, TDB - 88, TDB - 104). In many of the samples examined tremolite - actinolite is absent forming talc - serpentine schist. Most opaques are anhedral, but minor euhedral octahedral crystals (magnetite ?) are also observed. Fine grained magnetite can be seen in a hand specimen. The opaques form a network of veinlets which are common in the serpentine schist and some of this thin veinlets show staining due to oxidation. Serpentine is altered to talc but usually this alteration is zonal or localized. Talc often forms microveinlets which may be the result of hydration along some planes of weakness. Sample Nº TDB - 74 which is taken from the western part of this unit is composed of olivine (60 %), serpentine (30 %), and talc (10 %), yellowish gray colour, fine grained with mesh fabric, the septa of serpentines isolating the olivine nuclei. It is interpreted as serpentinized dunite (Plate 8). The unit is weakly to strongly schistosed in attitudes of N 40^0 W, N - S, upto N 80^0 E, but dominantly from N 20^0 E to N 30^0 E, and dip of 20^0 to 80^0 (dominantly 20^0 to 35^0) to the west (Fig. 5; Plate 9). But it is massive along the ridge top. Chromite, magnetite and green serpentine mineral (garnierite ?) are found as fracture filling and dissemination along strongly deformed and serpentinized part of this unit.

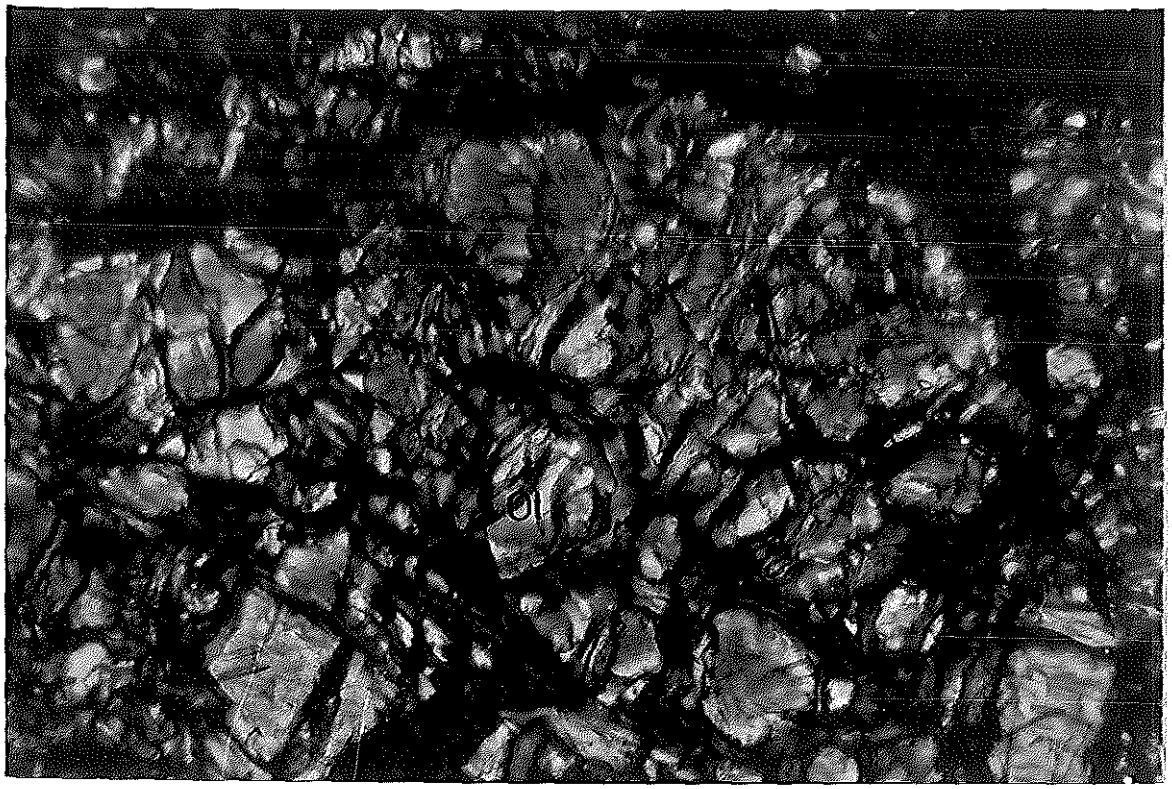

Plate 8. Alteration of olivine to serpentine in serpentinized dunite (TDB - 74), olivine (Ol) and serpentine (S). Crossed nicols, magnification (10X).

Plate 9. Westward dipping strongly deformed tremolite - actinolite - talc - serpentine schist.

2.2.1.5. Quartz Vein (Qv)

N - S trending dirty, milky white, glassy and sugary, about 20m wide and 30m long discontinuous quartz vein crops out mainly along the foot trails in the northwestern part being hosted by the talc schist. A milky white, glassy quartz vein fragments also occur along the contact between the biotite - muscovite - quartz schist and talc schist. In places the vein fragments are pegmatitic with potassic feldspar and quartz, and with illmenite crystals.

2.2.2. Structures

Both planar (foliation and fractures) and linear (mineral aggregate lineation) features were observed in the mapped area.

The foliation surfaces have a characteristic attitude of a N - S, NNE - SSW and NNW - SSE, strike directions and a shallow dip angle of (20^0 - 35^0) to W (Fig. 5). There are local variation due to later deformational features. It is marked by alignment of serpentine, chlorite, tremolite - actinolite and talc. In biotite - muscovite - quartz schist by alignment of biotite, muscovite, recrystallyzed and aligned quartz grains. Two sets of joints are present: N – S and E – W affecting almost all mapping units. The former joint set is seen cut by the latter. Hence the N – S joint set is older than the E – W joint set.

Mineral aggregate lineation is well developed in the southwestern part of the tremolite - actinolite - talc - serpentine schist on the polished surfaces (for example TDB - 4; Fig. 7). The lineation is made of an aggregate of tremolite, actinolite, talc, serpentine. Average linear attitude is measured at 270^0 / 30^0 (direction of plunge/ amount of plunge).

According to many works in the region (for example Kazmin, 1976; Woldehaimanot, 1995; Worku, 1996 and Yihunie and Tesfaye, 1998) and recognition of shallow angle westward dipping foliation during current mapping, may indicate the presence of thrust in an eastward tectonic transport direction. The works of Kazmin, 1976; Woldehaimanot, 1995; Worku, 1996; Yihunie and Tesfaye, 1998 suggest that this thrusting resulted in the obduction of metaultramafic slices of the Kenticha belt, which includes the study area onto the eastern high grade block along the Kenticha thrust front.

2.2.3. Metamorphism

From petrographic study and field observations the following metamorphic mineral assemblages and associated predominant alterations have been identified in altered ultramafic rocks of the Big Dubicha area:

Chlorite schist: **chlorite ± tremolite - actinolite ± epidote ± hornblende ± quartz**

Prediminant alterations: **chloritization (transformation of hornblende and tremolite - actinolite to chlorite)**

Talc schist: **talc + tremolite ± chlorite ± quartz ± serpentine**

Predominant alteration: **chloritization (alteration of tremolites to chlorite) and further hydration of serpentines to talc**

Tremolite - actinolite - talc - serpentine schist: **serpentine + tremolite - actinolite ± calcite ± olivine**

Predominant alteration: **sepentinization (transformation of olivine and tremolite-actinolites to serpentine), further hydration of serpentines to talc and little carbonation.** Here carbonates (calcites) are seen at few places within fractures in the tremolite - actnolite - talc - sepentine schist.

All mineral assemblages listed in all altered ultramafic rocks are consistent with lower greenschist facies, which represent the predominant serpentinization, chloritization and carbonation reactions resulted from low temperature water-rock interactions.

Metamorphic evolution of rocks of the region which include the Big Dubicha is described by numerous workers, including Gilboy, 1970; Worku, 1996, Kazmin, 1972; Kozyrev et al.,

1985; Yihunie and Tesfaye, 1998. Accordingly, the Mormora Group is represented by quartz - biotite, garnet - staurolite - quartz - biotite schist with lenses of chlorite and actinolite schist, and has the following mineral aassemblages (Yihunie and Tesfaye, 1998):

a. garnet + staurolite + biotite + muscovite + quartz + kyanite + sillimanite + opaque

b. biotite + microcline + quartz + tourmaline + opaque

c. biotite + microcline + quartz + muscovite

d. staurolite + garnet + biotite + muscovite + quartz + plagioclase

e. garnet + kyanite + sillimanite + K - feldspar + quartz + opaque

The above mineral assemblages are typical to various rock types of the Mormora Group, which are indicative of lower to upper amphibolite facies (Butcher and Frey, 1994). The Wadera Group is represented by quartzofeldspathic mylonite, biotite - plagioclase, microcline - quartz gniess and biotite granite and has the following mineral assemblages (Yihunie and Tesfaye, 1998):

a. microcline + plagioclase (An_{20}) + quartz + biotite

b. microcline + quartz + plagioclase (An_{20}) + biotite + muscovite

c. microcline + plagioclase + quartz + biotite

d. microcline + plagioclase + quartz + biotite

These assemblages are characteristic of the lower amphibolite facies (Butcher and Frey, 1994). As illustrated in the previous section the metamorphism of the study area is represented by assemblages of chlorite, tremolite - actinolite, talc, epidote, serpentine and quartz which indicate lower greenschist facies. Mineral assemblages of the country rocks (Mormora and Wadera Groups) fall within the amphibolite facies. This indicates the allochemical (allofacial) nature of the relationship between the Big Dubicha metaultramafic mass and the country rock (Fig. 8).

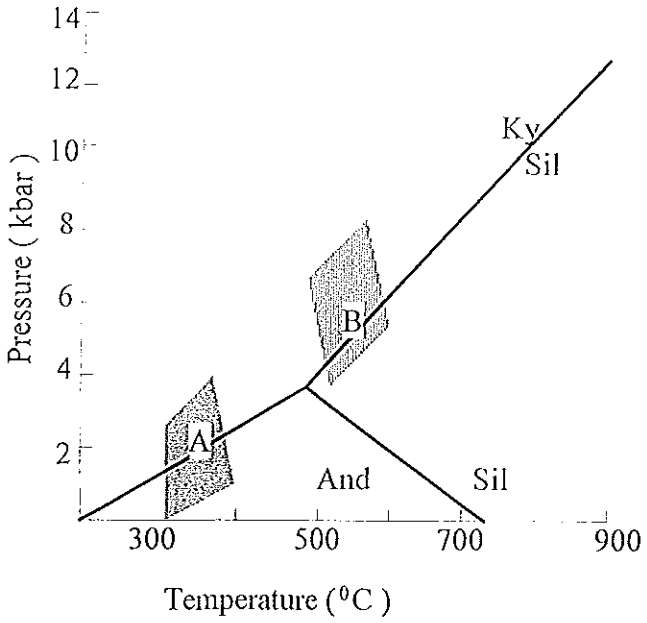

Figure 8. Approximate P - T stablity field for metamorphic mineral assemblages of A) Big Dubicha metaultramafics and B) country rock.

CHAPTER 3 - WHOLE ROCK GEOCHEMISTRY

Whole rock analysis of eighty three samples of altered ultramafics and three biotite - muscovite - quartz schist was conducted using an X-ray fluorescence (XRF) at Dipartimento di Scienze della Terra, University of Perujia, Italy. The result of the analysis is presented in this chapter; the location of the samples is given in Fig. 7 and the analytical data is presented in Appendix 4.

Theoretically once the mineral assemblage of rocks has been identified, it is convenient or even compulsory to represent the chemical composition of the minerals that constitute the assemblage on a chemography (a composition phase diagram). Composition phase diagram can be used to document the assemblages found in rocks of a given metamorphic terrain, such diagrams are an indispensable tool in the analysis of metamorphic characteristics and evolution of a terrain. The variables on the diagrams are concentrations or amounts of chemical entities. All other variables that control the nature of stable minerals must be constant. Compositional phase diagrams are isothermal-isobaric diagrams. It is useful to change the scale of the compositional variables from wt. % to mol %, mole fraction or mole numbers. Most chemographies use mol % or mole fraction as units for the composition variables. Ultramafic rocks consist predominantly of ferromagnesian silicates. Olivine, orthopyroxene and clinopyroxene dominate the modal composition of anhydrous ultramafitites. Most ultramafics contain hydrates (amphiboles, sheet silicates etc.) and very often carbonates. Therefore, H_2O and CO_2 must be added to the set of components in order to describe phase relationships in partially or fully hydrated (and/carbonated) versions of olivine + orthopyroxene + clinopyroxene rocks. The CaO - MgO - SiO_2 - H_2O - CO_2

(CMS-HC) system or subsystems thereof is adequate for discussion of metamorphism of ultramafic rocks. Hence here also CaO - MgO - SiO_2 - H_2O - CO_2 (CMS-HC) system is used to plot the analytical data to approximate the anhydrous mineralogy of the metaultramafics of the Big Dubicha area.

The objective is according to Butcher and Frey (1994): mantle fragments beneath the oceanic crust are often lherzolitic in composition and mantle fragments from subcontinental mantle occur in rock associations typical of continental crust, such ultramafitites are usually of harzburgitic (dunitic) in composition.

3.1. Tremolite - actinolite - talc - serpentine schist

The SiO_2 content ranges from 39.24 - 56.27 wt. %, Fe_2O_3 3.82 - 8.82 wt. %, Al_2O_3: from 0.17 - 2.37 wt. % and MgO: 24.72 - 40.78 wt. %. The high SiO_2 values of some samples may have resulted from secondary silicification processes. The concentrations of Ni and Cr range from 1412 - 13664 ppm and 1449 - 3693 ppm respectively; high values of Ni and Cr (e.g. Ni = 250 - 300 ppm, Cr = 500 - 600 ppm) indicate their derivation from mantle peridotite (Wilson, 1989). But the indicated very high values may be resulted from latter lateritic enrichment processes. Whole rock geochemical data examined in the system CaO - MgO - SiO_2 - H_2O - CO_2 for a tremolite - actinolite - talc - serpentine schist samples dominantly show harzburgitic anhydrous mineralogy (Fig. 9). According to Butcher and Frey (1994) they are part of tectonically implanted subcontinental mantle lithosphere. In MORB - normalized trace element distribution pattern (Fig. 11); generally low values are seen in high field strength elements (HFSE) (Y, Zr and Nb) and large ion lithophile elements (LILE) (Sr, K, Ba and Rb).

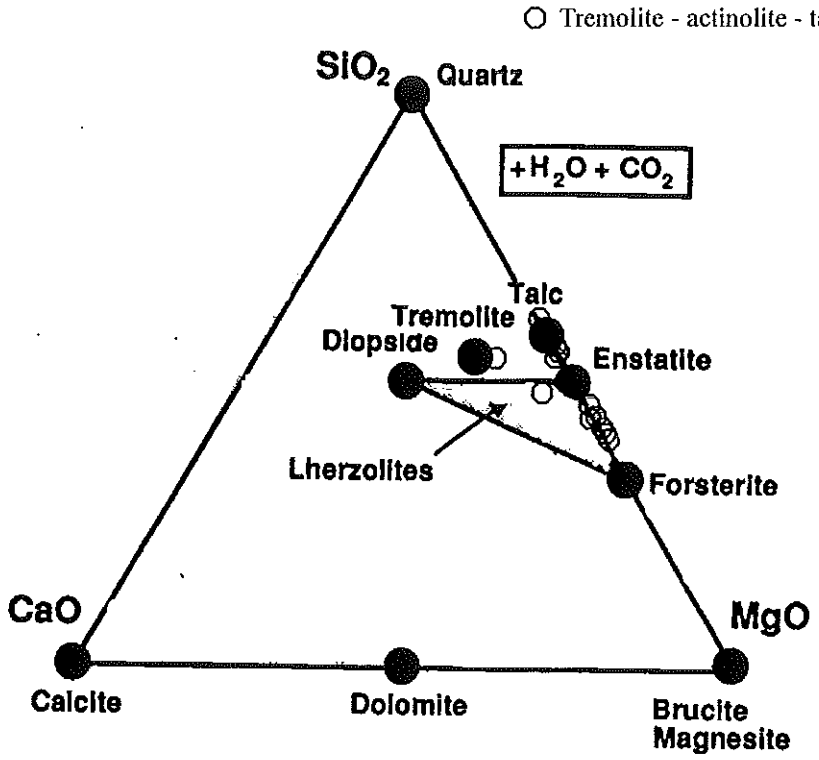

Figure 9. Chemography of tremolite - actinolite - talc - serpentine schist in the CaO-MgO-SiO_2-H_2O-CO_2 (CMS-HC) system (After Bucher and Frey, 1994).

Low in LILE may indicate the absence magmatic process that could have been resulted from continental process. The samples show positive Cr and Th anomaly. High Cr values indicate peridotitic mantle source, containing chromite, magnetite and pyroxene among others. Th positive anomaly is may be due to the supergene enrichment that is contributed from the continental crust.

3.2. Talc schist

A widespread in SiO_2 content (29.37 to 61.46 wt. %) is observed and most values are above 55 wt. %. This signifies the irregular silicification processes. With Fe_2O_3 content ranging from 2.8 - 11.34 wt. % and high MgO values (23.82 - 24.13 wt. %) correlates with modal talc. The CaO - MgO - SiO_2 - H_2O - CO_2 plot of the talc schist samples fall mostly out of the lherzolite composition triangle and lie along the edge with talc and enstatite end member minerals (Fig. 10). The anhydrous mineralogy could be pyroxenite and / or lherzolite. The trace element distribution pattern (Fig. 12) is similar to that of tremolite - actinolite - talc - serpentine schist.

3.3. Chlorite schist

The SiO_2 content varies between 22.55 - 40.85 wt. %, and the Fe_2O_3 content is between 8.14 - 18.54 wt. %. The latter may be related to the presence of abundant magnetite. The values of Al_2O_3 is between 11.1 - 20.11 wt. % and directly correlates with the amounts of amphiboles. MgO vary between 24.51 - 26.32 wt. % which is related with the ubiquitous chlorite. The TiO_2 content of this unit is relatively higher than the other units which vary

between 0.07 - 2.99 wt. %; the high values reflect the presence of illmenite and rutile. Chemographic representation in the system CaO - MgO - SiO_2 - H_2O - CO_2 (Fig. 13) approximate dunitic to harzburgitic anhydrous mineralogy, which may be interpreted as the result of obducted subcontinental mantle lithosphere (Butcher and Frey, 1994).

Trace element distribution diagram (Fig. 14) show positive spikes for Y and Th and low values in HFSE (Ti) and LILE (K and Sr). Similar to other lithologies low in LILE may indicate the absence of magmatic process. The unusual Th positive spike despite its high degree of mobility is attributed to supergene enrichment. The high Y value appears to correlate with presence of amphibole.

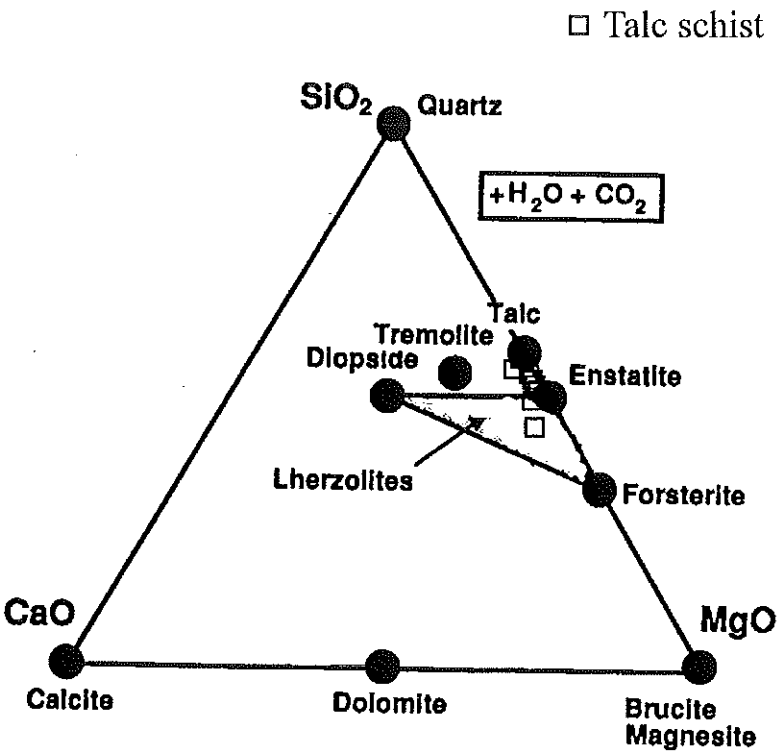

Figure 10. Chemography of talc schist in the CaO-MgO-SiO_2-H_2O-CO_2 (CMS-HC) system (After Bucher and Frey, 1994).

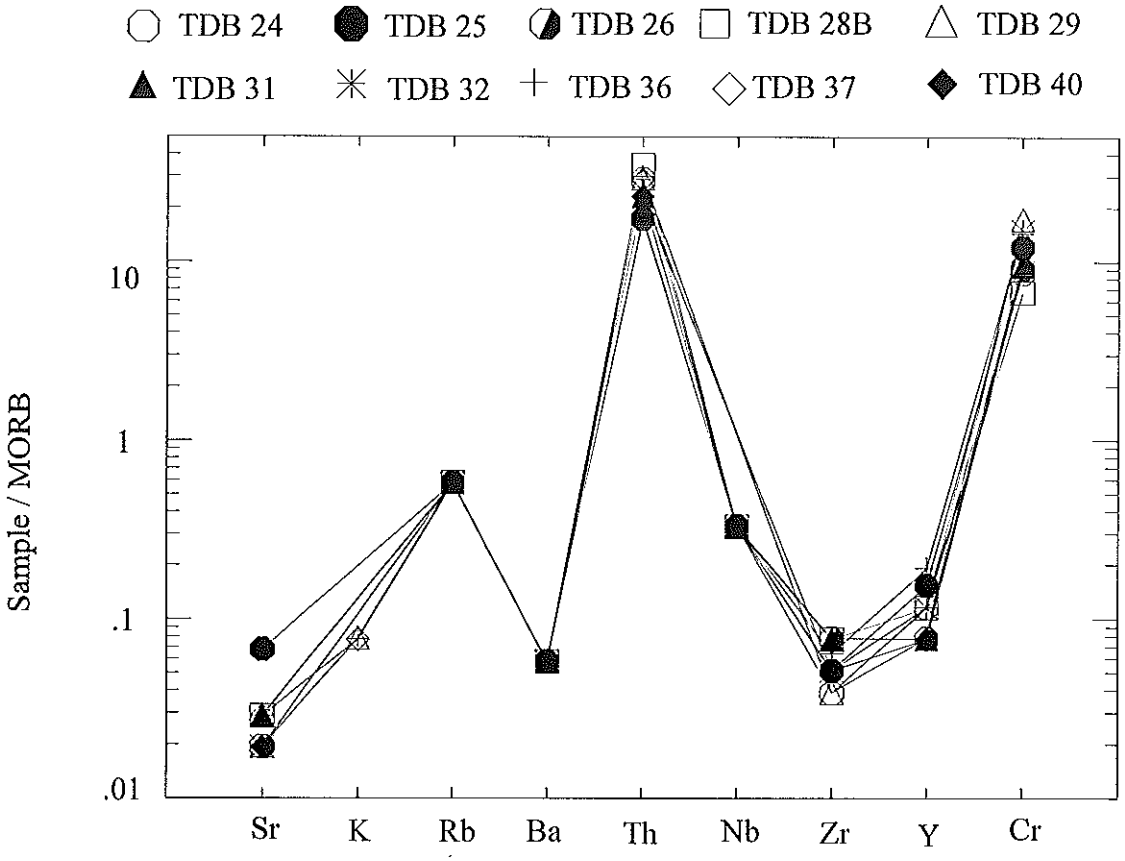

Figure 11. Trace element concentrations in tremolite - actinolite - talc - serpentine schist samples normalized to the composition of average MORB and plotted from left to right in order of increasing compatability. The normalizing values are those of Pearce (1983); Cr from Pearce (1982).

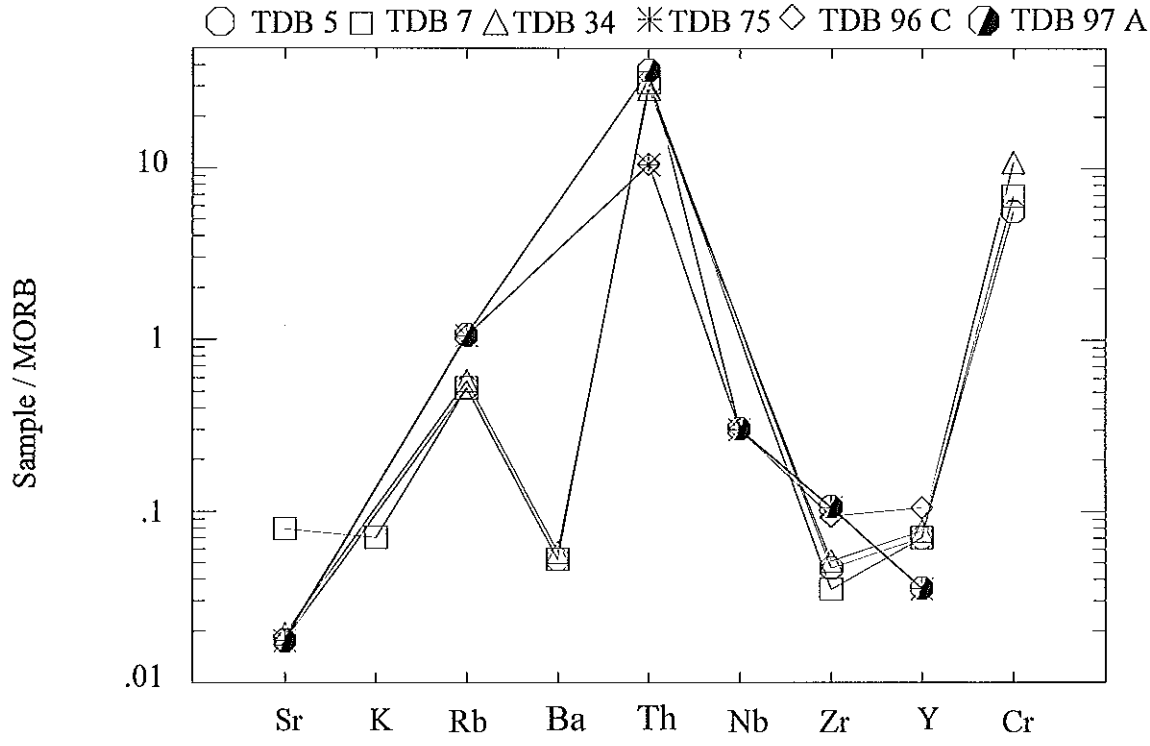

Figure 12. Trace element concentrations in talc schist samples normalized to the composition of average MORB and plotted from left to right inorder of increasing compatability. The normalizing values are those of Pearce (1983); Cr from Pearce (1982).

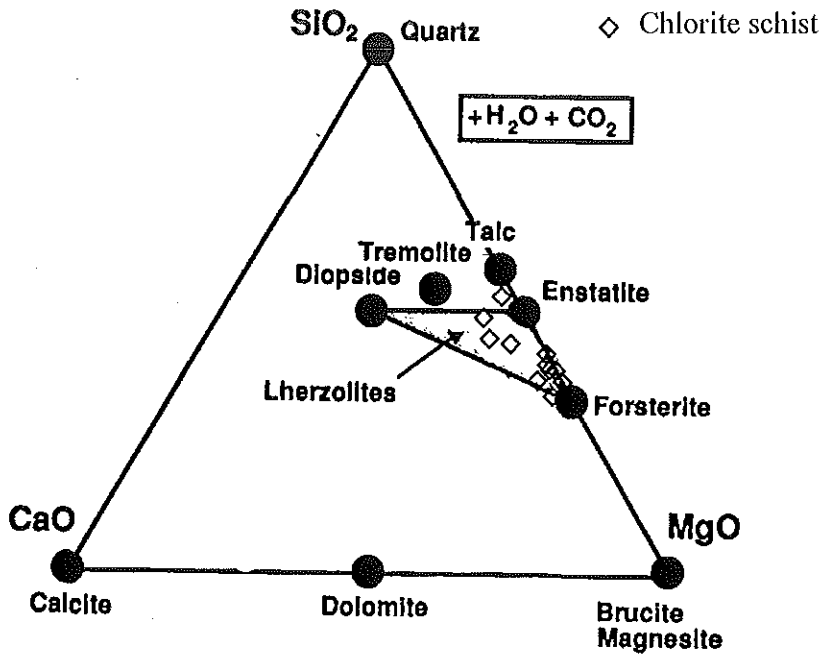

Figure 13. Chemography of chlorite schist in the CaO-MgO-SiO_2-H_2O-CO_2 (CMS-HC) system (After Bucher and Frey, 1994).

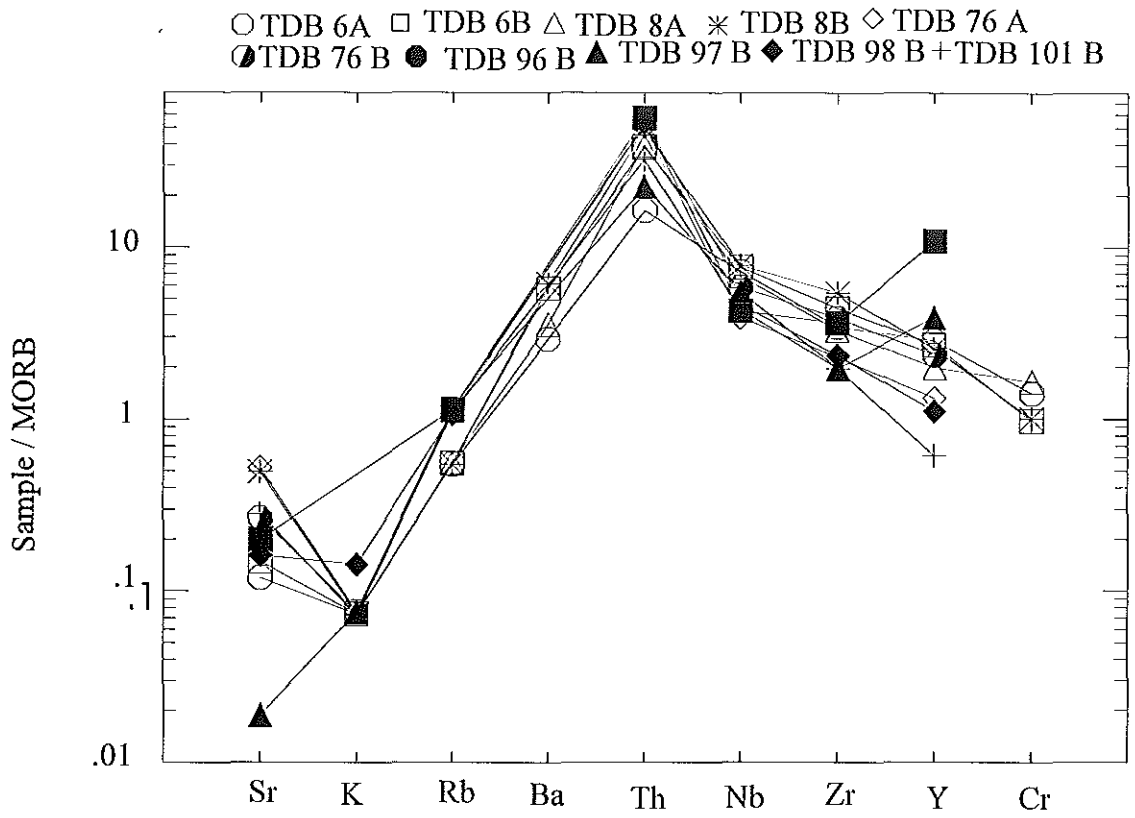

Figure 14. Trace element concentrations in chlorite schist samples normalized to the composition of average MORB and plotted from left to right in order of increassing compatability. The normalizing values are those of Pearce (1983); Cr from Pearce (1982).

CHAPTER 4 - EXPLORATION GEOCHEMISTRY

The aim of this survey is to outline the distribution and concentration of compatible elements with particular emphasis to Ni and Cr. This also helps to understand the primary and/or secondary processes that are responsible for the enrichment or deficiency of elements of economic interest.

4.1. Soil samples - Pedogeochemical Survey

During setting a reconnaissance exploration grid, the base line was cut in the N 30^0 E direction, which is parallel to the general strike direction of the lithologies. The profile lines were cut perpendicular to the base line in a 250m interval along the base line. About 500 gram soil samples were collected in 100m interval from hand dug pits with 30cm average depth along the profile line. Generally the area is characterized by poor development of soil profile. Hence most of the samples are collected from C-horizon. But there are also samples collected from B-horizon (zone of maximum accumulation of elements) within the areas where there is good development of soil horizons. The sampling sites are underlain by chlorite schist, talc schist and tremolite - actinolite - talc - serpentine schist. Twenty five soil samples were collected along the grid and six samples were from random locations outside the grid. The samples were air-dried and kept in plastic bags. The analytical data is discussed in this chapter and the results are presented in Appendix 1. The location of the samples is indicated on Figure 15 and 16.

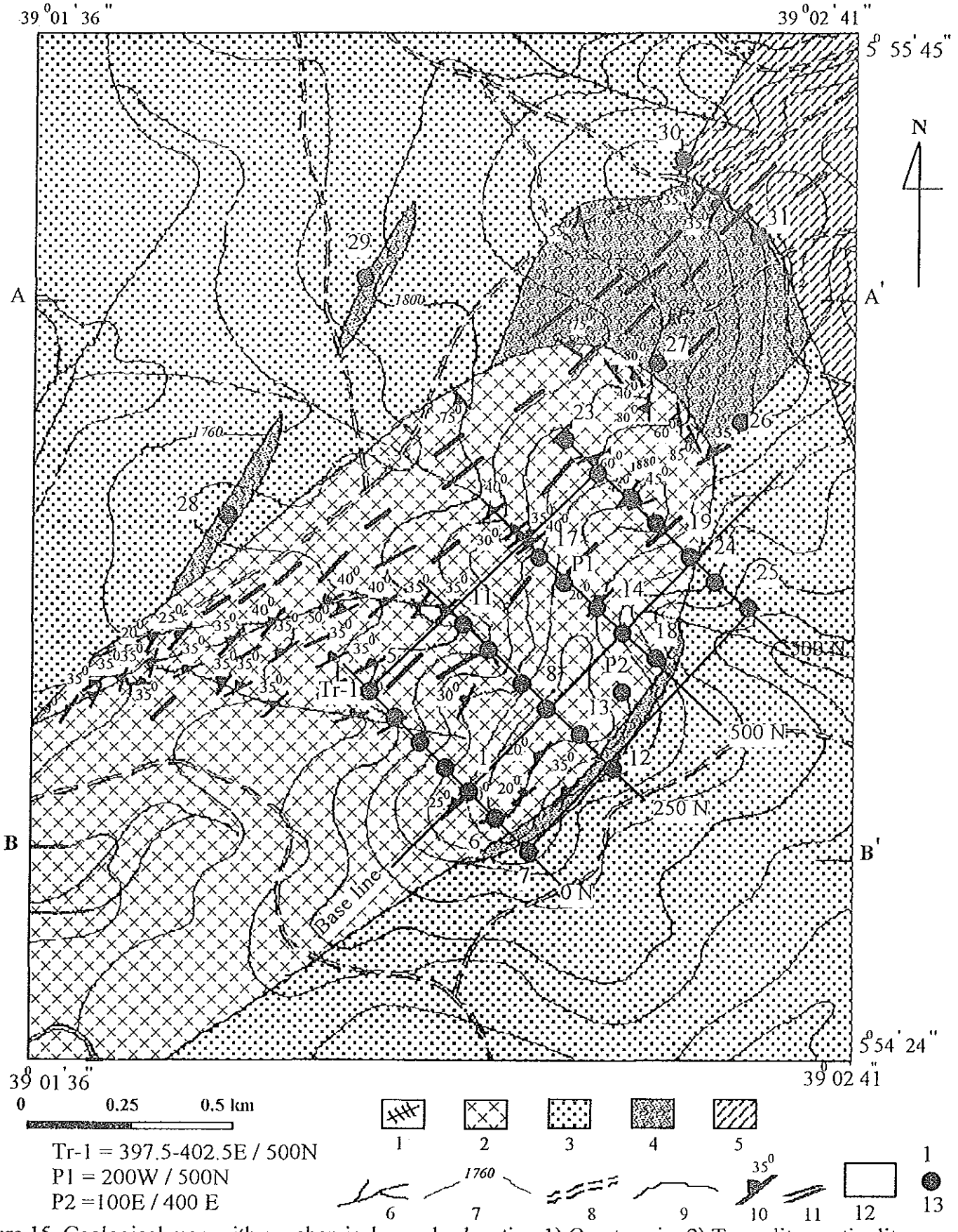

Figure 15. Geological map with geochemical samples location 1) Quartz vein, 2) Tremolite - actinolite - talc - serpentine schist,3) Talc schist, 4) Chlorite schist, 5) Biotite - muscovite - quartz schist, 6) Stream, 7) Contour,8) Foot trail, 9) Lithologic contact, 10) Strike and dip of foliation, 11) Strongly deformed zone, 12) Area covered by systematic soil sampling, 13) Soil sample location.

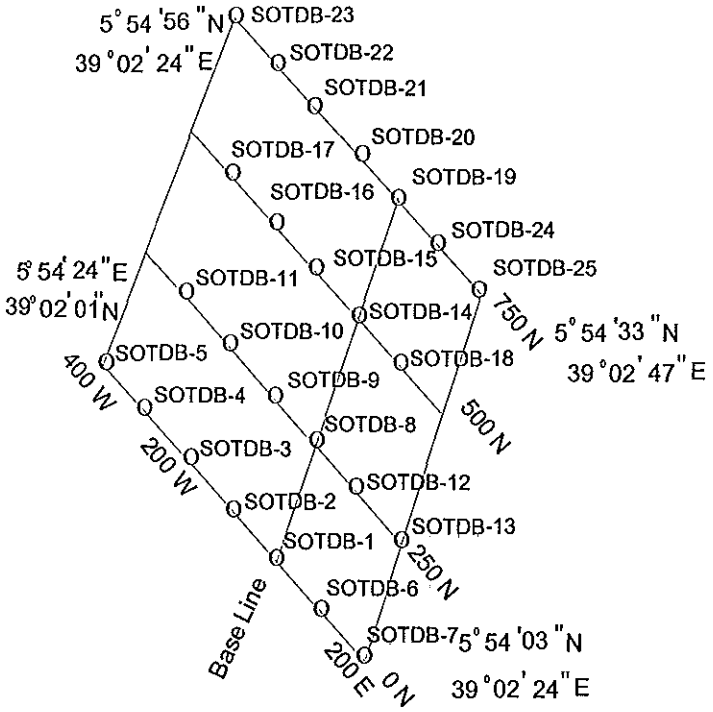

Profile interval = 250m
Sample interval = 100m
Base line orientation = 030^0
Profile line orientation = N 60^0 w
o SOTDB-1 = Soil sample location

Figure 16. Soil sample locations with established grid lines.

4.1.1. Gold (Au)

A total of 25 samples were analyzed for Au among which only two samples were found to contain below the detection limit (0.1 ppm). All the rest showed 0.1 ppm Au (Appendix 1). In addition, from six randomly collected soil samples (underlain by chlorite schist, talc schist and one from close proximity to quartz vein), four samples indicated Au. (Sample Nº SOTDB - 28) which was sampled above the western chlorite schist bedrock depicted 0.2 ppm Au. Average gold content for ultramafic rocks is 0.0032 ppm (Rose et al., 1979). Hence all the detected Au values from both systematic and randomly collected soil samples are above expected value for Au in the ultramafic rocks. Because of the identical analytical values for all samples (i.e. 0.1 ppm), no meaningful pattern of geochemical map can be contoured. All samples are collected from the ridge top to limit the effect of topography and drainage; hence Au associated with Big Dubicha metaultramafic is relatively high or reconcentrated during soil formation.

4.1.2. Cobalt (Co)

For 25 samples collected from the established grid of the Big Dubicha area, two populations were separated using cumulative probability frequency curve (Appendix 2a), i.e. 25 % (lower) and 75 % (upper) population. The threshold of the two populations are 84 ppm (P_1) and 244 ppm (P_2) respectively. From the summary statistics, the mean cobalt value for systematically collected 25 soil samples is 168.12 ppm with 10 ppm and 262 ppm minimum and maximum values respectively, 77 standard deviation (Table 3). The average Co value for

ultramafic rocks is 110 ppm (Rose et al., 1979). Hence the first (lower) population is considered as background and the second (upper) population is taken as anomalous.

Element	Minimum value (ppm)	Maximum value (ppm)	Mean value (ppm)	Standard deviation	Thresholds
Co	10	262	168.12	76.5	P1 = 84.168 P2 = 243.534
Ni	40	9330	5405.36	2652.318	P1= 1225.942 P2= 8352.207
Cu	40	86	19.2	21.333	P1= 7.974 P2 = 35.676
Zn	29	76	46.92	11.310	P1= 37.562 P2 = 58.296
Pb	0.05	10	2.574	2.989	P1 = 1.283 P2 = 7.713
Mn	194	1600	1084.56	389	P1 = 853.211 P2= 1441.608
Cr	33	4100	1947.32	1157.176	P1 = 1547.667 P2 = 3357.351

Table 3. Summary statistics for lognormal distribution of 25 soil samples collected from grided area.

The first (lower) population is associated with the eastern part, underlain by talc schist and containing pockets and lenses of chlorite schist. The second (upper) population, is considered as having anomalous Co value, is mainly underlain by altered tremolite - actinolite - talc - serpentine schist (Fig. 17). Anomalous values (> 220 ppm Co) are observed at grid

coordinates of 200 W – 400 W / 00 N – 500 N (Fig. 17). The anomaly opens towards the west, with similar patterns in the north at 200 W / 750 N; and closed anomaly is found between areas bracketed by coordinates of (00 E – 100 E / 400 N – 500 N). The maximum value 262 ppm is obtained from altered tremolite – actinolite – talc – serpentine schist, sample Nº SOTDB - 18, locality 100 E / 500 N.

A Cobalt values from the six randomly collected samples (five from those overlying chlorite schist and talc schist, and one from quartz vein) is low.

Cobalt generally shows positive correlation with Ni and Mn (Table 4; Fig. 25). The possible explanation for this pattern is that Co is associated with Mg and Ni in ultramafic rocks, and its intermediate mobility is controlled by adsorption and coprecipitation with Mn- and Fe- oxides (Rose et al., 1979). Cobalt also shows moderate positive correlation with Cr and Zn and negative correlation with Cu (Table 4; Figs. 24 and 25).

4.1.3. Nickel (Ni)

Cumulative probability frequency curve plot of nickel for systematically collected 25 soil samples indicates two populations (Appendix 2b) i.e. 20 % (lower) and 80 % (upper), with respective thresholds of 1226 ppm and 8352 ppm. Mean Ni value of the 25 soil samples is 5405.36 ppm, bracketed by minimum 40 ppm and maximum 9330 ppm; standard deviation is 2652 (Table 3). The average Ni content of ultramafic rocks is 2000 ppm (Rose et al., 1979). With the exception of five samples underlain by chlorite schist and talc schist, which are characterized with values below 540 ppm Ni, the rest of the samples obtained from grided

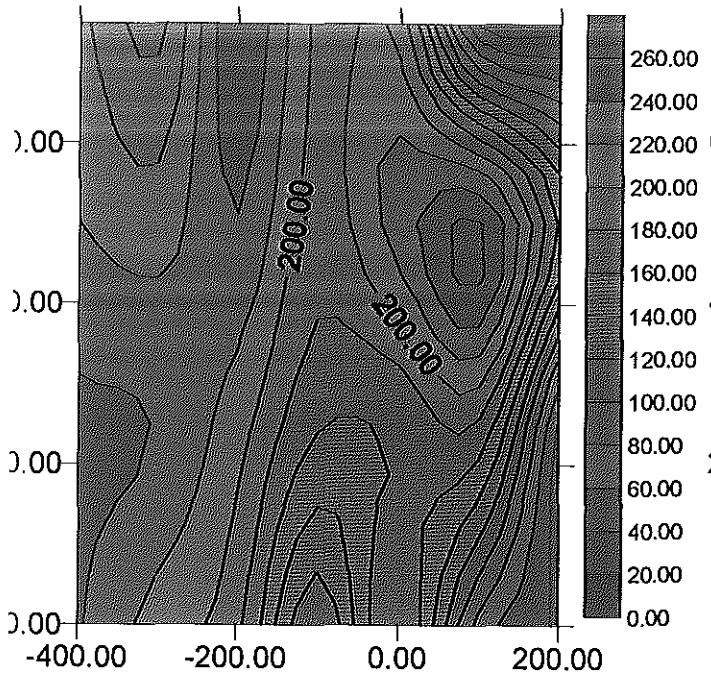

Figure 17. Geochemical map of Co (ppm).

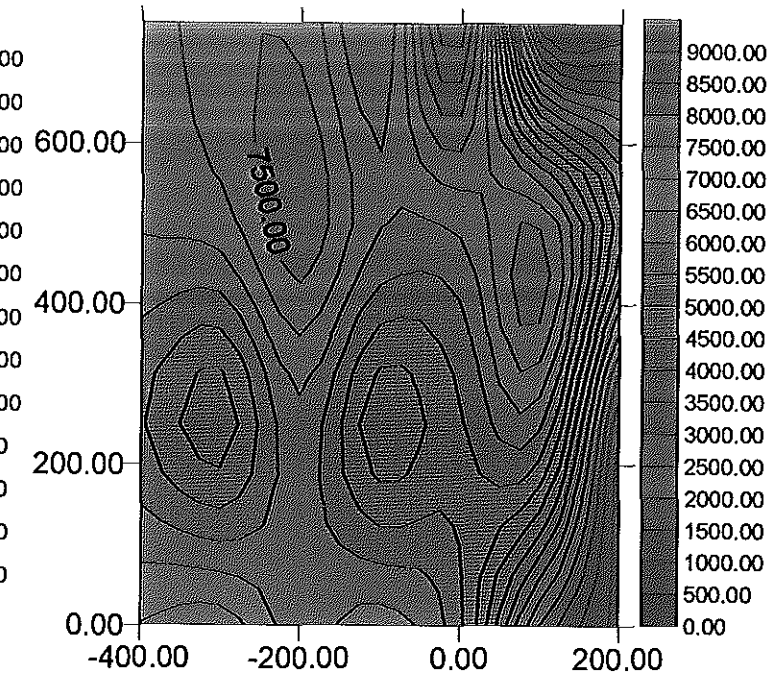

Figure 18. Geochemical map of Ni (ppm)

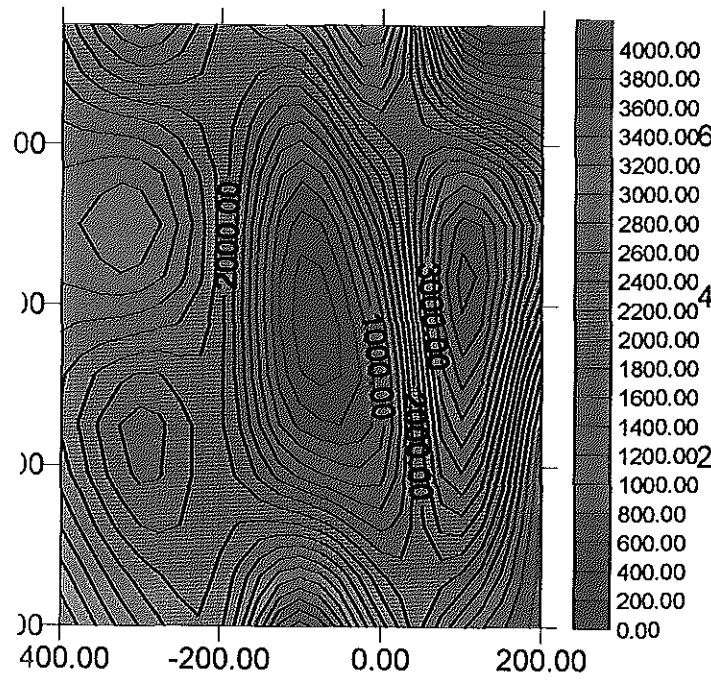

Figure 19. Geochemical map of Cr (ppm)

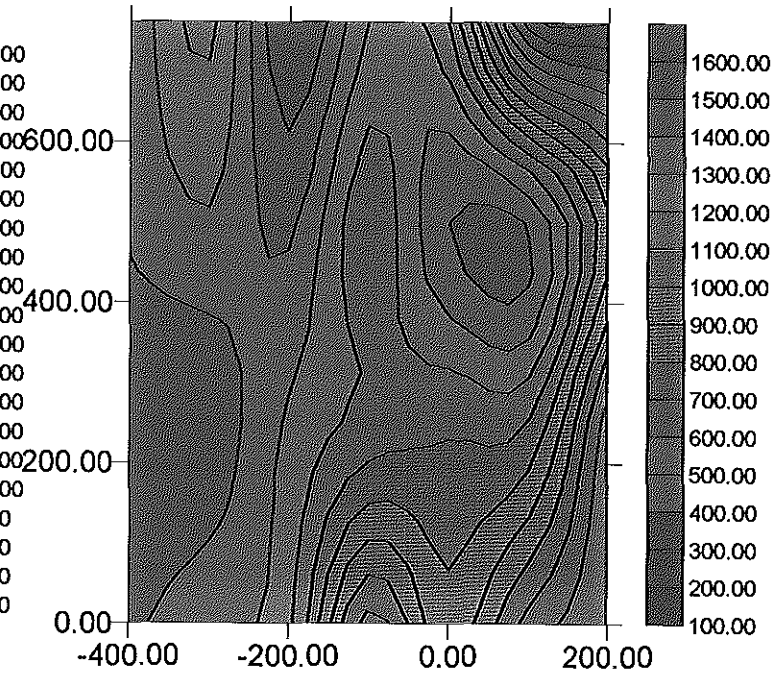

Figure 20. Geochemical map of Mn (ppm).

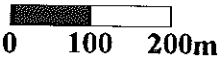

area gave values of above 2000 ppm (Appendix 1). The first population related to the chlorite and talc schists and represents a background value depicted on the eastern part of the area (Fig. 18). The second population is mostly associated with altered tremolite - actinolite - talc - serpentine schist and represents Ni anomaly. Nickel values in excess of 2000 ppm is observed west of 100 E in all grid lines. On the other hand, high Ni values (> 7000 ppm) are observed at locations bracketed by coordinates of 00 E – 100 E / 400 N to 750 N, 400 W / 00N and 200 W – 300 W / 400 N to 750 N (Fig. 18). Anomalous values characteristically developed on tremolite – actinolite – talc – serpentine schist. Another diagnostic feature of the anomalous samples is that the underlying rocks contain garnierite. The maximum value (9330 ppm) was obtained at 00 E / 750 N (Fig. 18) and the anomaly is open to the northeast out side of the area presently investigated.

Nickel has strong positive correlation with Co, Cr and Mn (Table 4; Fig. 24 & 25). This may be the result of Ni adsorption and copreciptation with Fe- and Mn- oxides or forming nickeliferous silicate (garnierite) in soils. The Ni pattern also show negative correlation with Cu and Zn (Table 4; Figs. 24 & 25), this is may be due to different chemical behavior or absence of sulfides.

All six randomly collected soil samples gave low Ni values which range from 13 ppm to 761 ppm. This may be due to the fact that the soil samples developed over the barren chlorite schist, talc schist and quartz vein.

4.1.4. Chromium (Cr)

Kozyrev et al., (1985) reported the presence of chromite lenses of upto 150 cm thick within the Kenticha, Dermidama, Katawicha and Dubicha serpentinites. Average Cr composition of ultramafic rocks is 2980 ppm (Rose et al., 1979). Based on the results of the 25 soil samples, two populations were identified from cumulative probability frequency curve plot (Appendix 2c), with 35 % (lower, P_1) and 65 % (upper, P_2). The respective threshold values are 1548 ppm and 3357 ppm. Minimum and maximum values are 33 ppm and 4100 ppm respectively, and a mean value is 1947 ppm, and standard deviation is 1157 (Table 3).

The first population (P_1) represents pure background value and the second population (P_2) is transitional between the background and anomalous values. Only values greater than the threshold value for the second population (> 3357 ppm), are considered anomalous.

Generally low values (< 1000 ppm) are observed in the eastern, northeastern, (00 – 200 W / 200 N – 600 N) parts of the grided area (Fig. 19). The eastern part is underlain by chlorite and talc schists. The pattern for the central part is closed and elongate, occupying the ridge top underlain by massive serpentinte devoid of lenses and disseminated chromite. From the geochemical map (Fig. 19), three distinct zones of anomalies can be identified: the first zone is below 00 N grid line and is open towards southwest, the second is a closed anomaly found between 00 – 100 E / 200 – 500 N and the third is an open anomaly observed at 00 E / 750 N. These anomalies are mostly related to the presence of chromite lense and disseminations within the serpentinized tremolite - actinolite - talc - serpentine schist. A maximum value of 4100 ppm is observed at 100 W / 00 N (Fig. 19) as part of the first anomalous zone.

Chromium shows strong positive correlation with Ni and Mn, and moderate positive correlation with Co and Zn (Table 4; Fig 24 & 25). Its behavior is consistent with those of other compatible elements including Mg and Ni. Other enrichment factor may be attributed to adsorption by Fe- and Mn- oxides in soils during weathering or lateritization processes (Rose et al., 1979). It also shows moderate negative correlation with Cu (Table 4), probably due to the absence of sulfides. Its moderate positive correlation with Zn may be due to limited ionic substitution in Fe- or Mn- oxides and / or Zn substitution in some Mg- silicates (Rose et al., 1979).

4.1.5. Manganese (Mn)

The average manganese content of ultramafic rocks is 1040 ppm (Rose et al., 1979). Two populations were identified from cumulative probability frequency curve (Appendix 3d): 28 % (lower; P_1) and 72 % (upper; P_2) with 853 ppm and 1442 ppm respective threshold values. The minimum and maximum values are 194 ppm and 1600 ppm respectively, the mean value is 1085.56 ppm and the standard deviation is 389 (Table 3).

The first population represents a background value and the second population a mixed (background and anomalous values); and values above the threshold limit (> 1442 ppm) are interpreted as pure anomalous values. The geochemical map of Mn (Fig. 20), illustrates low Mn (< 1000 ppm) values in the eastern part. Similar to other compatible element patterns, three zones of anomalies are observed: the first wider (open towards west) zone of anomaly stretches west of 200 W / 00 N to 500 N; the second zone has closed anomaly observed at 00 E to 100 E / 250 N to 500 N and the third anomaly which is located 100 W to 300 W / 500 N

to 750 N has an open pattern towards the north. Maximum value of 1600 ppm located at 100W / 750 N falls within the third anomalous zone. All the three anomalous zones developed on the tremolite - actinolite - talc - serpentine schist (Fig. 20), similar to other compatible elements discussed above.

Manganese has strong positive correlation with Ni, Co, Cr and Cu, and weak positive correlation with Zn (Table 4; Figs. 24 & 25). This is largely due to copreciptation and adsorption with Mn- oxides. The association of Mn with other intermediate to low mobile lithophile elements may allow substitution in Mg and Fe silicates (Rose et al., 1979).

4.1.6. Copper (Cu)

Two populations were identified with cumulative probability frequency curve plot (Appendix 2e): 55 % lower and 45 % upper population with the respective threshold values of 8 and 36 ppm (Table 3). The median value reported for Cu in ultramafic rocks is 42 ppm (Rose et al., 1979). Mean of the 25 samples is 19.2 ppm with minimum value of 4 ppm and maximum 86 ppm. Standard deviation is 21 (Table 3). Values greater than the threshold of the second upper population (> 36 ppm) are considered anomalous, and are localized in the southeastern part (Fig. 21), underlain by chlorite schist bearing talc schist. This is indirect contrast to the distribution pattern of the compatible elements. The maximum Cu concentration (86 ppm) is observed at 200 E / 250 N (Fig. 21). The soil samples found above the tremolite - actinolite - talc - serpentine schist bedrock is characterized by low Cu values (Fig. 21).

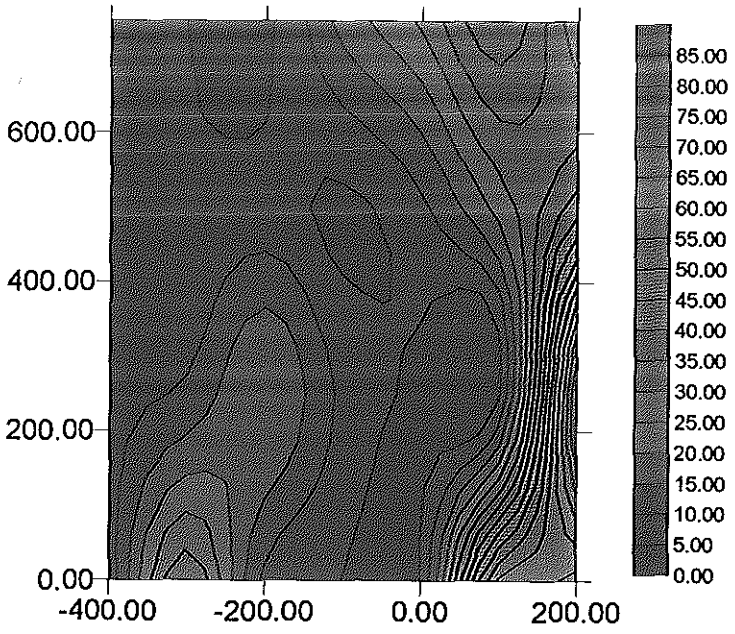

Figure 21. Geochemical map of Cu (ppm)

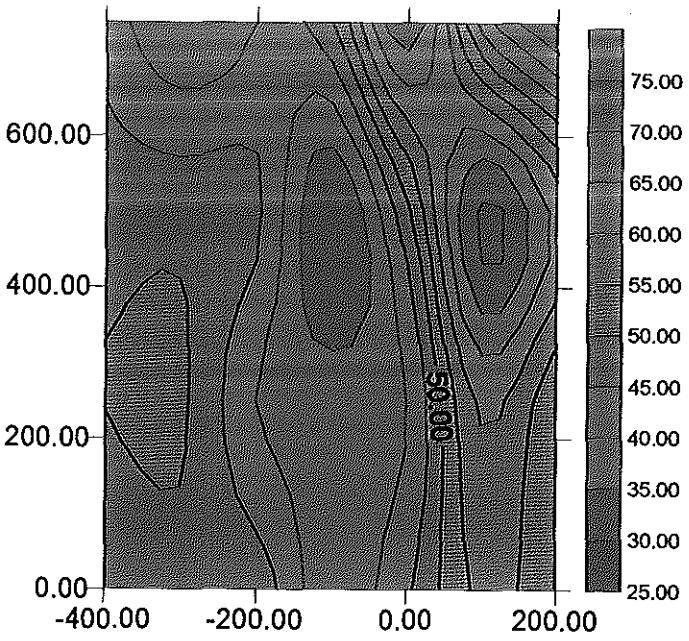

Figure 22. Geochemical map of Zn (ppm).

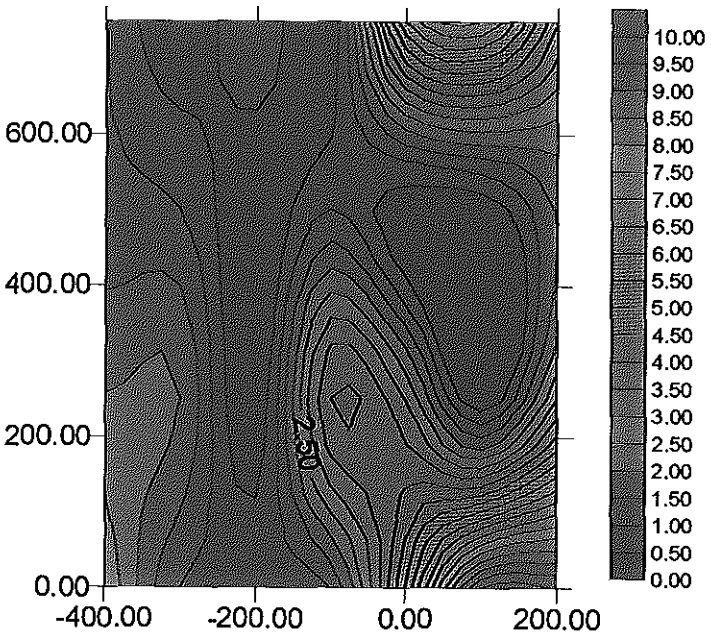

Figure 23. Geochemical map of Pb (ppm).

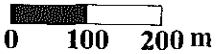

Copper has strong and weak positive linear correlation with Mn and Zn respectively (Table 4). The strong positive correlation with is due to it its adsorption to Mn- oxides and the weak positive correlation with Zn is mainly due to its similarity in chemical behavior. In addition Cu shows strong negative linear correlation with Ni and weak negative correlation with Co and Cr (Table 4; Figs. 24 & 25). This may be due to the significant difference in its chemical behavior with the compatible elements. The distribution of the compatible elements as discussed above is explained by the original enrichment in ultramafic rocks and enhanced enrichment by later serpentinization and lateritization processes.

Four of the six randomly collected soil samples show low Cu values; two of them, (sample Nº SOTDB – 27 and 28) and show values 78 and 69 ppm respectively, which are relatively higher.

4.1.7. Zinc (Zn)

Two populations (20 % lower; P_1 and 80 % upper; P_2) with 38 and 58 ppm threshold values respectively, were identified from cumulative probability frequency curve plot (Appendix 2f). A mean value of 46.92 ppm and standard deviation of 11 were obtained for minimum and maximum values 29 ppm and 76 ppm respectively (Table 3). Average Zn content for ultramafic rocks is 58 ppm (Rose et al, 1979). This value corresponds to the threshold of the second upper population and hence both population represent background values. Values above the threshold limit of the second population (> 58 ppm) may mark an anomaly.

Two zones of anomaly are identified in the area: the first is within grid coordinates bracketed by 100 E to 200 E / 250 N to 500 N and the second is located at 00 E / 750 N with open anomaly towards north and maximum value of 76 ppm is obtained at 100 E / 500 N within the first anomalous zone (Fig. 22). Similar to those for Ni, Co, Cr and Mn, both anomalies overly the tremolite - actinolite - talc - serpentine schist.

Zinc shows weak positive correlation with Co, Cr, Cu and Mn (Table 4; Figs. 24 & 25). This may be due to its substitution in Fe- and Mn- oxides, Mg- silicates, and its adsorption to organic matter in soils (Rose et al., 1979). The chlorite and talc schists and some parts of the tremolite - actinolite - talc – serpentine schist have low Zn values. In addition all randomly collected soil samples show low Zn concentration.

4.1.8. Lead (Pb)

Statistical computation from the 25 soil samples with 0.05 ppm and 10 ppm minimum and maximum values respectively, gave a mean value of 3 ppm and a standard deviation of 3 (Table 3). Two populations were identified with 60 % (lower; P_1) and 40 % (P_2; upper) having 1ppm and 8 ppm threshold limits respectively (Appendix 2g). The average Pb content for ultramafic rocks is 1 ppm (Rose et al., 1979). The first population represents background values ($\leq$ 1 ppm), and the second population represent anomalous values. Two open anomalies of Pb (one towards southeast and the other towards northeast) are observed (Fig. 23). These anomalies associated with the presence of quartz fragments in the soil.

The six randomly collected soil samples show relatively high Pb value (upto 11 ppm); one sample obtained from soil developed in close proximity to quartz vein, showed 43 ppm Pb.

6.1.9. Correlation

Correlation is a measure of similarity between paired data. The simple linear coefficient (r) lies between –1 and +1, where an absolute value of 1 means perfect correlation and a value of zero means no correlation. For variables x and y, n = 25, r can be expressed in terms of " sums of squares " (SS) notation as follows:

$$r = SS_{xy} / (SS_x . SS_y)^{0.5} \quad \text{Where : } SS_x = \sum_{i=1}^{n=25} (Xi - X_{mean})^2$$

$$SS_y = \sum_{i=1}^{n=25} (Xi - X_{mean})^2$$

$$SS_{xy} = \sum_{i=1}^{n=25} (Xi - X_{mean})^2$$

Au and Pb are not included in the matrix, because almost all soil samples have similar Au concentrations (0.1 ppm) and Pb values less than the detection limit (< 1ppm).

Correlation coefficient (r) > 0.1845 is significant at 95 % of confidence level (Snedecor and Cochran, 1976). The correlation matrix of the 25 samples (Table 4) show strong correlation among compatible elements (Co, Cr, Ni and Mn), strong negative correlation between Cu and Co, Ni, and Cr. Zinc shows positive linear correlation with other elements except Ni (Table 4). The correlation coefficient (r) of Mn and Ni is near to the ideal positive linearity, (r = 0.8326); and near to an ideal negative linearity is observed between Cu and Ni, which is marked by r = - 0.7150.

r	Co	Ni	Cr	Mn	Cu	Zn
Co	1.0000					
Ni	0.6024	1.0000				
Cr	0.3065	0.6967	1.0000			
Mn	0.6570	0.8326	0.5158	1.0000		
Cu	-0.1940	-0.7150	-0.3122	0.6608	1.0000	
Zn	0.3633	-0.1120	0.4555	0.1667	0.2971	1.0000

Table 4. Linear coefficient (r) matrix for 25 grid soil samples.

Figure 32 and 33 are presented to show the graphic correlation that exists between the analyzed elements.

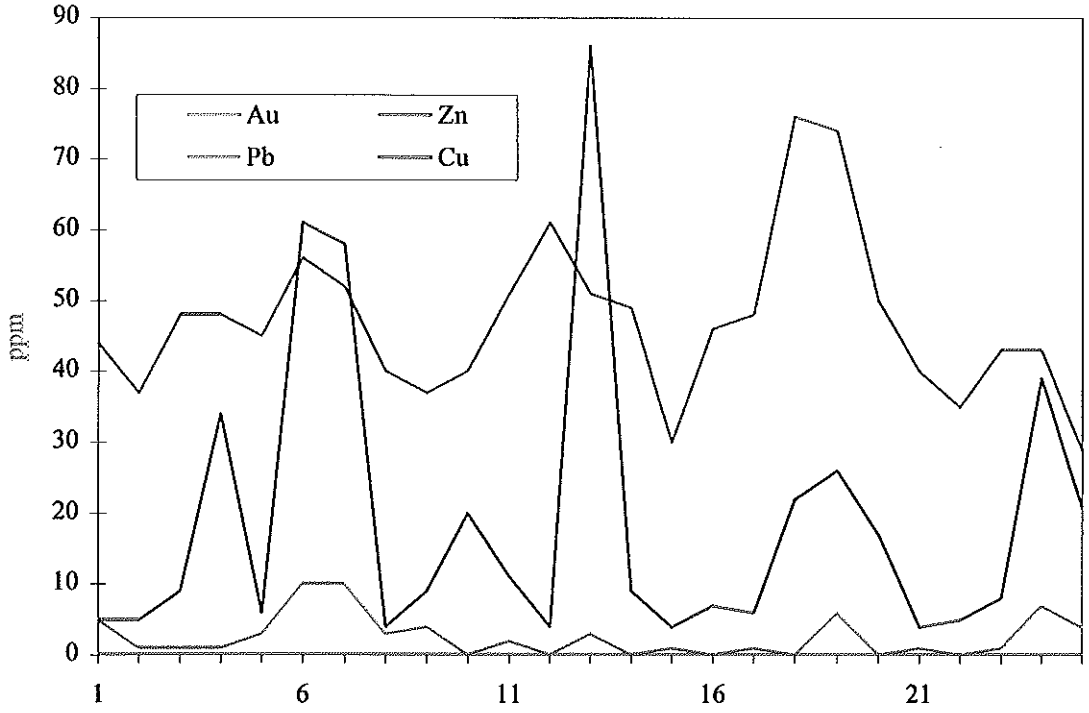

Fig. 25. Correlation graph between Au, Cu, Zn and Pb in soil samples of Big Dubicha.

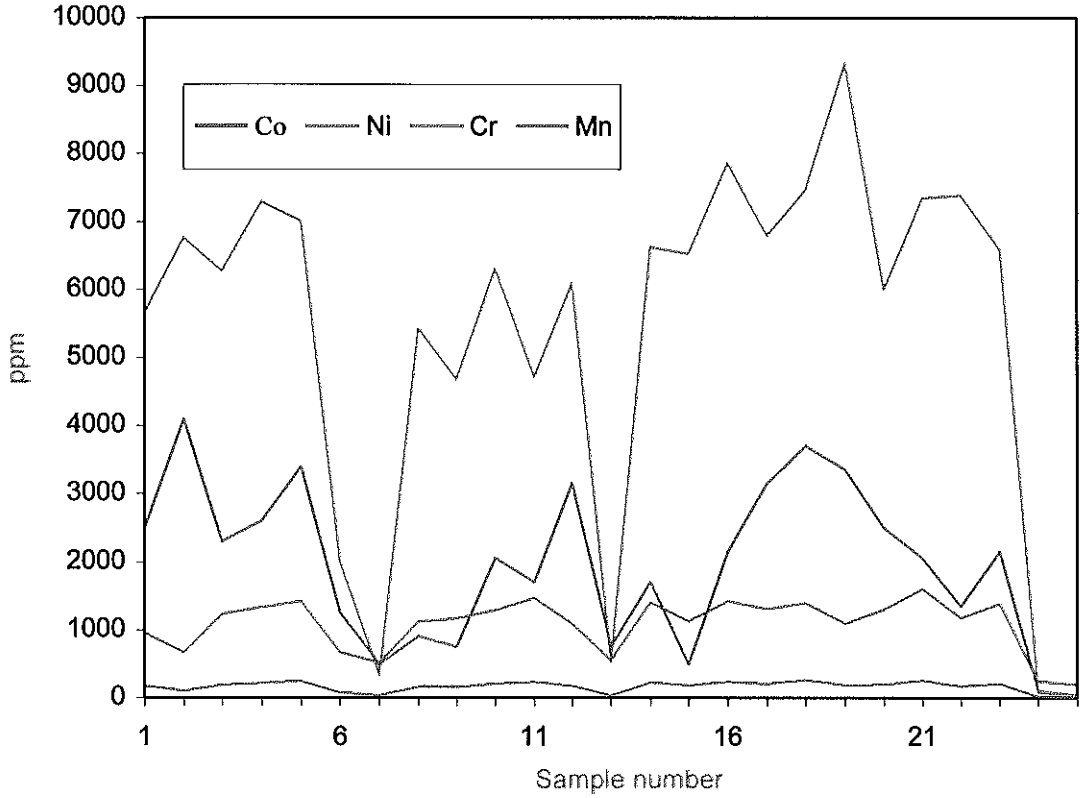

Fig. 26. Correlation graph between Co, Ni, Cr and Mn in soil samples of Big Dubicha.

	Lithology				
Element	Ttss	Cs	Ts	Bmqs	Remark
Co (ppm)	58 - 142	45 - 101	45 - 142	14 - 74	Soil anomaly is > 84 ppm
Ni (ppm)	1412 - 13664	666 - 2079	89 - 1664	18 - 333	Soil anomaly is > 2000 ppm
Cr (ppm)	1449 - 3693 mostly above 2000 ppm	1325 - 2350 mostly not analyzed	70 - 2195 mostly not analyzed	140 only one sample was analyzed	Soil anomaly is > 3357
Cu (ppm)	1 - 54	2 - 93	1 - 93	6 - 64	Soil anomaly is > 36 ppm
Zn (ppm)	18 - 74	33 - 115	59 - 150	25 - 79	Soil anomaly is > 58 ppm
Pb (ppm)	3 - 18	4 - 17	2 - 14	16 - 56	Soil anomaly is >1 ppm

Table 5. Trace element composition range of the different lithologies of the area (Ttss = tremolite - actinolite - talc - serpentine schist, Ts = talc schist, Cs = chlorite schist and Bmqs = biotite - muscovite - quartz schist).

Table 5 clearly shows that the tremolite - actinolite - talc - serpentine schist (Ttss) bedrock is relatively rich in compatible elements often in excess of background values. For example Nickel values are greater than 2000 ppm and Co values greater than 84 ppm. In the case of Cr, the samples analyzed from tremolite - actinolite - talc - serpentine schist fall in the mixed upper population of the soil samples. From this observation the anomalies in the soil overlying the tremolite - actinolite - talc - serpentine schist bedrock are interpreted as residual (Figs. 17, 18, 19 & 20). Following the insitu weathering of the bedrock, lateritization process further reconcentrated elements such as Ni and Co.

In contrast to the anomalies observed in the soil samples Zn is rich in chlorite and talc schist samples (Fig. 22). These marked differences are attributed to higher mobility of Zn. The rock samples collected from talc and chlorite schists (see Table 5 and Appendix 4) contain a relatively higher Cu values. This pattern is in good agreement with Cu anomaly observed in the soil samples (Fig. 21). For both anomalies of Pb recognized (Fig. 23) Pb concentration in soil samples increases with the presence of quartz vein fragments in the soil. This may suggest hydrothermal activity in the concentration of Pb or the presence of Lead sulfides associated with the quartz vein.

6.2. Stream sediment samples

The stream sediment samples were collected from first and second order intermittent streams of the Big Dubicha area. The aim of this stream sediment sampling is to identify the anomalous zones, and then to compare the distribution patterns with those of the soil samples. Six stream sediment samples (sample Nº SDTDB – 1 to 6; Fig. 26) were collected, of which

sample Nº SDTDB – 1 to 5 are from the streams draining the tremolite - actinolite – talc - serpentine schist bedrock and SDTDB – 6 is from the stream draining the chlorite schist containing talc schist bedrock. The Atomic Absorption Spectrometry (AAS) results of the six samples are given in Table 6.

Sample Nº	Lithology	Co (ppm)	Ni (ppm)	Cr (ppm)	Mn (ppm)	Cu (ppm)	Zn (ppm)	Pb (ppm)	order of streams
SDTDB-1	Ttss	242	4950	2600	1421	13	57	2	2nd
SDTDB-2	Ttss	211	4820	2450	1394	13	56	4	1st
SDTDB-3	Ttss	218	4410	5000	1424	17	78	5	1st
SDTDB-4	Ttss	251	5230	2400	1497	9	54	2	1st
SDTDB-5	Ttss	121	3210	9400	813	16	101	5	1st
SDTDB-6	Ts	27	386	570	308	11	35	5	2nd

Table 6. Trace element concentrations in stream sediment samples (Ttss = tremolite - actinolite - talc - serpentine schist, Ts = talc schist).

As illustrated in Table 6, Co, Ni, Mn, Cr and Zn show high values in streams sediments collected from streams draining the tremolite - actinolite - talc - serpentine schist. This indicates the source of anomalies seen in soil geochemical maps of Co, Ni, Mn, Cr and Zn is the underlying tremolite - actnolite - talc - serpentine schist.

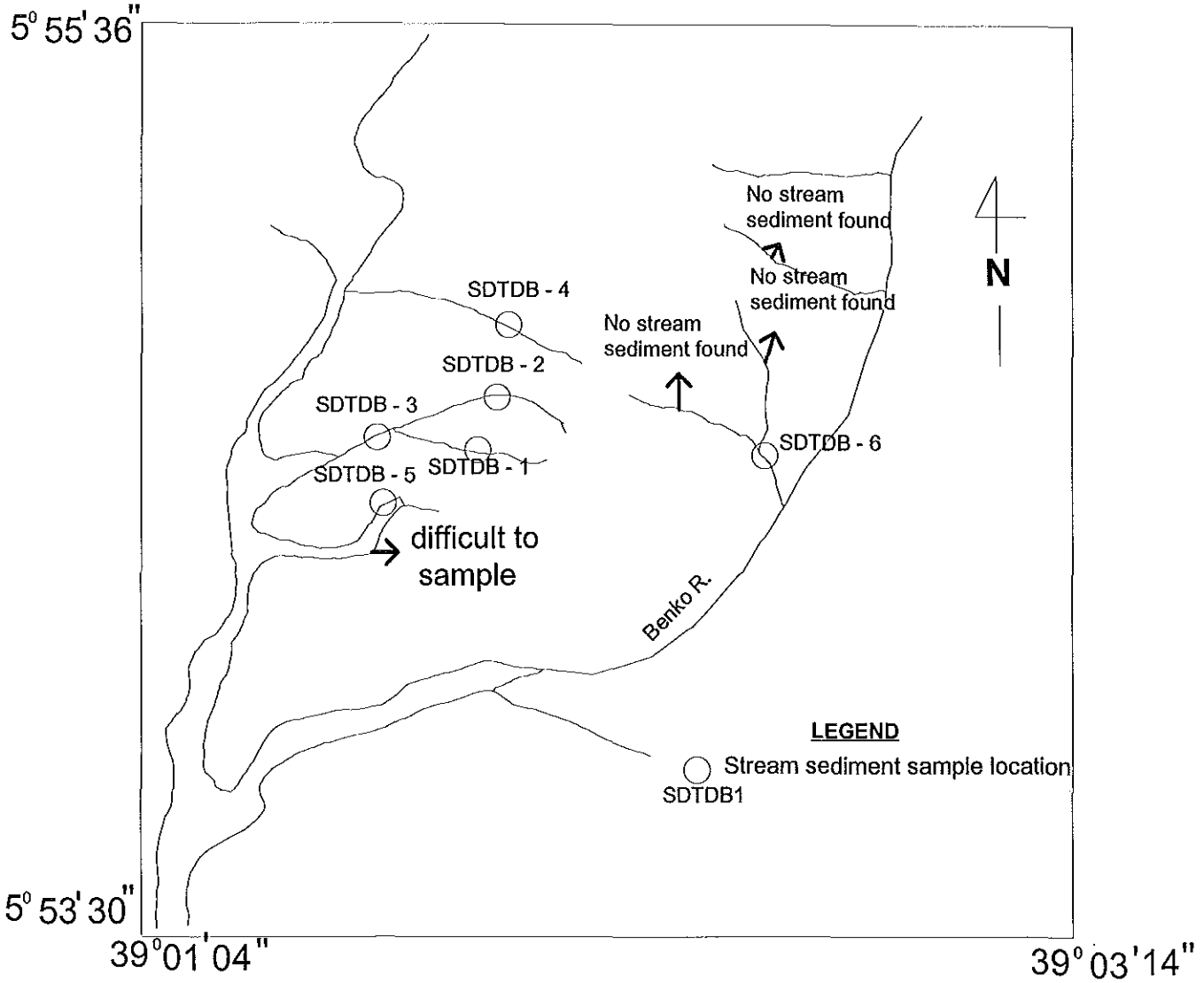

Figure 26. Stream sediment samples location map.

4.3. Pit channel soil samples

PIT - 1 (Fig. 27 a) is a rectangular pit located at 200 W / 500 N (Fig. 15) based on the northerly open soil anomalies of Co and Mn (Figs. 17 & 20), and the closed anomaly of Ni (Fig. 18). The eastern and western wall of the pit was mapped and sampled. Both walls indicate high values for Co, Mn and Ni. In addition, the concentrations increase upsection from bottom to top of the pit (Table 7). The pit shows very high values of Ni for top most samples of both walls (8070 ppm and 7550 ppm, at eastern and western walls respectively). This Ni enrichment trend corresponds to the enrichment of Fe, suggesting the presence of Ni bearing Fe- oxides. The concentration of Co, Ni and Mn overlap anomalies outlined from soil survey (Fig. 17, 18 and 20). The above observation suggests that Ni enrichment is controlled by lateritization process and the soil anomaly is residual, which resulted from the insitu weathering of the tremolite - actinolite - talc - serpentine schist.

PIT - 2 (Fig 27 b) was dug at 100 E / 400 N (Fig. 15) to test the closed soil anomalies of Co, Ni, Cr, Mn and Zn (Figs. 17, 18, 19, 20 and 22) encountered from the grid soil maps and to understand the trend of vertical variation. Sampling was carried out from the eastern and western wall of the pit. The pit samples yielded high values for Co, Ni, Mn, Cr, Fe and Zn, in agreement with the soil geochemical maps. Cobalt shows vertical enrichment trend from bottom to top; 234 ppm to 347 ppm for the eastern wall and from 193 ppm to 295 ppm for the western wall (Table 7) which implies lateritic enrichment. Values from the top samples also coincide with the anomalous values obtained in soil samples (Fig. 17).

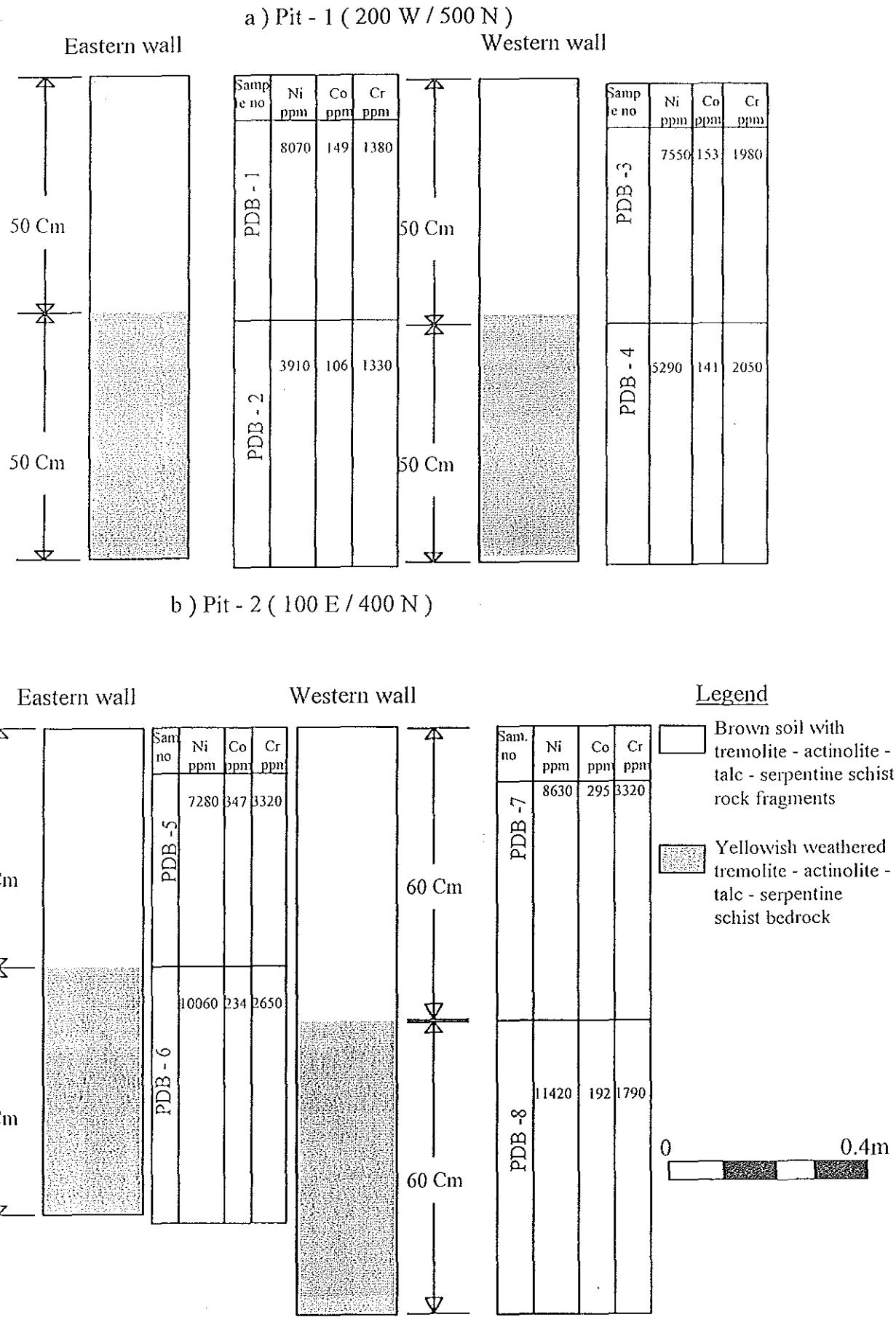

Figure 27. Geological map of ; a) Pit - 1 and b) Pit - 2

Sample No	Pit grid location	Pit No.	Wall dire.	Depth (m)	Co ppm	Ni ppm	Mn ppm	Cr ppm	Fe %	Cu ppm	Zn ppm	Pb ppm	Ag ppm	Remark
PDB - 1	200 W / 500 N	1	eastern	0 - .5	149	8070	1340	1380	11.2	4	46	< 1	< .1	Brownish soil with Ttss fragment
" - 2	"	1	"	.5 - 1	106	3910	990	1330	9.5	4	44	< 1	< .1	Yellowish green weathered Ttss
" - 3	"	1	western	0 - .5	153	7550	1310	1980	12.5	5	42	< 1	< .1	Brownish soil with Ttss fragment
" - 4	"	1	"	.5 - 1	141	5290	1200	2050	11.1	5	41	< 1	< .1	Yellowish gray weathered Ttss
" - 5	100 E / 400 N	2	eastern	0 -.6	347	7280	2990	3320	13.1	21	64	< 1	< .1	Brownish soil with Ttss fragments
" - 6	"	2	"	.6 - 1.2	234	10060	1680	2650	12.6	10	49	< 1	< .1	Yellowish magnetite, chromite and garnierite bearing Ttss
" - 7	"	2	western	0 - .6	295	8630	2510	3320	13.2	24	83	< 1	< .1	Brownish soil with Ttss fragment
" - 8	"	2	"	.6 - 1.2	192	11420	1490	1750	10.1	8	44	< 1	< .1	yellowish brown weathered Ttss

Table 7. Pit channel soil samples AAS analytical result.

But Ni values for the bottom samples are 10,060 ppm for the eastern wall and 11,420 ppm for the western wall. These values decrease upsection; 7280 ppm and 8630 ppm at eastern and western walls respectively (Table 7). These values correspond with the anomalous values observed on the geochemical map of Ni (Fig. 18) for this pit location. The high values from the bottom of the pit are attributed to the presence of garnierite that is observed in the weathering mantle of the bedrock.

Mn, Cr and Fe also show increasing values upsection. The Cr and Fe contents are enhanced with the presence of disseminated and lenses of chromite and magnetite in the weathered bedrock (tremolite - actinolite - talc - serpentine schist). Zinc also shows an upward enrichment trend at both walls. This coincides with the geochemical map of Zn (Fig. 22; Table 7).

4.4. Trench channel soil samples

A trench with dimensions of 5m long and about 1m deep (TR - 1) was dug at 00 N / 397. 5 to 402.5 W to evaluate the lateral variation of the eastward open anomalies of Co, Ni, Cr and Mn (Figs. 17, 18, 19 & 20).

Figure 28. Geological map of trench (Tr - 1).

Trench No.- 1 (Tr - 1) 00N / 307.5 W - 402.5 W

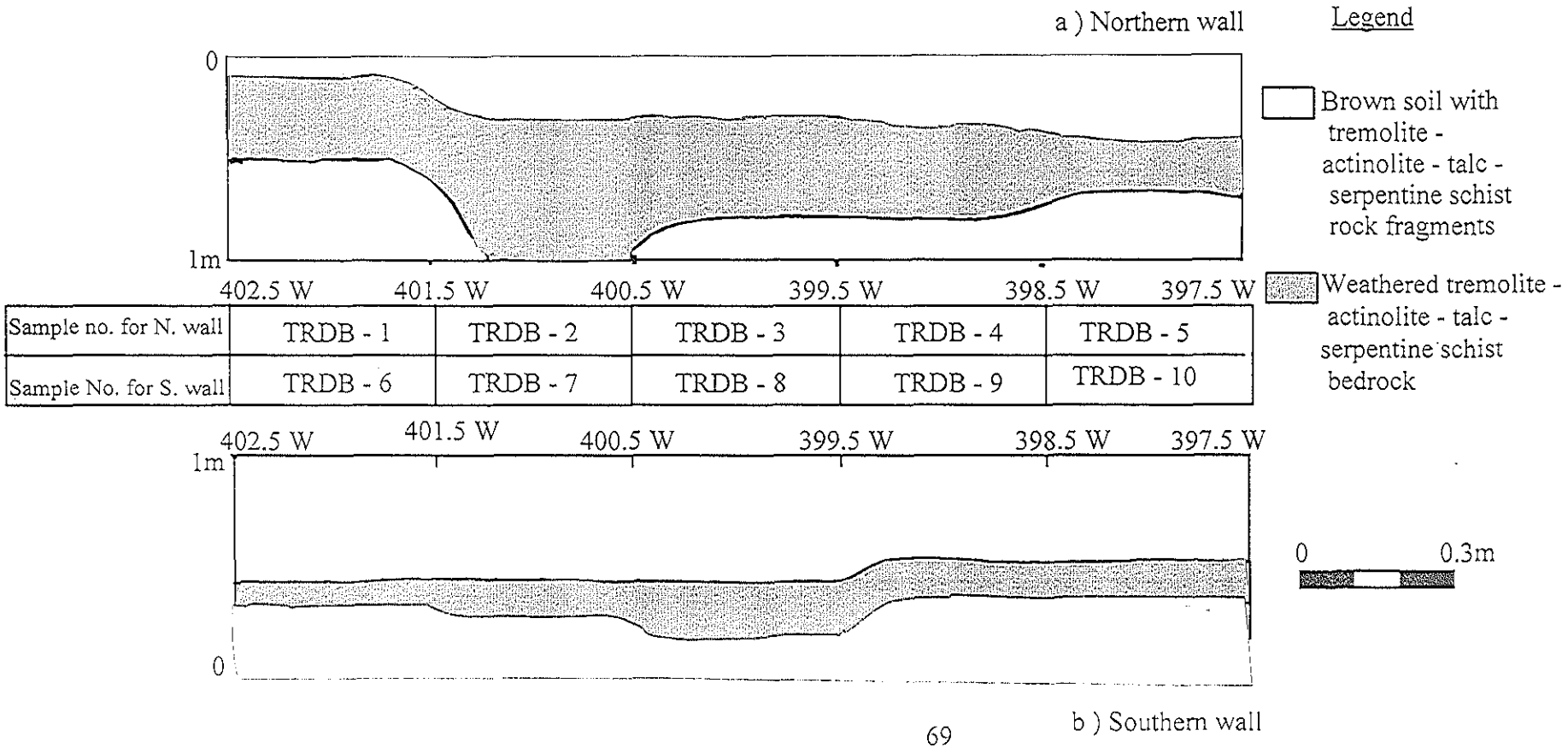

Sample No	wall direction	sample location 00 N / 400 W	Co ppm	Ni ppm	Mn ppm	Cr ppm	Fe %	Cu ppm	Zn ppm	Pb ppm	Cu ppm	Remark
TRDB –1	northern	402. 5 - 401.5 W	102	3560	910	1380	7.9	3	39	<1	1.0	strongly weathered yellowish gray Ttss fragments were noticed
" - 2	"	401.5 - 400. 5 W	138	4370	1200	1540	10.2	5	45	<1	1.0	"
" - 3	"	400.5 - 399. 5 W	135	7330	1200	1490	10.1	9	46	<1	< 1	"
" - 4	"	399.5 - 398.5 W	131	5900	1130	1250	10.7	6	44	<1	< 1	"
" - 5	"	398.5 - 397.5 W	155	5170	1090	1260	12.3	5	45	<1	< 1	"
" - 6	southern	402. 5 - 401.5 W	160	6580	1470	1700	12.2	6	45	<1	< 1	"
" - 7	"	401.5 - 400. 5 W	180	6550	1740	1680	12.1	4	49	<1	< 1	"
" - 8	"	400.5 - 399. 5 W	146	7120	1330	1810	11.1	9	44	<1	1.0	"
" - 9	"	399.5 - 398.5 W	153	5680	1300	1820	11.1	7	49	<1	< 1	"
" - 10	"	398.5 - 397.5 W	175	7380	1610	2870	14.1	7	48	<1	< 1	"

Table 8. Trench channel soil samples of TR - 1 AAS analytical result. Ttss = Tremolite - actinolite - talc - serpentine schist

The northern and southern walls of the trench were mapped and sampled at 1m interval. The trench is underlain by a strongly weathered tremolite - actinolite - talc - serpentine schist. The geological map is given on (Fig. 28) and the AAS result of the channel soil samples is presented on (Table 8).

Generally Co values are high for the channel soil samples of both walls (102 ppm upto 155 ppm, in the northern wall and 140 ppm upto 180 ppm in the southern wall). The values are anomalous for soil samples (> 84 ppm) and are also in excess of the 110 ppm average content for ultramafic rocks, (Rose et al., 1979). The lateral variation between samples within each wall is insignificant. An eastward open Co anomaly seen in the geochemical map (Fig. 17), is interpreted as resulting from insitu weathering of tremolite - actinilite - talc - serpentine schist and subsequent reconcentration by lateritization process.

Nickel concentration is high in all samples; samples of the southern wall showing relatively higher values than the northern wall. The samples of the northern wall show a range of value between 3560 and 7330 ppm and the southern wall from 5680 upto 7380 ppm. Values indicated on the geochemical map of Ni (Fig. 18) at 400 W / 00N is above 6500 ppm, and most values from the southern wall exceed this value, but the northern wall samples have lower value. The average Ni content for ultramafic rocks is 2000 ppm (Rose et al., 1979). Channel samples of both walls yielded values greater than the Clark value, and the lateral variation of Ni in the northern wall is higher than that of the southern wall. Hence all values can be considered anomalous for weathered bedrock which subsequently enriched through lateritization process. Manganese obtained from the systematic soil samples at grid location (400 W / 00 N) is above 1400 ppm (Fig. 20). The Clark value for ultramafic rocks is 1040 ppm (Rose et. al, 1979). The southern wall samples have relatively higher values (1680

to 2870 ppm) than the northern wall (1910 to 1200 ppm), but southern wall show significant lateral variation. With the exception of one sample from the northern wall, all the samples gave higher values than the Clark value. Some samples of the southern wall showed even greater values than recognized anomaly in the geochemical map (Fig. 20). Hence the anomaly observed in the soil samples may have been the result of the weathering of the tremolite - actinolite - talc - serpentine schist. An eastward open anomaly of Cr outlined on the geochemical map is above 3200 ppm (Fig. 19), but values from both walls are below this value. Similar to the other elements, the southern wall has relatively high values (1680 to 2870 ppm) than the northern wall which range between 1250 and 1540 ppm. The average Cr content for ultramafic rocks is 2980 ppm (Rose et al., 1979). Generally all the channel sample values are below the average value, with the southern wall samples having comparable values to the average content. This indicates the significance of the latter reconcentration processes in forming the soil anomaly. Though there is a slight variation in the southern wall, Fe shows near uniform distribution for all channel samples. Due to their low concentrations in the channel samples, the distribution and behavior of the rest of the elements is not considered.

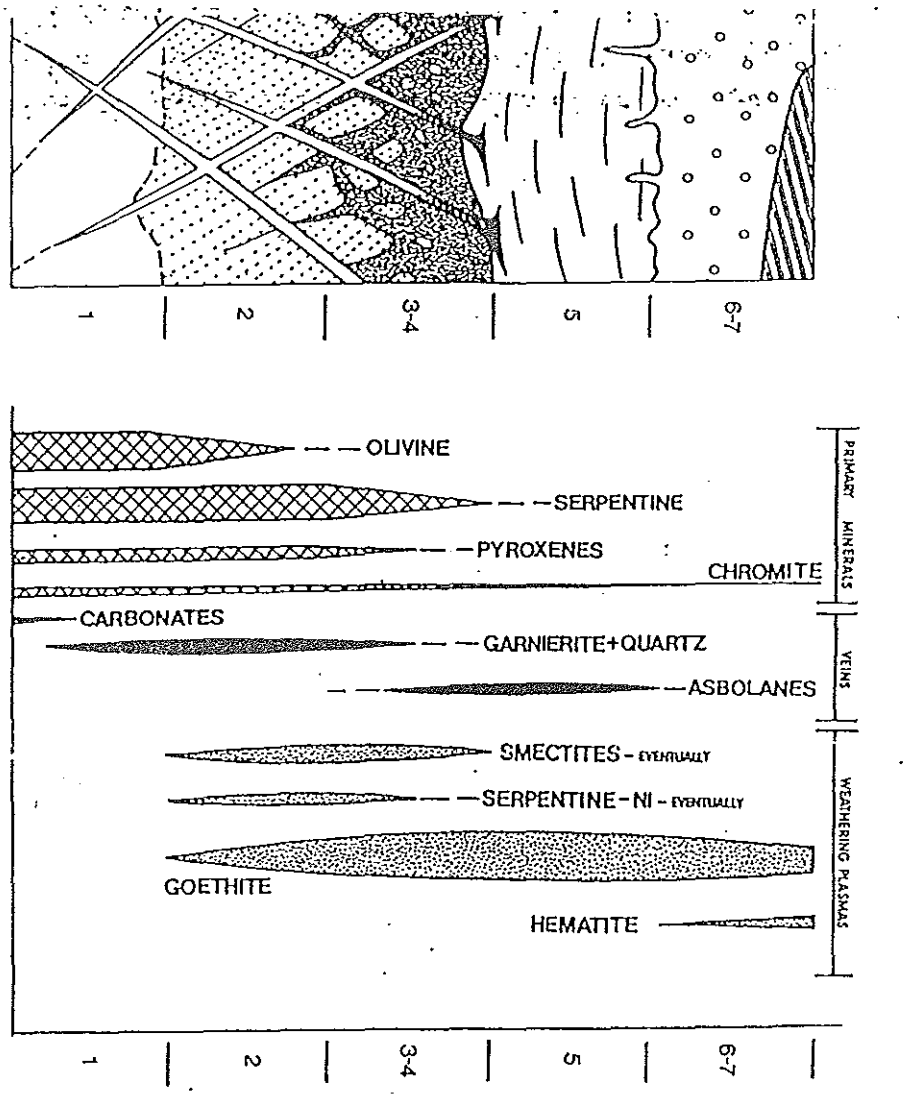

Figure 29. Ni - lateritic profile with the mineralogical composition of the successive layers (1- 7 indicate the various layers) (After Paquet and Clauer, 1977).

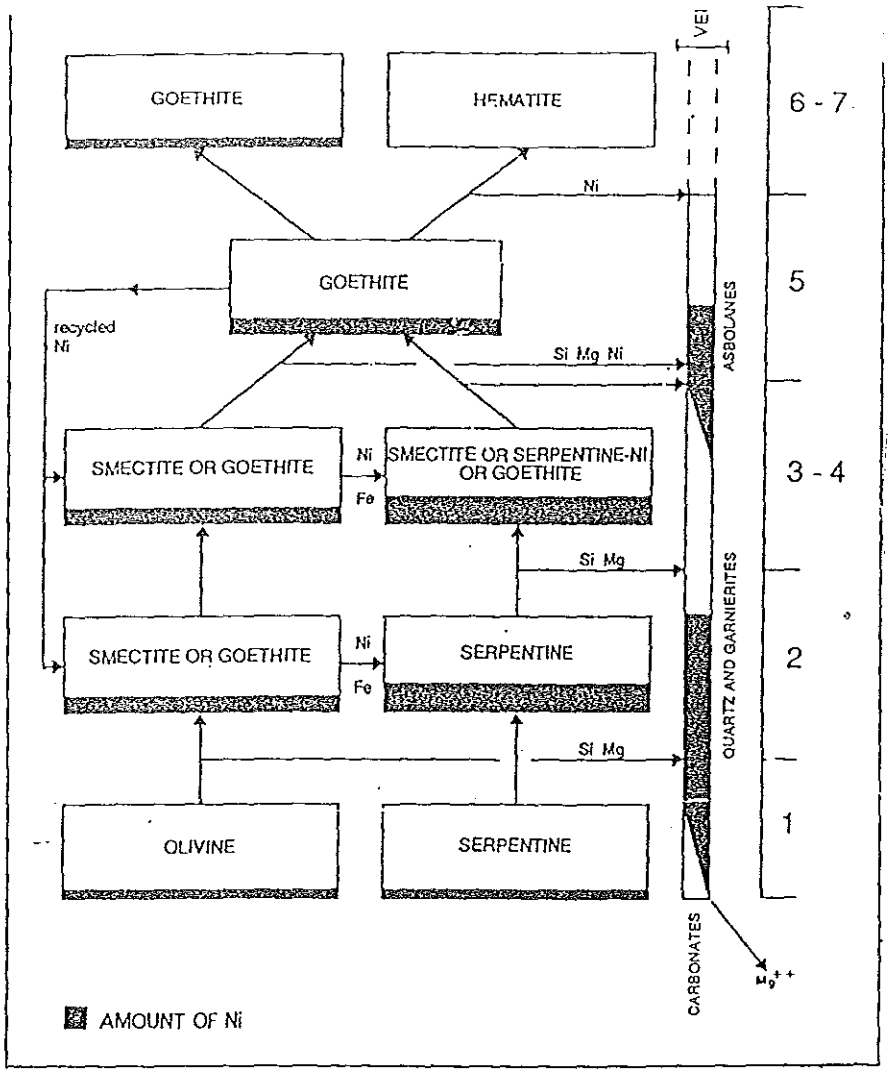

Figure 30. Main mineralogical sequence and chemical element transfer occurring during laterite weathering of ultramafic rocks (After Paquet and Clauer, 1977).

Figure 29 and 30 illustrate the primary and secondary minerals with associated veins formed in the different layers of the laterite; and their control in Ni and other compatible elements enrichment. The main Ni bearing secondary minerals in the figures are Ni bearing serpentines and Fe- oxides. As indicated in the previous sections, anomalies of the compatible elements in soil samples are associated with the strongly deformed and serpentinized tremolite - actinolite - talc - serpentine schist. The concentration of these compatible elements increase upsection with Fe in pit samples, indicating the formation Ni bearing Fe- oxides in the upper layers during weathering. Nickel especially shows very high values both in soils and garnierite bearing weathered zone of the tremolite - actinolite - talc - serpentine schist. These all agree with the processes seen in Figure 29 & 30. Hence the source of the anomalies of the compatible elements seen in the soil geochemical maps is the lateritic weathering of the underlying tremolite - actnolite - talc - serpentine schist.

5. DISCUSSION

The altered ultramafic rocks of the Big Dubicha area are: chlorite schist, talc schist and tremolite - actinolite - talc - serpentine schist. The metamorphic mineral assemblages of the Big Dubicha altered ultramafic rocks are dominated by **chlorite + talc + tremolite-actinolite + serpentine ± epidote ± quartz ± green hornblende ± calcite.** This assemblage is characteristic of lower greenschist facies, representing serpentinization, chloritization and carbonation reactions. These reactions are resulted from low temperature water-rock interactions. Mineral assemblages of the country rock fall within the lower to middle amphibolite facies, indicating the allochemical (disequlibrium) state of the assemblages between the Big Dubicha metaultramafic mass and the host rock. This suggests the presence of allofacial relationship between the Big Dubicha altered ultramafic rocks and the enveloping rock.

The CaO-MgO-SiO_2-H_2O-CO_2 plot of the chlorite and tremolite - actinolite - talc - serpentine schists approximate harzburgitic to dunitic anhydrous mineralogy. According to Butcher and Frey (1994) such compositional spectrum suggest a tectonically implanted subcontinetal mantle lithosphere. This is supported by the absence of magmatic process, which is interpreted from depletion of LILE in spider diagrams of all altered ultramafic rocks of the Big Dubicha area.

The soil geochemical anomalies of the compatible elements (Co, Ni, Cr and Mn) consistently overlap the strongly deformed and serpentinized; garnierite, chromite and magnetite lenses

and disseminations containing tremolite - actinolite - talc - serpentine schist. The anomalies are also consistent with high values obtained from the whole rock geochemical data of the tremolite - actinolite - talc - serpentine schist. Nickel characteristically shows high values in both soils and weathered garnierite bearing tremolite - actinolite - talc - serpentine schist. These are interpreted as evidences for a residual nature of the anomaly, which is resulted from the insitu weathering of the bedrock (tremolite - actinolite - talc - serpentine schist) and subsequent lateritization processes.

6. CONCLUSION AND RECOMMENDATIONS

6.1. CONCLUSION

1. Metamorphic mineral assemblages of the Big Dubicha altered ultramafic rocks represent lower greenschist facies. The enveloping rock assemblages fall within the lower to middle amphibolite facies, suggesting the presence of allofacial relationship between the Big Dubicha metaultramafic rocks versus the enveloping rock.

2. Geochemical investigations and limited metamorphic and structural observations suggest that the Big Dubicha altered ultramafic mass is a tectonic slice or fragment of subcontinental mantle lithosphere.

3. The strongly deformed and serpentinized tremolite - actinolite - talc - serpentine schist is the source of lateritic Ni and other compatible elements enrichment.

6.2. RECOMMENDATIONS

1. Further whole rock Rare earth element (REE) analysis, isotopic work and mineral chemistry are necessary to adequately constrain the geological evolution.

2. Systematic detailed geochemical survey should be done to further map the dispersion patterns of the compatible elements.

7. REFERENCES

AYALEW, T. BELL, K., MOORE, J.M., AND PARRISH, R.R., 1990. U – Pb and Rb – Sr geochronology of western Ethiopian Shield. *Geological Society of America*, Bulletin 102: 1309 – 1316, Boulder.

AYALEW, T. AND GICHILE, S., 1990. Preliminary U - Pb ages from southern Ethiopia. Extended abstracts, *15th Colloquium African Geology*, 127 - 130, Nancy.

BERHE, S.M., 1990. Ophiolites in northeast Africa: implications for crustal growth, *Journal of Geological Society of London*, **147**: 41 – 57, London.

BUTCHER, K. AND FREY, M.,1994. Petrogenesis of Metamorphic Rocks, 6th edition, 318p, Berlin.

CHATER, A. M., 1971. The Geology of the Megado area of southern Ethiopia. Unpublished Ph. D. Thesis, University of Leeds, United Kingdom.

DE WIT, M. J., AND CHEWAKA, S., 1981. Plate tectonic evolution of Ethiopia and origin of its mineral deposits: an overview. In: S.CHEWAKA & M. J. DE WIT (eds), Plate Tectonics and Metallogenesis: Some guide lines to Ethiopian mineral deposit. *Ethiopian Institute of Geological Surveys*, Bulletin No 2, 115 - 129, Addis Ababa.

ETHIOPIAN MAPPING AGENCY (EMA), 1981. National Atlas of Ethiopia. Preliminary edition, Ethiopian Government. Addis Ababa.

GASS, I.G., 1981. Pan – African (Upper Proterozoic) plate tectonics of the Arabian – Nubian shield. In: A. Kroner, (ed.) *Precambrian plate tectonics* : 387 - 405, Elsiever, Amsterdam.

GILBOY, C. F., 1970. The geology of the Gariboro region, southern Ethiopia. Unpub. Ph. D. thesis, University of Leeds, United Kingdom.

HOLMES, A., 1951. The sequence of Precambrian Orogenic Belts in south & central Africa. 18 th International Geological Congress, **14**: 254 - 269, London.

JELENC, D., 1966. Mineral occurrences of Ethiopia. *Ethiopian Institute of Geological Surveys*, 720p, Addis Ababa.

KAZMIN, V., 1971. Geology of Ethiopia, *Geological survey of Ethiopia*, Ministry of Mines, Imperial Ethiopian Government.

_____, 1972. Geology of Ethiopia (Explanatory Note to Geological Map of Ethiopia, 1: 2, 000,000).

_____, 1975. The Precambrian of Ethiopia and some aspects of the geology of Mozambique belt. *Geophysical Observatory, Bulletin* **15**: 27 – 45.

_____, 1976. Ophiolites in the Ethiopian Basement. *Ethiopian Institute of Geological Surveys*, Note no. 35, Addis Ababa.

KAZMIN, V., SHIFERAW, A., AND BALCHA, T., 1978. The Ethiopian Basement: stratigraphy and possible manner of evolution. *Geologische Rundschau* **67**: 531 – 546, Stuttgart.

KOZYREV, V. , KEBEDE, G., SAFANOV, V., WOLDEMICHEAL, B., GURBANOVICH, G., TEWELDEMEDHIN, T. , KAITUKOV, M., KUZNATSOV, J.,TULIANKIN, U. AND ARIJAPOV, A., 1985. Regional geological and exploration work for gold and other minerals in the Adola Goldfields: Regional geological mapping and prospecting. *Ethiopian Mineral Resources Development Corporation*, V. 2, Addis Ababa.

KRONER, A.,1993. The Pan – African Belt of Northeastern and Eastern Africa, Madagascar, southern India, Sirilanka, East Antarctica: Terrane Amalgamation during formation of the Gondwana Supercontinent. In: U. Thorweihe and H. Schandelmier (eds.) *Geoscientific Reaserch in northeast Africa,* 3 –9, Balkema, Rotterdam.

LEVITTE, D. AND KENT, G., 1968. Nickeliferous laterites of Sidamo. *UN – Ethiopia Mineral Survey*, Unpub rep., Addis Ababa.

PAQUET, H. AND CLAUER, N., 1977. Soils and sediments: Mineralogy and Geochemistry, 125 - 138.

PEARCE, J. A., 1982. Trace element characterstics of lavas from destructive plate boundaries. In: R.S. THORPE (ed.). Andesites, 525 - 548, Wiley, Chichester.

_____, 1983. Role of the subcontinental lithosphere in magma genesis at active continental margins. In: C. J. HAWKESWORTH and M. J. NORRY (eds.), " Continental Basalts and Mantle Xenoliths, ". Shiva Publishing Limited, 230 - 249.

ROSE, W., HAWKES, H. E. AND WEBB, J. S., 1979. Geochemistry in Mineral Exploration. 2nd edition, Acadamic Press Inc, 657p, London.

SCHEMROLD, R., 1988. Report on field trip to the Adola Goldfield (Sidamo), unpublished report, *Ethiopian Institute of Geological Surveys,* Addis Ababa.

SNEDECOR G. W. AND COCHRAN W. G. 1976. Statististcal methods, New Delhi.

STERN, R. J., 1993. Tectonic evolution of the Late Proterozoic East African Orogen: Constrains from crustal evolution of the Arbian –Nubian Shield and the Mozamibque Belt. In: U. THORWEIHE AND H. SCHANDELMIER (eds.) *Geoscientific research in northeast Africa*, 73 - 74, Balkema, Rotterdam.

STERN, R. J., 1994. Arc assembly and continental collision in the Neoproterozoic East African Orogen: Implications for the consolidation of Gondwana land. *Annu. Rev. Earth Planet. Sci. letters* **23**: 319 – 351.

TEKLAY, M. KRONER, A., AND OBERHANSLI, R., 1993. Reconnaissance Pb – Pb zircon ages and Nd – Sr isotope composition of Precambrian rocks from southern and eastern Ethiopia and an attempt to define crustal provinces. In : U. THRRWEIHE AND H. SCHANDELMEIER (eds.), *Geoscientific Research in Northeast Africa*, 133 - 138, Balkema, Rotterdam.

VAIL, J. R., 1976. Outline of the Geochronology and tectonic units of the basement complex of Northeast Africa. *Proceedings of Royal Society*, London, Series A - **350**: 97 - 114

VAIL, J. R. 1983. Pan – African crustal accerètion in northeast Africa. *Journal of African Earth Science.* **1**: 285 – 294, Oxford.

WILSON, M., 1989., Igneous petrogenesis. Unwin Hyman, 466p, London.

WOLDEHAIMANOT, B., 1995. Structural Geology and Geochemistry of the Neoproterozoic Adobha and Adola Belts (Eritrea and Ethiopia) Pub. Ph. D. thesis, *Giessener Geogische Schriften,* **54**, 218p, Germany.

WOLDEMARIAM, M., 1970. An atlas of Ethiopia, Revised edition, Ministry of Education and Fine Arts, Addis Ababa.

WORKU, H., 1996. Geodynamic development of Adola Belt (Southern Ethiopia) in the Neoproterozoic and its control on gold mineralization Pub. Ph. D. thesis, Tech. Univ. of Berlin. *Wissenschaftiliche Schriftenreihe Geologie und Bergbau,* Band 5, 156p.

WORKU, H., AND YIFA, K., 1989. The tectonic evolution of the precambrian metamorphic rocks of the Adola Belt (Southern Ethiopia) and in its implication on Gold Mineralization, Tec. Report, *Ethiopian Institute of Geological Surveys*, Addis Ababa.

YIHUNIE, T., AND TESFAYE, M., 1998. Geology of the Negele area, *Ethiopian Institute of Geological Surveys*, Memoir 11, Addis Ababa.

8. APPENDICES

1. AAS analytical result (ppm) for geochemical samples of Big Dubicha area.

Sample No.	Sample type	Au ppm	Co ppm	Ni ppm	Cu ppm	Zn ppm	Pb ppm	Mn ppm	Cr ppm	Location	Horizon	Topgraphy	Bed rock	Alteration	Depth (cm)
SOTDB - 1	Soil	<0.1	179	5660	5	44	5	962	2500	0 E / 0 N	C	Flat	Ttss	Serp.	30
SOTDB - 2	Soil	0.1	104	6760	5	37	1	667	4100	100 W / 0 N	C	Gentle	Ttss	Serp.	25
SOTDB - 3	Soil	0.1	187	6270	9	48	1	1233	2300	200 W / 0 N	C	Gentle	Ttss	Serp.	30
SOTDB - 4	Soil	0.1	212	7290	34	48	1	1318	2600	300 W / 0 N	C	Gentle	Ttss	Serp.	21
SOTDB - 5	Soil	0.1	243	7010	6	45	3	1425	3400	400 W / 0N	C	Gentle	Ttss	Serp.	22
SOTDB - 6	Soil	0.1	74	2004	61	56	10	667	1250	100 E / 0 N	B	Flat	Ts	Chl.	25
SOTDB - 7	Soil	0.1	37	336	58	52	10	518	500	200 E / 0 N	B	Gentle	Ts	Chl.	27
SOTDB -8	Soil	0.1	163	5430	4	40	3	1116	900	0 E / 250 N	C	Flat	Ttss		
SOTDB - 9	Soil	0.1	162	4680	9	37	4	1168	750	100 W / 250 N	C	Steep	Ttss	Serp.	22
SOTDB - 10	Soil	0.1	209	6310	20	40	<1	1286	2050	200 W / 250 N	B	Steep	Ttss	Serp.	30
SOTDB - 11	Soil	0.1	239	4720	11	51	2	1470	1700	300 W / 250 N	C	Steep	Ttss	Serp.	20
SOTDB - 12	Soil	0.1	177	6090	4	61	<1	1093	3150	100 E / 250 N	C	Flat	Ttss	Serp.	20
SOTDB - 13	Soil	<0.1	38	540	86	51	3	551	750	200 E / 250 N	B	Gentle	Ts	Serp.	30

1. Continued

Sample No.	Sample type	Au ppm	Co ppm	Ni ppm	Cu ppm	Zn ppm	Pb ppm	Mn ppm	Cr ppm	Location	Horizon	Topography	Bed rock	Alteration	Depth (cm)
SOTDB - 14	Soil	0.1	230	6620	9	49	<1	1400	1700	0 E / 500 N	C	Gentle	Ttss	Serp.	32
SOTDB - 15	Soil	0.1	190	6530	4	30	1	1134	500	100 W / 500 N	C	Gentle	Ttss	Serp	21
SOTDB - 16	Soil	0.1	239	7860	7	46	<1	1422	2150	200 W / 500 N	C	Gentle	Ttss	Serp.	30
SOTDB - 17	Soil	0.1	210	6800	6	48	1	1310	3150	300 W / 500 N	C	Gentle	Ttss	Serp.	32
SOTDB - 18	Soil	0.1	262	7460	22	76	<1	1391	3700	100 E / 500 N	B	Gentle	Ttss	Serp.	32
SOTDB - 19	Soil	0.1	192	9330	26	74	6	1090	3350	0 E / 750 N	B	Gentle	Ttss	Serp.	40
SOTDB - 20	Soil	0.1	194	6000	17	50	<1	1298	2500	100 W / 750 N	B	Flat	Ttss	Serp.	25
SOTDB - 21	Soil	0.1	256	7340	4	40	1	1600	2050	200 W / 750 N	C	Gentle	Ttss	Serp.	25
SOTDB - 22	Soil	0.1	174	7380	5	35	<1	1174	1350	300 W / 750 N	B	Gentle	Ttss	Serp.	35
SOTDB - 23	Soil	0.1	206	6590	8	43	1	1381	2150	400 E / 750 N	C	Gentle	Ttss	Serp.	30
SOTDB - 24	Soil	0.1	16	84	39	43	7	246	100	100 E / 750 N	C	Gentle			30
SOTDB - 25	Soil	0.1	10	40	21	29	4	194	33	200 E / 750 N	B	Gentle			32
SOTDB - 26	Soil	0.1	31	400	16	18	6	228	700	out of grid	C	Gentle	Cs	Chl.	30

1. Continued

Sample No.	Sample type	Au ppm	Co ppm	Ni ppm	Cu ppm	Zn ppm	Pb ppm	Mn ppm	Cr ppm	Location	Horizon	Topgraphy	Bed rock	Alteration	Depth (cm)
SOTDB - 27	Soil	<0.1	50	695	78	50	11	309	700	out of grid	B	Gentle	Ts		30
SOTDB - 28	Soil	0.1	77	761	16	49	8	727	1050	out of grid	B	Gentle	Cs	Chl.	35
SOTDB - 29	Soil	0.1	38	701	18	16	3	219	850	out of grid	C	Flat	Cs	Chl.	30
SOTDB - 30	Soil	0.1	27	116	69	37	43	240	150	out of grid	B	Flat	Q V		30
SOTDB - 31	Soil	<0.1	9	13	23	60	3	372	11	out of grid	B	Flat	Bqcs	Sericitization	30

Ttss = tremolite - actinolite - talc - serpentine schist, Ts = talc schist Cs = chlorite schist,

Bqcs = biotite - quartz - cericite schist Q V = quartz vein, Serp.= serpentinization Chl.= chloritization

2a) Probability plot of Co

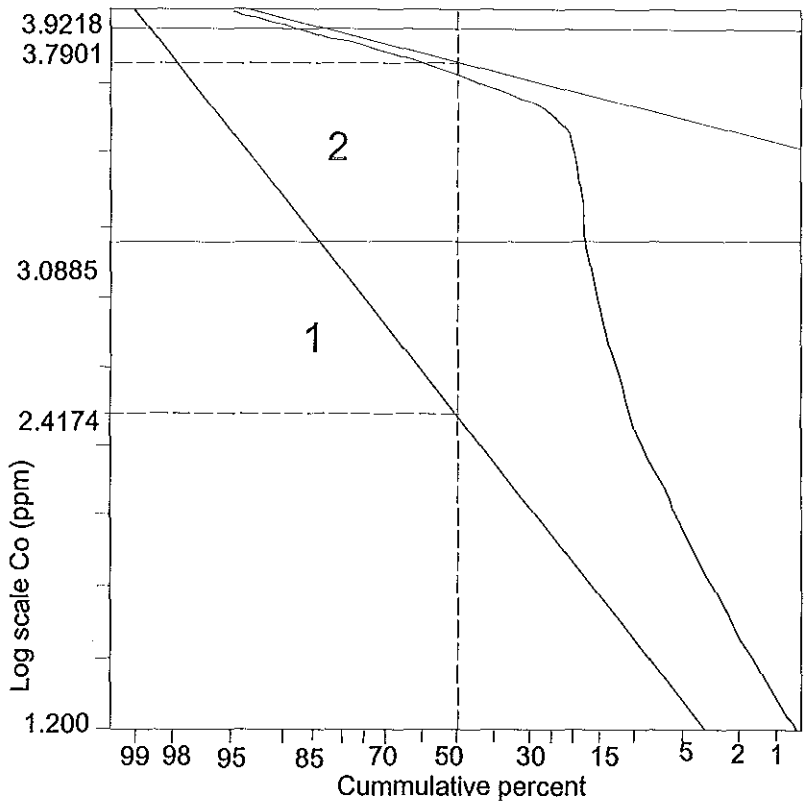

Pop	Mean	S.d	Threshold	%
1	2.4174	0.6711	3.0885	20
2	3.7901	0.1317	3.9218	80

2b) Probability plot of Ni

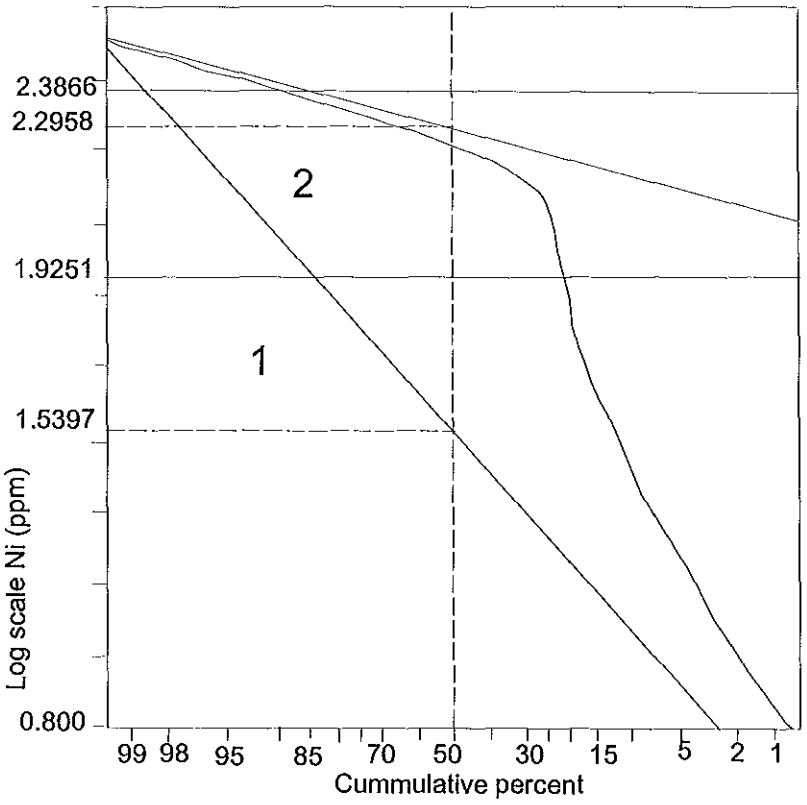

Pop	Mean	S.d	Threshold	%
1	1.5397	0.3854	1.9251	25
2	2.2958	0.0908	2.3866	75

2c) Probability plot of Cr

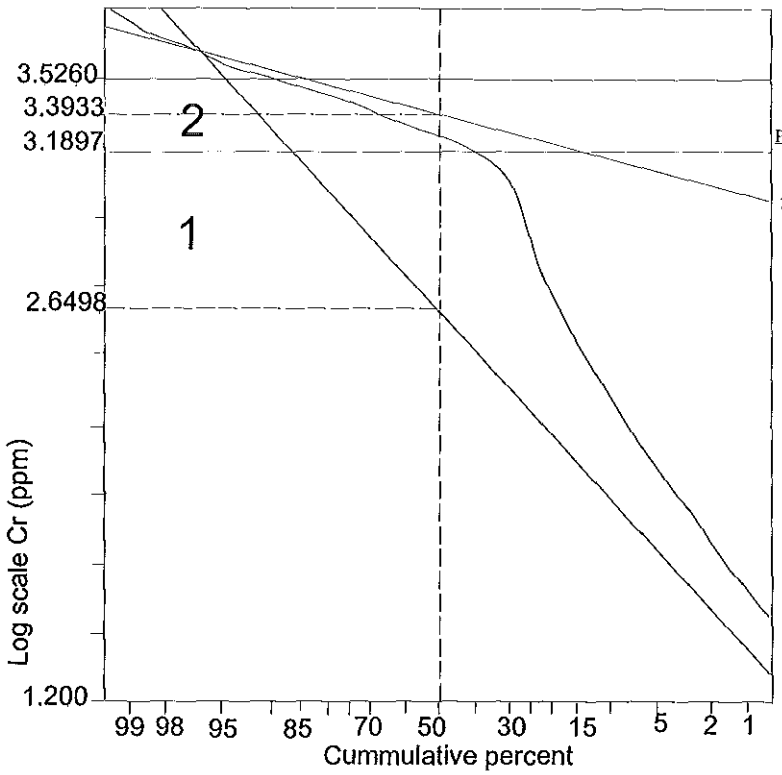

Pop	Mean	S.d	Threshold	%
1	2.6498	0.5399	3.1897	35
2	3.3933	0.1327	3.5260	65

2d) Probability plot of Mn

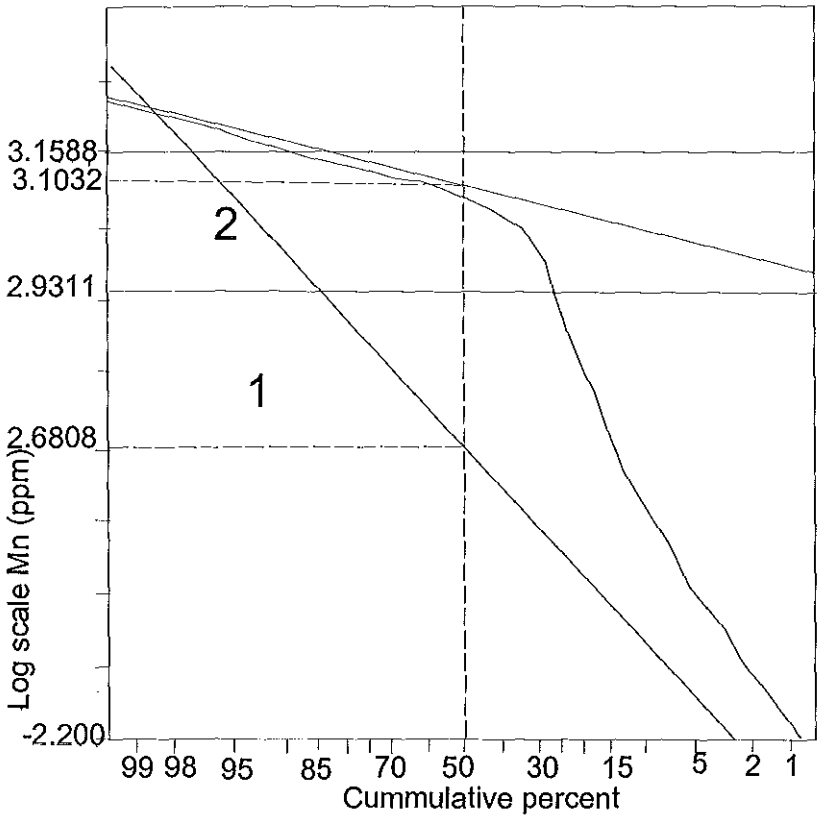

Pop	Mean	S.d	Threshold	%
1	2.6808	0.2503	2.9311	28
2	3.1032	0.0557	3.1588	72

2e) Probability plot of Cu

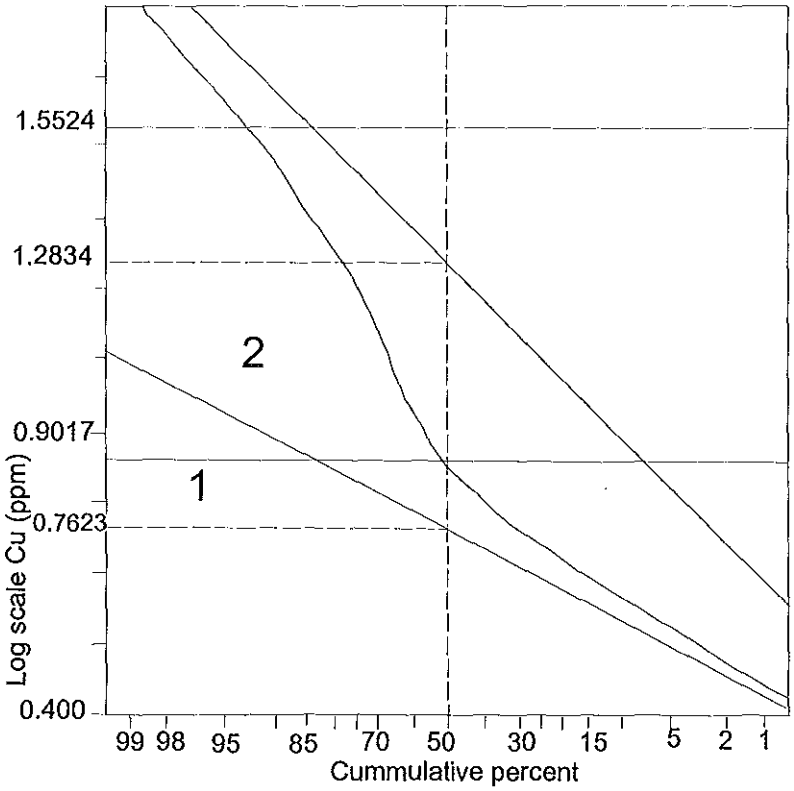

Pop	Mean	S.d	Threshold	%
1	0.7623	0.1394	0.9017	55
2	1.2834	0.2689	1.5524	45

2f) Probability plot of Zn

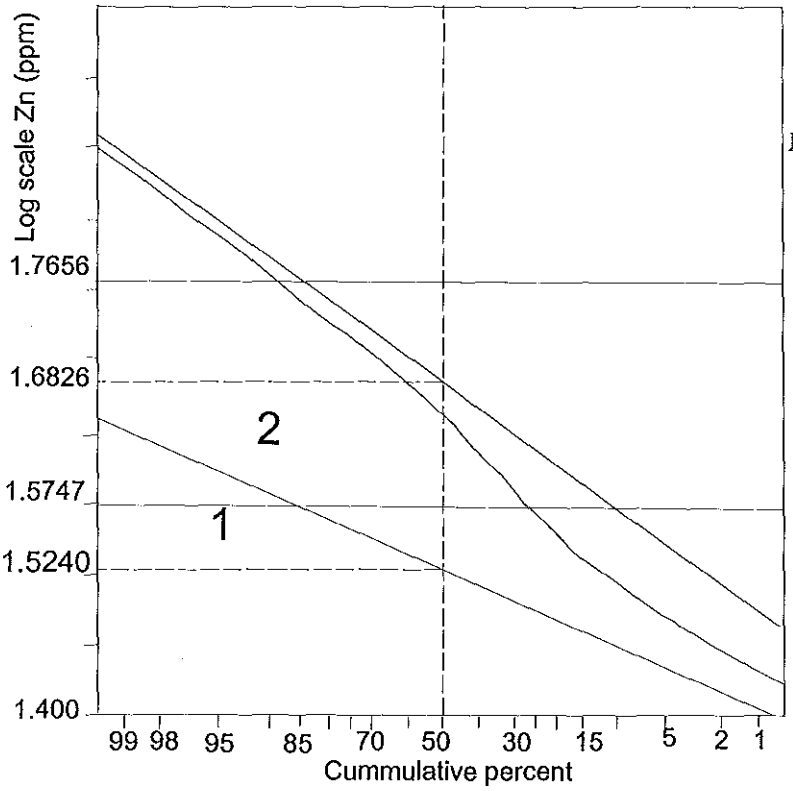

Pop	Mean	S.d	Threshold	%
1	1.5240	0.0508	1.5747	20
2	1.6826	0.0831	1.7656	80

2g) Probability plot of Pb

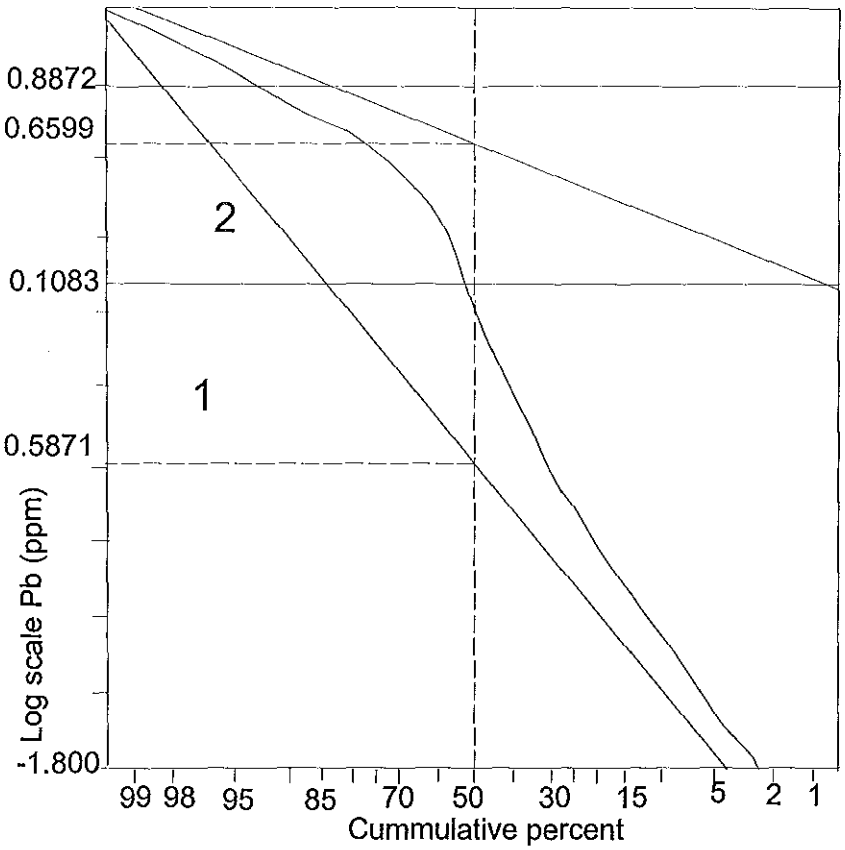

Pop	Mean	S.d	Threshold	%
1	0.5871	0.6954	0.1083	60
2	0.6599	0.2273	0.8872	40

3. Mineralogical compositions of thin - sections

3a. Biotite - muscovite - quartz schist

Sample No	Biotite %	Muscovite %	Quartz %	others %	Texture	Alteration	Rock name
TDB - 13 A	20	15	60	5 (hbl)	Schistosed	seric.	Cbqs
" - 99	20	25	50	"	"	-	Bmqs
" - 100	-	60	35	5 (opaque)	"	-	Qms
" - 106	-	30	50	20 (opaque)	"	-	Mqs
" - 107	10	30	40	5 (opaque) 5 plag. + microcline	"	-	Bmqs

hbl = hornblende Cbqs = Cericite - biotite - quartz schist Bmqs = Biotite - muscovite - quartz schist Qms = Quartz - muscovite schist Mqs = Muscovite - quartz schist seric. = sericitization

3b. Chlorite schist

Sample No	Tre - act (%)	Talc (%)	Chlo. (%)	Opaque (%)	others (%)	Texture	Alter ation	Rock name
TDB - 6 A			94	5	1 epidote	Schistosed	Chl.	Cs
" - 6 B			95	5		"	"	Cs
" - 8 A			95	5		"	"	Cs
" - 8 B			90	5	5 quartz	"	"	Cs
" - 9 B			98	2		"	"	Cs
" - 35 A			95	5		"	"	Cs
" - 35 B			90	10		"	"	Cs
" - 64 A			80	20		"	"	Cs
" - 64 B			93	5	2 epidote	"	"	Cs
" - 76 A			96	4		"	"	Cs
" - 76 B			90	10		"	"	Cs
" - 78			80	10	10 quartz	"	"	Cs
" - 91 A	5		65	30		"	"	Cs
" - 91 B	10		45	40		"	"	Cs
" - 92 A	20	10	70	trace		Schistosed	Chl.	Tcs
" - 92 B	30	65	5				"	Tcs
" - 93 A	40		60	tr.		"	"	Tcs
" - 96 B			93	5	2 (epi)	"	"	Cs
" - 97 B			90	10		"	"	Cs
" - 98	40		55	5		"	"	Tcs
" -101 B	43		45	12		"	"	Tcs
" - 103 B	10		25	trace		"	"	Achs

3c. Talc schist

Sample No	Talc	Tre - act. (%)	Chlo. (%)	Opaque (%)	Others (%)	Texture	Alteration	Rock name
TDB - 5	95			5		Schistosed		Ts
" - 7	90	5		5		"		Ts
" - 13 B	60	40						Tts
" - 34	90			10		"		Ts
" - 65	68		30	2		"		Cts
" - 66	98			2		"		Ts
" - 75	80			20		"		Ts
" - 77	95			5		"		Ts
" - 93 B	90			10		"		Ts
" - 94	39	25	34	1	1	"		Tcts
" - 95 B	80	10		10		"	T	Ts
" - 95 C	70	20	10			"	T	Tts
" - 96 A	98			2		"		Ts
" - 96 C	85	5		5		"	T	Ts
" - 97 A	95			5		"		Ts
" - 98 A	95	5				"		Ts
"- 101 A	48	40		5	7 quartz	"	T	Tts
"- 102 A	75	25				"	"	Tts

3d. Tremolite - actinolite - talc - serpentine schist

Sample No	Tre - act. (%)	Talc (%)	Serp. (%)	Chlo. (%)	Opaques	Others	Texture	Alteration	Rock name
TDB - 1	5	10	80		5		Schistosed	Ser. + T	Tss
" - 3		10	85		5		"	T	"
" - 4		30	60		10		"	"	"
" - 13 C	99				tr.	Tr. (car)	"		Ta s
" - 14		10	85		5		massive	T	Serpentinite
" - 15			95				schistosed		Ss
" - 16		10	85		5		"	T	Tss
" - 17	5	10	80		5		"	Ser. + T	"
" - 18		10	85		5		"	T	"
" - 22		5	85		5		"	T	Ss
" - 24			90		10		"		Ss
" - 25		15	84		1		"	T	Tss
" - 26		10	80		10		"	T	Tss
" - 27	10	10	75		5		"	Ser. + T	Ttss
" - 28 B		10	85		5		"	T	Tss
" - 29		10	80		10		"	T	"
" - 31		10	80		10		"	T	"
" - 32		10	80		10		"	T	"

3d. Continued.

Sample No	Tre - act. (%)	Talc (%)	Serp. (%)	Chlo. (%)	Opaques	Others	Texture	Alteration	Rock name
TDB - 36		30	69		1		"	T	"
" - 37	10	10	79		1		"	T	Ttss
" - 40	5	10	80		5		"	Ser. + T	Tss
" - 45 A		5	95						Tss
" - 45 B	10	20	50		20		"	Ser. + T	Ttss
" - 46 B	10	10	70		10		"	Ser. + T	"
" - 49		2	93		5		"	T	Ss
" - 53		5	90		5		"	T	"
" - 56	5	10	80		5		"	Ser. + T	Tss
" - 60		5	95		tr.		"	T	Ss
" - 61		10	80		10		"	T	Tss
" - 62 A		10	85		5		"	T	"
" - 62 B		10	85		5		"	T	"
" - 63		5	90		10		"	T	Ss
" - 67		10	88		2		"	T	Tss
" - 68		10	70		20		"	T	"
" - 69	10	10	68		2		"	Ser. + T	Ttss
" - 74		10	30			60 olivine	massive		Sd

3d. Continued.

Sample No	Tre - act. (%)	Talc (%)	Serp. (%)	Chlo. (%)	Opaques	Others	Texture	Alteration	Rock name
TDB - 73	20	20	55		5		schistosed	Ser. + T	"
" - 88			80		20		"		Ss
" -103 A	90				10		"		Tas
" - 104			98		2		"		Ss
" - 105		10	80				"	T	Tss

Tre - act = Tremolite - actinolite Serp. = Serpentine Chlo. = Chlorite Biot. = Biotite Car. = Carbonates Ser. = Serpentinization T = transformation of serpentne to talc Ttss = Tremolite - actinolite - talc - serpentine schist Tss = talc serpentine schist Ss = Serpentine schist Tas = Tremolite - actinolite schist Sd = Serpentinized dunite Chl. = chloritization epi = epidote quartz Cs = Chlorite schist Ts = Talc schist Ttcs = Tremolite - actinolite - talc -chlorite schist Tcts = Tremolite - actinolite - chlorite - talc schist Tts = Tremolite - actinolite - talc - schist Tcs = tremolite - actinolite - chlorite schist Achs = Actinolite - chlorite - hornblende schist

Talc schist XRF analytical data (n=16)

Sample	Major oxides (wt. %)											Trace elements (ppm)																
No	SiO_2	TiO_2	Al_2O_3	Fe_2O_3	MnO	MgO	CaO	Na_2O	K_2O	P_2O_5	LOI	Total	V	Cr	Co	Ni	Cu	Zn	Ga	Rb	Sr	Y	Zr	Nb	Ba	La	Pb	Ce	Th
TDB - 5	61.48	0.00	0.44	4.18	0.05	29.11	0.00	0.00	0.00	0.00	4.73	99.99	6	1325	61	1341	9	38	0.00	1	2	2	4	0.00	1	1	8	0.00	6
TDB - 7	58.78	0.01	1.07	4.89	0.07	29.20	1.43	0.00	0.01	0.01	4.54	100.01	6	1651	64	1281	2	74	0.00	1	9	2	3	0.00	1	2	14	0.00	6
TDB - 13 B	56.96	0.02	0.84	5.53	0.13	29.11	4.01	0.00	0.02	0.04	3.33	99.99	9	1866	73	1428	7	81	4.00	1	6	2	5	1.00	1	9	4	0	2
TDB - 34	51.95	0.02	1.70	5.11	0.05	28.09	0.03	0.00	0.00	0.01	13.04	100.00	59	2350	45	839	93	47	2	1	2	2	4	0.00	1	0.00	7	0.00	5
TDB - 65	58.14	0.02	1.06	2.8	0.04	32.05	0.05	0.00	0.00	0.01	5.83	100.00	*	*	51	1577	10	35	4	2	3	1	10	0.00	*	*	12	*	7
TDB - 66	55.98	0.01	1.54	3.18	0.06	33.63	0.03	0.00	0.00	0.00	5.57	100.00	*	*	75	1519	2	39	8	2	2	3	8	0.00	*	*	16	*	6
TDB - 75	55.92	0.01	1.67	5.48	0.07	32.13	0.03	0.00	0.00	0.00	4.69	100.00	*	*	71	1131	11	59	6	2	2	1	9	1	*	*	4	*	2
TDB - 77	55.35	0.02	2.81	4.35	0.05	32.03	0.06	0.00	0.01	0.02	5.31	100.01	*	*	64	1423	16	50	3	2	2	4	9	0.00	*	*	10	*	4
TDB - 93B	56.27	0.01	0.75	3.82	0.04	34.13	0.01	0.00	0.00	0.00	4.97	100.00	*	*	63	1687	5	46	4	2	2	2	8	0.00	*	*	14	*	7
TDB - 94	46.64	0.47	6.71	9.19	0.12	28.98	1.63	0.00	0.01	0.08	6.17	100.00	*	*	93	1310	12	106	11	2	6	17	78	8	*	*	13	*	10
TDB - 96A	57.95	0.02	1.8	5.28	0.06	29.89	0.02	0.00	0.01	0	4.97	100.00	*	*	67	1648	11	41	3	2	2	1	7	0.00	*	*	18	*	6
TDB - 96C	55.35	0.02	1.95	5.79	0.08	31.88	0.04	0.00	0.00	0.00	4.88	99.99	*	*	88	2079	14	46	1	2	2	3	8	1	*	*	11	*	2
TDB - 97A	55.74	0.02	3.54	5.04	0.06	29.92	0.02	0.00	0.00	0.00	5.65	99.99	*	*	48	1015	53	54	6	2	2	1	9	1	*	*	17	*	7
TDB - 98A	55.32	0.03	2.18	5.07	0.06	32.21	0.07	0.00	0.00	0.00	5.06	100.00	*	*	80	1636	12	33	6	2	2	1	9	0.00	*	*	17	*	7
TDB - 102B	57.47	0.02	1.76	5.32	0.08	29.28	1.95	0.00	0.01	0.02	4.1	97.01	*	*	69	1431	5	57	1	2	11	2	10	1	*	*	12	*	6
TDB - 103A	50.02	0.36	4.26	9.26	0.14	23.82	8.78	0.00	0.04	0.17	3.15	99.98	*	*	79	666	15	67	4	2	46	6	42	6	*	*	9	*	3

Chlorite schist XRF analytical data (n=22)

Sample	Major oxides (wt. %)											Trace elements (ppm)																
No	SiO_2	TiO_2	Al_2O_3	Fe_2O_3	MnO	MgO	CaO	Na_2O	K_2O	P_2O_5	LOI	Total	V	Cr	Co	Ni	Cu	Zn	Ga	Rb	Sr	Y	Zr	Nb	Ba	La	Pb	Ce	Th
TDB - 6A	26.05	1.58	18.29	18.54	0.12	27.28	0.41	0.00	0.01	0.26	7.46	100.00	380	323	121	89	68	109	16	1	13	78	281	23	53	18	5	69	3
TDB - 6B	25.51	2.01	15.56	16.43	0.12	30.89	0.55	0.00	0.01	0.39	8.54	100.01	264	221	116	135	50	96	16	1	16	73	357	24	104	47	3	139	7
TDB - 8A	25.51	1.56	18.43	15.73	0.14	26.32	1.33	0.00	0.00	0.96	10.02	100.00	180	365	116	367	21	142	21	1	50	53	263	21	63	41	2	60	7
TDB - 8B	22.55	2.37	15.80	19.11	0.14	29.64	1.66	0.00	0.01	1.24	7.48	100.00	353	230	93	114	93	117	19	1	54	70	445	25	112	69	2	149	9
TDB - 9B	30.27	0.54	15.25	8.14	0.11	34.51	0.02	0.00	0.00	0.01	11.15	100.00	123	2195	86	1006	5	93	11	1	2	2	8	3	1	0.00	8	0.00	4
TDB - 35A	26.57	0.43	20.11	12.48	0.11	29.74	0.05	0.00	0.00	0.02	10.48	99.99	474	70	69	73	6	77	11	1	3	5	14	2	1	0.00	2	0.00	0.00
TDB - 35b	30.24	0.23	13.59	9.00	0.06	35.74	0.01	0.00	0.00	0.00	11.14	100.01	220	272	89	139	5	59	7	1	2	5	23	4	1	0.00	3	0.00	4
TDB - 64A	22.78	2.99	15.21	17.21	0.14	33.08	1.5	0.00	0.01	1	6.08	100.00	*	*	138	325	10	108	11	2	20	63	219	36	*	*	-7	*	-2
TDB - 64B	26.78	1.46	19.13	11.13	0.11	30.56	0.29	0.00	0.00	0.13	10.4	99.99	*	*	92	222	5	101	22	2	20	32	164	14	*	*	5	*	4
TDB - 76A	29.14	0.57	17.29	9.58	0.12	31.57	0.37	0.00	0.01	0.18	11.19	100.02	*	*	45	150	6	97	16	2	55	35	180	12	*	*	9	*	9
TDB - 76B	27.18	0.87	19.56	11.44	0.17	29.4	0.19	0.00	0.01	0.1	11.09	100.01	*	*	36	144	7	150	16	2	28	62	306	18	*	*	15	*	10
TDB - 78	27.93	1.49	15.15	9.57	0.11	31.09	3.03	0.00	0.00	1.82	9.8	99.99	*	*	75	577	6	99	16	2	210	47	833	30	*	*	6	*	17
TDB - 91A	27.01	0.23	16.93	14.48	0.15	31.87	0.33	0.00	0.00	0.01	9	100.01	*	*	152	2061	24	153	20	2	5	13	17	2	*	*	2	*	1
TDB - 91B	27.92	1.87	16.45	14.57	0.17	29.38	0.66	0.00	0.01	0.09	8.87	99.99	*	*	135	930	9	134	19	2	8	37	221	25	*	*	3	*	0.00
TDB - 92A	31.21	0.05	16.07	10.97	0.13	30.38	0.08	0.00	0.01	0.01	11.09	100.00	*	*	117	1644	29	110	43	2	2	2	14	0.00	*	*	16	*	3
TDB - 92B	29.37	0.42	15.73	11.34	0.11	31.9	0.85	0.00	0.01	0.03	10.25	100.00	*	*	101	1875	13	115	14	2	6	19	56	7	*	*	5	*	1
TDB - 93A	40.85	0.07	11.1	8.74	0.15	27.18	4.79	0.00	0.04	0.07	7.02	100.01	*	*	79	1484	29	95	10	2	18	3	9	1	*	*	12	*	4
TDB - 96B	27.54	0.8	20.75	11.78	0.1	27.54	0.13	0.00	0.00	0.09	11.29	100.02	*	*	95	701	16	99	23	2	21	30	286	13	*	*	14	*	10
TDB - 97B	27.16	0.81	18.42	12.05	0.09	30.72	0.06	0.00	0.01	0.01	10.68	100.01	*	*	63	374	11	85	13	2	2	103	156	17	*	*	2	*	4
TDB - 98B	36.5	0.93	13.09	10.12	0.17	26.5	6.02	0.00	0.02	0.46	6.19	100.00	*	*	97	744	71	123	17	2	18	31	196	15	*	*	12	*	10
TDB - 101B	34.9	0.94	13.47	10.91	0.14	28.56	3.97	0.00	0.01	0.32	6.78	100.00	*	*	83	930	5	119	17	2	31	17	163	14	*	*	12	*	6
TDB - 103B	39.36	0.8	10.94	9.74	0.16	27.8	5.81	0.00	0.03	0.19	5.18	100.01	*	*	105	1167	28	85	15	2	23	17	96	11	*	*	9	*	6

Biotite - muscovite - quartz schist XRF analytical data (n=3)

Sample	Major oxides (wt. %)											Trace elements (ppm)																
No	SiO_2	TiO_2	Al_2O_3	Fe_2O_3	MnO	MgO	CaO	Na_2O	K_2O	P_2O_5	LOI	Total	V	Cr	Co	Ni	Cu	Zn	Ga	Rb	Sr	Y	Zr	Nb	Ba	La	Pb	Ce	Th
TDB - 13A	55.37	1.06	11.93	15.48	0.25	5.64	5.49	0.68	0.44	0.28	3.36	99.98	25	140	14	333	45	79	32	10	828	10	181	5	102	20	56	28	21
TDB - 99	66	0.49	15.52	3.25	0.07	2.77	1.12	4.74	4.61	0.23	1.2	100	*	*	41	19	6	59	20	111	214	17	163	2	*	*	25	*	10
TDB - 100	61.56	0.71	21.36	3.93	0.05	1.71	0.44	0.68	6.13	0.31	3.13	100.01	*	*	42	18	8	30	25	110	95	10	113	4	*	*	22	*	6

* = not analyzed